p. 163

A Variational Assimilation Method for Satellite and Conventional Data: Development of Basic Model for Diagnosis of Cyclone Systems

G. L. Achtemeier, R. W. Scott,

and J. Chen

Illinois State Water Survey

Champaign, Illinois 61820

FINAL REPORT

Prepared for

George C. Marshall Space Flight Center

under Grant NAG8-059

June 1991

Table of Contents

omit to p.11

Chapter I

Background and Overview of Document

I. Introduction

The following summarizes the progress toward completion of a comprehensive diagnostic objective analysis system based upon the calculus of variations. The approach was to first develop the objective analysis subject to the constraints that the final product satisfies the five basic primitive equations for a dry inviscid atmosphere: the two nonlinear horizontal momentum equations, the continuity equation, the hydrostatic equation, and the thermodynamic equation. Then, having derived the basic model, there would be added to it the equations for moist atmospheric processes and the radiative transfer equation.

The remainder of this section is organized into subsections as follows. A brief review of the problem design and progress to the beginning of the current completed grant period is given in I.1. This first period is designated as Phase I. Then subsection I.2 summarizes progress under this grant (Phase II) and references following chapters that give results in greater detail.

The reader should pay particular attention to the findings presented in Chapter V. A conceptual error within one of the

mathematical derivations was discovered while preparing Chapter V. The outcome is that some of the negative conclusions regarding the meaningful incorporation of satellite thermodynamic data into the meteorological data mainstream are no longer valid.

I.2. Background of Initial Project and Phase I Summary

By 1981, most quantitative satellite data for the troposphere consisted of TIROS-N temperature retrievals (Smith and Woolf, 1976), some cloud wind vectors, early VAS soundings (Smith, 1970; Chesters, et al., 1981), and initial SASS surface winds (Jones, et al., 1979). Although these data revealed new and interesting phenomena, it was becoming apparent that satellite data could not be used to quantify the dynamics of the troposphere without being supplemented by conventional data.

The tools available to dynamically assimilate satellite data with conventional data consisted mostly of initialization methods for numerical prediction models. For example, normal mode initialization (Baer, 1977; Machenhaur, 1977) improved the dynamic coupling between the observations and numerical models. Early comparisons between numerical predictions with and without satellite temperature data using initialization schemes of the time were inconclusive (Phillips, 1976; Tracton et al., 1981; Ghil et al., 1979). The impact of satellite data was highly dependent on the capability of the analysis and forecast system used for the impact testing.

There was, therefore, a need for other methods for blending satellite data with conventional data. The direct variational methods presented by Sasaki (1958, 1970) are applicable to a diagnostic data assimilation method. Achtemeier (1975) applied Sasaki's method to blend diverse conventional data to satisfy the primitive equations. This work revealed the potential of the direct variational method as well as some of the inherent difficulties. The purpose of the variational objective analysis project funded by NASA was to extend the Achtemeier method to blend satellite data with conventional data.

The general goals of the project which began in 1982 (see Achtemeier, et al., 1986) were to:

(1) Modify the Achtemeier (1975) numerical variational model for the assimilation or merging of weather data (constraints: the nonlinear set of dynamical equations for atmospheric flow plus the radiative transfer equation) collected remotely from space with conventional weather data.

(2) Translate the variational theory into a practical model that can be used by other scientists within the NASA Global Scale Atmospheric Processes Research Program and elsewhere.

(3) Design the variational assimilation to be independent from numerical forecast models - that is, make it diagnostic. This does not preclude the method from being used to develop initial fields for numerical models nor the blending of model forecast fields with satellite and conventional data.

(4) Apply the variational model to estimate minimal data

requirements (data type, sampling frequency, density, accuracy) for accurate diagnosis of atmospheric structure that could be useful for the design of future satellite-borne instruments.

The project began with a review of the Achtemeier (1972, 1975, 1979) applications of the Sasaki (1958, 1970) variational methods by a mathematical consultant. This review confirmed that the applications of Sasaki's methods were mathematically sound. We then commenced the development of a general numerical variational model that includes the following dynamical constraints: the two nonlinear horizontal momentum equations, the hydrostatic equation, the continuity equation, the thermodynamic equation for moist convective processes, a moisture conservation equation, and the radiative transfer equation. From the experience gained from the previous studies, it was known that the application of the direct variational method to the above dynamic constraints presented three formidable mathematical problems.

(1) Courant (1936) showed that the number of subsidiary conditions (dynamic constraints) must be at least one less than the number of adjustable dependent variables. Inclusion of the same number of constraints as dependent variables, such as the five primitive equations with five dependent variables, overdetermines the problem and a solution is not guaranteed. Achtemeier (1975) originally attempted to circumvent this

problem through a parameterization of the tendency terms of temperature and the velocity components that required the exact solution of the integrated continuity equation. However, this method (a variational adjustment within a variational adjustment) was considered a failure after an extensive analysis (Achtemeier, 1979) found unrealistically large velocity component tendencies where actual velocity changes over a 12-hr period were small.

(2) Application of the direct variational method to the local tendencies of temperature and the horizontal velocity components yield terms in the Euler-Lagrange equations that are local tendencies of Lagrange multipliers. Boundary conditions for these terms are unknown. The problem of time consistency in variational problems has been examined by Lewis (1980, 1982) and Lewis et al (1983). More recently, the time consistency problem has been found more tractable through use of the adjoint method (Lewis and Derber, 1985; Talagrand and Courtier, 1987).

(3) The Euler-Lagrange equations produced by Sasaki's method include the dynamical constraints plus variational equations which are equal in number to the number of dependent variables to be blended and equal in complexity to the complexity of the original constraints. This set of complicated nonlinear partial differential equations presents formidable programming

problems and is difficult to solve by traditional methods. Achtemeier (1975) developed a cyclical solution method which, upon scaling the equations and expressing the terms in powers of the Rossby number, places higher order terms in forcing functions, solves the equations as a linear set and updates the higher order terms with the new solutions. The method, which converges rapidly, was modified for this project.

To better assure progress toward the development of the general variational analysis model, the task was divided into four variational models of increasing complexity. MODEL I, including the two horizontal momentum equations, the hydrostatic equation, and an integrated continuity equation as dynamical constraints, addresses the problems that arise from applying the direct variational method to local tendency terms. The cyclical solution method developed by Achtemeier (1975) is applied to the MODEL I finite differencing scheme. A nonlinear vertical coordinate reduces the need to vertically interpolate satellite-derived temperatures. MODEL II, which includes MODEL I plus the thermodynamic equation for a dry atmosphere, focuses on the overdetermined solution problem posed by Courant. MODEL III includes MODEL II plus the radiative transfer equation as a dynamical constraint and the radiance as a dependent variable. MODEL IV incudes moisture and its parameterizations.

The theoretical development and initial evaluations of MODEL I are given by Achtemeier (1986a), Achtemeier et al. (1986a,

1986b), and Kidder and Achtemeier (1986). In MODEL I, the tendency terms for the horizontal velocity components were separated into advective and developmental components; the advective component explains local changes caused by disturbances moving in a basic current and the developmental component explains local tendencies caused by changes in the structures or intensities of the disturbances. The advective components were incorporated into the dynamic equations through time to space conversion, and the developmental components became dependent variables.

MODEL I successfully diagnosed local tendencies of the horizontal velocity components. Diagnosed local tendencies of the horizontal velocity components compared favorably with observed three hour tendencies, whereas local tendencies calculated from direct substitution of unadjusted fields of data into the dynamic constraints did not.

I.2 Summary of Results under Phase II

Theoretical development, programming, and evaluation of MODEL II was completed early in 1987. MODEL II included the five primitive equations for a dry atmosphere as dynamic constraints ie., MODEL I plus the thermodynamic equation. The partition of the horizontal velocity tendencies with the definition of the developmental components as dependent variables increased the number of dependent variables from five to seven. Therefore, we have solved the problem of overdetermining the solution (Courant,

1936).

Evaluation of MODEL II revealed that the tendency term formulations remained stable (Achtemeier, 1988c). However, first order terms that contain the divergence adjustment cancel out in the cyclical solution formulations. The divergence adjustment must then be carried in second order terms and through other variables. Formulating the continuity equation as an ancillary constraint to be satisfied at each cycle - a variational model within a variational model - and "nudge" the solution does not always provide the desired dynamic balance with the divergent part of the wind. Details of the MODEL II evaluation are presented in Chapter II.

Further examination of MODEL II found that the divergent component of the wind can be made to satisfy the continuity equation subject to the satisfaction of an additional mathematical constraint. That constraint requires the adjusted wind field to satisfy a particular solution of the integrated vorticity equation. The particular solution satisfies the conditions that the sum of the terms of the vorticity equation vanish when integrated from the surface to the top of the domain and that the divergence vanishes when integrated from the surface to the top of the domain. This latter condition satisfies the integrated continuity equation.

Both MODEL I and MODEL II were reformulated mathematically and reprogrammed into a new version MODEL IIB. MODEL IIB is the subject of Chapter III. It forms the new basic 5-primitive equation variational objective analysis model that must be

satisfied before any additional dynamic constraints can be added to increase the complexity of the objective analysis technique. The successful completion of MODEL IIB therefore, is the focus of the Phase II research effort.

The need to rederive the basic variational models also changed the focus of this research. The original objective to develop an analysis tool for the incorporation of satellite data into the mainstream of meteorological data was changed from applied research to basic research. Rather than take an existing method and modify it to produce a product, it became necessary to prove that the variational method fundamentally was workable.

Several other research efforts aimed at expanding the variational objective model beyond the basic model were pursued commensurate with the development of MODEL IIB. A variationally constrained temperature profile analysis was derived with the dynamic constraints being the four radiative transfer equations for the microwave channels used to sample within the troposphere. Rawinsonde temperature and the four brightness temperatures are the adjustable variables. Chapter IV presents the results from this study. Then, in Chapter V, the radiative transfer equations were combined with the equations for a geostrophic, hydrostatic atmosphere as part of a theoretical study to determine the impact of the radiative transfer equations upon the variational analysis.

Additional effort was directed to the goal was to make the variational analysis more responsive to the original observations. The gridding of meteorological data is the first step in performing

objective analysis and is done independently from the variational adjustments. Therefore our first efforts in achieving this goal was to improve upon the objective analysis method. Chapter VI presents a study of the effects of influence radius upon an objective analysis and Chapter VII presents a modification of a successive corrections technique for improved derivative calculations.

Chapter II

A Variational Assimilation Method for Satellite and Conventional Data: MODEL II (Version 1)

Gary L. Achtemeier
Office of Climate and Meteorology
Division of Atmospheric Sciences
Illinois State Water Survey
Champaign, Illinois 61820

1. Introduction

The MODEL II variational data assimilation model is the second of the four variational models designed to blend diverse meteorological data into a dynamically constrained data set. MODEL II differs from the MODEL I developed during Phase I in that it includes the thermodynamic equation as the fifth dynamical constraint.

Thus MODEL II includes all five of the primitive equations that govern atmospheric flow for a dry atmosphere. The reason for delaying the introduction of the thermodynamic equation until MODEL II is as follows. Courant (1936) showed that the number of subsidiary conditions (dynamic constraints) must be at least one less than the number of adjustable dependent variables. The five primitive equations form a closed set of equations with five dependent variables. Inclusion of the same number of constraints as dependent variables overdetermines the problem and a solution is not guaranteed. Achtemeier (1975) attempted to circumvent this problem through a parameterization of the tendency terms of the velocity components and the temperature that required the exact solution of the integrated continuity equation. This method, a variational adjustment within a variational adjustment, was considered a failure after an extensive analysis (Achtemeier, 1979) found unrealistically large velocity component tendencies where actual velocity changes over a 12-hr period were small.

The approach taken in the development of MODEL I was to make

possible the inclusion of the five primitive equations by increasing the number of dependent variables. We defined two new dependent variables, the developmental components of the horizontal velocity tendencies, which increased the number of dependent variables from five to seven. Though this solves the problem of the number of subsidiary conditions, the extent of internal coupling among the variables and within the equations could not be determined fully until the development and evaluation of MODEL II.

2. MODEL II: Thermodynamic Equation as a Dynamic Constraint

Upon defluxing and omitting the dissipation term of the thermodynamic equation in Anthes and Warner (1978), the thermodynamic equation as it appears as a dynamical constraint in MODEL II is,

$$\frac{\partial T}{\partial t}+m\left(u\frac{\partial T}{\partial x}+v\frac{\partial T}{\partial y}\right)+\dot{\sigma}\frac{\partial T}{\partial \sigma}-\frac{RT\omega}{c_p p}-\frac{Q}{c_p}=0 \qquad (1)$$

The omega-term (term 4) of the thermodynamic equation can be transformed into the nonlinear sigma coordinate system through the definition,

$$\sigma=\beta\left(p-p^*\right)^3+\sigma^*\frac{p-p_u}{p^*-p_u} \qquad (2)$$

where the superscript, *, and the subscript, u, identify, respectively, the variables at the reference pressure level and at the top of the model atmosphere. For more information on the nonlinear vertical coordinate system, refer to Appendix A.1. Furthermore,

$$\beta = [1-\sigma^* \frac{p_s-p_u}{p^*-p_u}] \, (p_s-p^*)^{-3} \tag{3}$$

where the subscript, s, refers to quantities measured at the surface. We differentiate (2) with respect to time. If

$$\alpha = \frac{\sigma^*}{p^*-p_u} \tag{4}$$

and

$$J = [3\beta \, (p-p^*)^2+\alpha] \, (p-p^*) \tag{5}$$

then we may define two coefficients such that

$$q_3 = \frac{p-p^*}{Jp} \tag{6}$$

and

$$q_4 = \frac{J_s}{Jp}\left(\frac{p-p^*}{p_s-p^*}\right)^4 \tag{7}$$

for $p>p^*$, and

$$q_3 = \frac{1}{\alpha p} = \frac{p^* - p_u}{\sigma^* p} \tag{8}$$

and

$$q_4 = 0 \tag{9}$$

for $p < p^*$.

The thermodynamic equation in the nonlinear sigma coordinates is, upon substitution for the omega-term,

$$\frac{\partial T_W}{\partial t} + m\left(u\frac{\partial T_W}{\partial x} + v\frac{\partial T_W}{\partial y} + \dot{\sigma}\frac{\partial T_W}{\partial \sigma} - \frac{RT\omega}{c_p}\right)(q_3\dot{\sigma} + q_4\omega_s) - \frac{Q}{c_p} = 0 \tag{10}$$

Here the subscript, W, refers to the whole temperature, $T_W = T_R + T$, where T_R is a reference temperature for the layer and is always in hydrostatic balance and T is the departure from the reference temperature that is subject to adjustment within the variational model. Substitution for the whole temperature yields the thermodynamic equation in the adjustable part of the temperature,

$$\frac{\partial T}{\partial t} + m\left(u\frac{\partial T}{\partial x} + v\frac{\partial T}{\partial y}\right) + \dot{\sigma}\frac{\partial T}{\partial \sigma} - \frac{R}{c_p}(T_R - T)(q_3\dot{\sigma} + q_4\omega_s) + \dot{\sigma}\frac{\partial T_R}{\partial \sigma} - \frac{Q}{c_p} = 0 \tag{11}$$

Now nondimensionalize the thermodynamic equation. Letting

$$u=Uu',\ v=Uv',\ \Delta t=(L/C)\Delta t',\ \Delta x=L\Delta x',$$
$$T_R=\theta T_R'=(gH/R)\,T_R',\ \Delta T=(gH/R)\,(F/R_o)\,\delta T' \qquad (12)$$
$$p=Pp',\ \dot{\sigma}\sim(C/L)\,\dot{\sigma}',\ \omega_s\sim(PC/L)\,\omega_s'$$

and dividing through by $(C/L)(gH/R)(F/R_o^2)$, the nondimensionalized thermodynamic equation with primes suppressed is,

$$R_o\left[\frac{\partial T}{\partial t}+m\left(u\frac{\partial T}{\partial x}+v\frac{\partial T}{\partial y}\right)+\dot{\sigma}\frac{\partial T}{\partial \sigma}\right]$$
$$-R_o\frac{R}{C_p}\left(\frac{R_o}{F}T_R'+T\right)\left(q_3\dot{\sigma}+q_4\omega_s\right)-\left[\frac{LRR_o^2}{CgHF}\right]\frac{Q}{C_p}=0 \qquad (13)$$

Dividing by the additional R_o renders (13) into the same order of magnitude as the other dynamic equations of MODEL II. In addition, it can be shown that the two terms that include T_R combine to form the static stability,

$$\sigma_\sigma=\frac{R_o^2}{F}\left[\frac{\partial T_R'}{\partial \sigma}-q_3\frac{R}{C_p}T_R'\right] \qquad (14)$$

Therefore, the thermodynamic equation reduces to

$$R_o\left[\frac{\partial T}{\partial t}+m\left(u\frac{\partial T}{\partial x}+v\frac{\partial T}{\partial y}+\dot{\sigma}\left(\frac{\partial T}{\partial \sigma}-\frac{R}{C_p}Tq_3\right)\right)\right]$$
$$+\dot{\sigma}\sigma_\sigma-\left[\frac{LRR_o^2}{CgHF}\right]\frac{Q}{C_p}-R_oq_4\omega_s\frac{R}{C_p}\left(\frac{R_o}{F}T_R+T\right)=0 \qquad (15)$$

Next, the thermodynamic equation is converted to finite differences and made compatible with the Arakawa D-grid finite difference template developed for MODEL I (Achtemeier, et al., 1986). Fig. 1 shows the template with the locations of the variables that appear in the thermodynamic equation. Note that the local tendency of temperature has been defined as the dependent and adjustable variable, E_T. The finite difference version of the thermodynamic equation is,

$$
\begin{aligned}
& R_o [E_T + (\overline{m})^{xy} (\overline{u})^{x\sigma} (\overline{T_x})^{y} + (\overline{m})^{xy} (\overline{v})^{y\sigma} (\overline{T_y})^{x} \\
& + \dot{\sigma} [(\overline{T_\sigma})^{xy\sigma} - \frac{R}{C_p} (\overline{q_3})^{xy} (\overline{T})^{xy}]] + \sigma_o \dot{\sigma} \\
& - R_o (\overline{q_4})^{xy} \omega_s \frac{R}{C_p} [\frac{R_o}{F} (\overline{T_R}) + (\overline{T})^{xy}] - [\frac{LRR_o^2}{CgHF}] \frac{Q}{C_p} = 0
\end{aligned}
\tag{16}
$$

where the various overbar averages are defined in Achtemeier, et al., (1986).

3. MODEL II. Variational Equations

The variational analysis melds data from various measurement systems at the second stage of a two-stage objective analysis. All data are gridded independently in the first stage and are combined in the second stage. The gridded observations to be modified are meshed with the dynamic constraints through Sasaki's (1970) variational formulation which requires the minimization of the integrand of an adjustment functional. Now it is not necessary to reproduce the full derivation of MODEL I plus the thermodynamic

equation in order to get MODEL II. Each term of the equations is a linear combination with the other terms. Therefore, all that is required is to perform the variational operations upon the thermodynamic equation and add the resulting terms to the appropriate adjustment equations of MODEL I. Let,

$$I=2\lambda_5 m_5+\pi_8 (E_T-E_T^o)^2 \tag{17}$$

where π_8 is the precision modulus weight for the temperature tendency and m_5 is equation (16). Performing the variations upon each of the dependent variables that appear in the thermodynamic equation yields the following terms to be added to the respective variational equations.

$$\delta E_T=\pi_8 (E_T-E_T^o)+R_o\lambda_5=0 \tag{18}$$

$$\delta u=R_o(\overline{m})^{y}(\overline{\lambda_5(\overline{T_x})^{y}})^{x\sigma} \tag{19}$$

$$\delta v=R_o(\overline{m})^{x}(\overline{\lambda_5(\overline{T_y})^{x}})^{y\sigma} \tag{20}$$

$$\delta\dot{\sigma}=R_o\lambda_5\left[(\overline{T_\sigma})^{xy\sigma}-\frac{R}{C_p}(\overline{q_3})^{xy}(\overline{T})^{xy}\right]+\lambda_5\sigma_\sigma \tag{21}$$

$$\begin{aligned}\delta\overline{T}=&-R_o\left[(\overline{m})^{x}(\overline{u})^{x}(\overline{\lambda_5})^{y\sigma}\right]_x-R_o\left[(\overline{m})^{y}(\overline{v})^{y}(\overline{\lambda_5})^{x\sigma}\right]_y\\&-R_o\left[(\dot{\overline{\sigma}}\overline{\lambda_5})^{xy\sigma}\right]_\sigma-R_o\frac{R}{C_p}\left[(\dot{\overline{\sigma}}\overline{\lambda_5})^{xy}q_3+(\overline{\omega_s\lambda_5})^{xy}q_4\right]\end{aligned} \tag{22}$$

Table 1 summarizes the modifications of the existing MODEL I equations that are required to implement MODEL II. The first column labeled "variable referenced" locates the variable in the grid templet shown in Fig. 1 to which the new terms are referenced. For example, the new terms to be added to the existing function F_1 (first line in Table 1) are calculated for the location of u in Fig. 1. Also included are two new equations, the latter being the thermodynamic equation. This brings to 13 the number of linear and nonlinear equations to be solved.

4. MODEL II: Evaluation

The purpose of this section is to demonstrate whether MODEL II performs as predicted by theory. In our evaluation of the variational assimilation models, we have used three criteria which have found use in the verification of diagnostic analyses (Krishnamurti, 1968; Achtemeier, 1975; Otto-Bliesner, et al., 1977). These criteria are measures of, first, the extent to which the assimilated fields satisfy the dynamical constraints, second, the extent to which the assimilated fields depart from the observations, and third, the extent to which the assimilated fields are realistic as determined by pattern recognition. The last criterion requires that the signs, magnitudes, and patterns of the hypersensitive vertical velocity and local tendencies of the horizontal velocity components be physically consistent with respect to the larger scale weather systems.

The strong constraint formalism requires that the dynamical constraints; the nonlinear horizontal momentum equations, the hydrostatic equation, an integrated form of the continuity equation, and the thermodynamic equation be satisfied exactly (to within truncation). Therefore, it is appropriate that the first evaluation of the variational model determine whether indeed the adjusted fields of meteorological variables are solutions of these physical equations.

In solving the Euler-Lagrange equations, we substituted observed or previously adjusted variables into the nonlinear terms and other terms that are products with the Rossby number or are higher order terms and treated these terms as forcing functions. This approach made the linearized equations easier to solve but several cycles with the forcing terms updated with newly adjusted variables were required for the method to converge to a solution.

The technique for determining whether the method converges to a solution is as follows. First, we note that any variable is found from the algebraic sums of all other terms of an equation. Thus the residual obtained by substituting variables back into the equation will be identically zero - the equation is satisfied exactly. This does not mean that the variational method has converged. Entirely different values for all of the variables may be found at the next cycle. Therefore, the adjusted variables are averaged over two successive cycles. Then the averaged variables are reintroduced into the dynamic constraints. Residuals are computed as remainders of algebraic sums of the terms of each

constraint. The root-mean-squares (RMS) of these differences (Glahn and Lowry, 1972) vanish when variables at two successive cycles are unchanged. When this happens, the constraints are satisfied and the method has been judged to converge to a solution. A convenient measure of how rapidly the method is converging to a solution is the percent reduction of the initial unadjustment given by,

$$\Delta r(\%) = 100\left(1 - \frac{r^{o} - r^{\tau}}{r^{o}}\right) \qquad (23)$$

The performance of MODEL II is assessed through the percentage reductions in the RMS differences from the initial unadjustments through the first four cycles of the solution sequence. The calculations are done for the eight adjustable levels in the model. Table 2 shows the percentages for the two nonlinear horizontal momentum equations. These results compare favorably with the MODEL I percentage residual reductions. The initial unadjustments are approximately halved at each cycle to about 90 percent after four cycles.

The percentage reductions of the initial unadjustment for the integrated continuity and hydrostatic equations are shown in Table 3. The RMS differences for the integrated continuity equation are reduced by from 96 to 99 percent at the second cycle and improve slowly to near 100 percent by the fourth cycle. These improvements are, of course, dependent upon the magnitudes of the initial unadjustment. We set the initial vertical velocity to zero. Then

the initial unadjustment is equal to the divergence integrated upward. The MODEL I cyclical solution order subjects the adjusted velocity components to a second adjustment to satisfy the integrated continuity equation. In this case, the averages of the adjusted velocity components are just averages of two solutions of the integrated continuity equation. Therefore the unadjustment should approach zero by the second cycle.

The initial unadjustments for the hydrostatic equation at levels 4 through 8 are halved at each cycle and the percentage reduction increases to near 94 percent by the fourth cycle. Convergence is much slower at levels 1 and 2. There is a 65 percent reduction in the initial unadjustment at the second cycle at level 2. There is no change during the third cycle and a slight increase in the initial unadjustment is observed at cycle 4. Given that the only difference between the adjustments presented here and the adjustments presented for MODEL I is the introduction of the fifth constraint, we are led to suspect that the degradation is directly related to the thermodynamic equation.

Table 4 gives the percentage reductions of the initial unadjustment for the thermodynamic equation. Negative percentages occur where the RMS differences exceed the initial unadjustment. Table 4 shows that the initial unadjustment was reduced by nearly 90 percent by the fourth cycle at levels 2 and 9. At the remaining levels, first cycle reductions of from 48 to 63 percent were followed by increases in the RMS differences that by the fourth cycle exceeded the initial unadjustment at levels 6 and 7.

Further analysis of the behavior of the convergence of MODEL II has revealed the following:

1. The breakdown in the assimilation was almost exclusively in temperature. The initial unadjustments in the horizontal momentum equations and the continuity equation were reduced as was done with MODEL I. Only the first two levels in the hydrostatic equation showed any response to the temperature unadjustment and this was somewhat unexpected given that the most severe departures from convergence in the thermodynamic equation occurred at higher levels.

2. The patterns of winds and heights generated by MODEL II (not shown) were unchanged from the winds and heights generated by MODEL I. The pattern analysis was an additional confirmation that the breakdown in convergence in MODEL II was largely confined to the thermodynamic equation.

3. The initial unadjustment in the thermodynamic equation was found to be approximately an order of magnitude larger than the initial unadjustments for the other dynamic constraints and was approximately two orders of magnitude larger in the stratosphere. Although this is not the cause for the breakdown in convergence, it does show that a gross imbalance existed in the initial gridded fields of meteorological variables when those variables were substituted into the thermodynamic

equation.

4. Analysis of the patterns of the residuals remaining after the fourth pass found that they were almost identical to the patterns of vertical velocity.

Our analysis of the large RMS differences in the thermodynamic equation remaining after four cycles reveals the following concerning how the initial and adjusted vertical velocity adversely impacted upon the analyses. First, the initial vertical velocity was calculated kinematically and subjected to the variational adjustment by O'Brien (1970). This method can transfer error from the lower levels into the upper levels of the troposphere and generate large and noisy vertical velocity patterns there. Furthermore, there is no consideration given for the change in static stability between the troposphere with its relatively large vertical velocities and the stratosphere with its relatively small vertical velocities. The kinematic vertical velocities were unrealistically large in the stratosphere and, when coupled with the large static stability, produced large and uncompensated terms in the thermodynamic equation. Therefore, the magnitudes of the initial unadjustments were approximately two orders of magnitude larger than were the initial unadjustments for the other dynamical constraints.

Second, further theoretical analysis has revealed that the adjustment for the divergent part of the wind is the "weak link" in

this variational assimilation model. First order terms that contain the divergence adjustment cancel out in the cyclical solution formulations. The divergence adjustment must then be carried in second order terms and through other variables. Our solution for this problem has been to require the adjusted horizontal velocity components to satisfy the continuity equation constraint after each cycle, a variational model within a variational model, then allow for the second order terms and the readjusted velocity components to "nudge" the solution toward the desired dynamic balance. The result was that the RMS differences grew after the first cycle when the vertical velocity was released to converge slowly toward another equilibrium.

5. Coupling the Vertical Velocity in MODEL I.

In this section, we propose solutions for the vertical velocity related problems of very large initial unadjustments for the thermodynamic equation and the buildup of RMS differences in MODEL II.

The solution for the problem of very large initial unadjustments in the thermodynamic equation is the implementation of a blended vertical velocity algorithm such as the variational method presented by Chance (1986). This method, developed as part of this variational assimilation project but not included in the version of MODEL II evaluated as part of this study, blends the divergence of the horizontal wind with the vertical velocity

calculated from the adiabatic method. The relative weighting given the horizontal and the vertical velocity is a function of the stability, relative humidity, and satellite observed cloud cover. The divergence of the horizontal wind receives the greatest weight when the conditions of low stability, near saturation, or dense cloud cover at levels with near saturation prevail. The adiabatic vertical velocity receives greatest weight at locations where stability is high. Division by large stability reduces the magnitude of the vertical velocity in the stratosphere and forces the vertical velocity to near zero at the tropopause rather than at the arbitrarily defined top of the model domain.

The formula for the modified vertical velocity is

$$\dot{\sigma}_M(k) = \frac{\dot{\sigma}_M(k-1) + D(k)\,\Delta\sigma + a\dot{\sigma}_T(k)}{1-a} \qquad (24)$$

The modified vertical velocity at level k is the weighted sum of the modified vertical velocity at level k-1 plus the incremental vertical velocity obtained through the continuity equation and the vertical velocity obtained by the adiabatic method. The weight, a, carries the theoretical relative accuracies of the two methods for calculating vertical velocity as obtained through standard errors of observation for the observed variables. The weight also carries the relative importance of the vertical velocities as determined by meteorological considerations. For example, the adiabatic vertical velocities are assigned the greatest weight in the stratosphere because the adiabatic method carries information regarding static stability,

$$\sigma_o = \left(\frac{\partial}{\partial\sigma} - \frac{R}{c_p} q_3\right)\left(T + \frac{R_o}{F} T_R\right) \qquad (25)$$

However, in the lowest layers of the analysis domain, a=0 to account for the near adiabatic conditions within the planetary boundary layer.

Preliminary studies with the blended vertical velocity show that large magnitude centers of either sign developed by the kinematic method in the upper troposphere and lower stratosphere are reduced or eliminated. Therefore the large initial unadjustments that exist because of the use of the kinematic vertical velocities will be reduced or eliminated also.

The solution for the problem of buildup of RMS differences in MODEL II is to reformulate the MODEL I variational equations so that the solution sequence will better couple the vertical velocity with the dynamic adjustment. Achtemeier, et al. (1986) have shown that the derivations in MODEL I required to reduce the number of dependent variables and equations to a single diagnostic equation in geopotential cancel out the zero order divergence adjustment terms. The adjustment of the divergent part of the wind is therefore forced into higher-order nonlinear terms which do not sufficiently impact upon the final adjustment to bring about compatibility with the continuity equation. The continuity equation was satisfied through the second variational step which forced an adjustment of the adjusted velocity components. The

problem was that the two variational steps could not be connected in a way that allowed adjustments required for satisfaction of the thermodynamic equation to feed back to the continuity equation.

This analysis of MODEL II reveals that the second variational step must be eliminated and the coupling of the vertical velocity with the remainder of the adjusted variables must be part of a single variational model. It was found that the divergent part of the wind obtained from the first step adjustment is a function of the nonlinear terms of the horizontal momentum equations. If F_5 represents the nonlinear terms of the u-component equation and F_6 represents the nonlinear terms of the v-component equation, then the horizontal momentum equations can be expressed as

$$m_1 = -v + \frac{\partial \phi}{\partial x} + F_5 = 0 \tag{26}$$

$$m_2 = u + \frac{\partial \phi}{\partial y} + F_6 = 0 \tag{27}$$

Forming the divergence from (23) and (24) and integrating through the depth of the analysis domain gives

$$\int (u_x + v_y)\, d\sigma = -\int (F_{6x} - F_{5y})\, d\sigma = 0 \tag{28}$$

Equation (25) is an integral of the vorticity equation. The constraint upon the divergent part of the wind, and hence the vertical velocity, that must be satisfied in order for all MODEL I dynamic constraints to be satisfied is as follows. A particular

solution of the vorticity equation must integrate to zero at the top of the model domain - the particular solution being that the divergent component of the same adjusted wind field must also satisfy the integrated continuity equation.

The incorporation of the integrated vorticity equation into the variational formalisms is the subject of MODEL IIB derived in Chapter III.

Acknowledgements

This research was supported by the National Aeronautics and Space Administration (NASA) under Grant NAG8-059. The programming efforts of Mrs. Julia Chen are gratefully acknowledged.

REFERENCES

Achtemeier, G. L., 1979: Evaluation of a variational initialization method. Preprints, 4th Conf. Num. Wea. Pred., Amer. Meteor. Soc. 1979, 1-8.

_____, 1975: On the Initialization problem: A variational adjustment method. Mon. Wea. Rev., 103, 1090-1103.

_____, H. T. Ochs, III, S. Q. Kidder, R. W. Scott, J. Chen, D. Isard, and B. Chance, 1986: A variational assimilation method for satellite and conventional data: Development of basic model for diagnosis of cyclone systems. NASA Con. Rept. 3981, 223 pp.

Anthes, R. A., and T. T. Warner, 1978: Development of hydrodynamic models suitable for air pollution and other mesometeorological studies. Mon. Wea. Rev., 106, 1045-1078.

Chance, B. A., 1986: Application of satellite data to the variational analysis of the three dimensional wind field. NASA Con. Rept. 4022, 86 pp.

Courant, R., 1936: Differential and Integral Calculus, Vol. 2, (E. J. McShane, translator), Wiley - Interscience, p198.

Glahn, H. R., and D. A. Lowry, 1972: The use of model output statistics (MOS) in objective weather forecasting. J. Appl. Meteor., 11., 1203-1211.

Krishnamurti, T. N., 1968: A diagnostic balance model for studies of weather systems of low and high latitudes. Rossby number less than one. Mon. Wea. Rev., 96, 197-207.

O'Brien, J.J., 1970: Alternative solutions to the classical vertical velocity problem. J. Appl. Meteor., 9, 197-203.

Otto-Bliesner, B., D. P. Baumhefner, T. W. Schlatter, and R. Bleck, 1977: A comparison of several data analysis schemes over a data-rich region. Mon. Wea. Rev., 105, 1083-1091.

Sasaki, Y., 1970: Some basic formalisms in numerical variational analysis. Mon. Wea. Rev., 98, 875-883.

FIGURE CAPTIONS

Fig. 1. The grid template for the variational assimilation model.

Table 2. Percent reduction of the initial unadjustment in the horizontal momentum equations after 4 cycles.

Cycle No.	Level 2	3	4	5	6	7	8	9
				u-component				
0	0	0	0	0	0	0	0	0
1	54	54	52	51	50	50	51	51
2	81	78	77	75	74	75	76	76
3	92	89	87	86	86	87	87	87
4	94	93	90	89	91	91	90	90
				v-component				
0	0	0	0	0	0	0	0	0
1	54	53	52	53	51	51	50	50
2	78	80	77	80	77	76	76	73
3	88	89	87	90	88	88	87	84
4	93	92	91	92	91	91	91	88

Table 3. Percent reduction of the initial unadjustment in the integrated continuity and hydrostatic equations after 4 cycles.

Cycle No.	Level 2	3	4	5	6	7	8	9
				Integrated Continuity				
0	0	0	0	0	0	0	0	0
1	-	-	-	-	-	-	-	-
2	97	98	98	99	99	99	99	99
3	96	98	98	99	99	99	99	99
4	96	98	99	99	99	99	99	99
				Hydrostatic				
0	0	0	0	0	0	0	0	0
1	51	50	50	50	50	50	50	50
2	73	65	75	75	75	75	75	75
3	83	65	88	88	88	88	88	88
4	86	62	94	94	94	94	94	94

Table 4. Percent reduction of the initial unadjustment in the thermodynamic equation after 4 cycles.

Cycle No.	Level 2	3	4	5	6	7	8	9
				Thermodynamic Equation				
0	0	0	0	0	0	0	0	0
1	54	60	62	63	61	63	63	48
2	81	80	74	55	24	39	76	72
3	89	73	61	32	-12	9	62	83
4	88	65	50	14	-38	-12	49	89

Table 1. Modifications to variational equations in MODEL 1 to obtain MODEL 2.

Variable Referenced	Existing Function	New Terms to be Added
u	F_1	$R_o(\overline{m})^{y}(\overline{\lambda_5(\overline{T_y})^{y}})^{x\sigma}$
v	F_2	$R_o(\overline{m})^{x}(\overline{\lambda_5(\overline{T_y})^{x}})^{y\sigma}$
$\dot{\sigma}$	F_3	$\lambda_5\sigma_\sigma+R_o\lambda_5[(\overline{T_\sigma})^{xy\sigma}-\frac{R}{C_p}(\overline{q_3})^{xy}(\overline{T})^{xy}]$
$\overline{T}$	*Eq 34 p 39 Achtem.etal 1986*	$F_8=-\{[(\overline{m})^{x}(\overline{u})^{x}(\overline{\lambda_5})^{y\sigma}]_x+[(\overline{m})^{y}(\overline{v})^{y}(\overline{\lambda_5})^{x\sigma}]+[(\overline{\sigma\lambda_5})^{xy\sigma}]_\sigma+\frac{R}{C_p}[(\overline{\sigma\lambda_5})^{xy}q_3+(\overline{\omega_s\lambda_5})^{xy}q_4]\}$
$\overline{T}$	*Eq 47 p 41 Achtem.etal 1986*	F_8/γ
$\dot{\sigma}$	*New Equation*	$\lambda_5=-\frac{\pi_8}{R_o}(E_T-E_T^o)$
$\dot{\sigma}$	*New Equation*	$E_T=-\{[(\overline{m})^{xy}(\overline{u})^{x\sigma}(\overline{T_x})^{y}+(\overline{m})^{xy}(\overline{v})^{y\sigma}(\overline{T_y})^{x}]+\dot{\sigma}[(\overline{T_\sigma})^{xy\sigma}-\frac{R}{C_p}(\overline{q_3})^{xy}(\overline{T})^{xy}]+\frac{\sigma_\sigma}{R_o}\dot{\sigma}-(\overline{q_4})^{xy}\omega_s\frac{R}{C_p}[\frac{R_o}{F}\overline{T_R}+(\overline{T})^{xy}]\}$

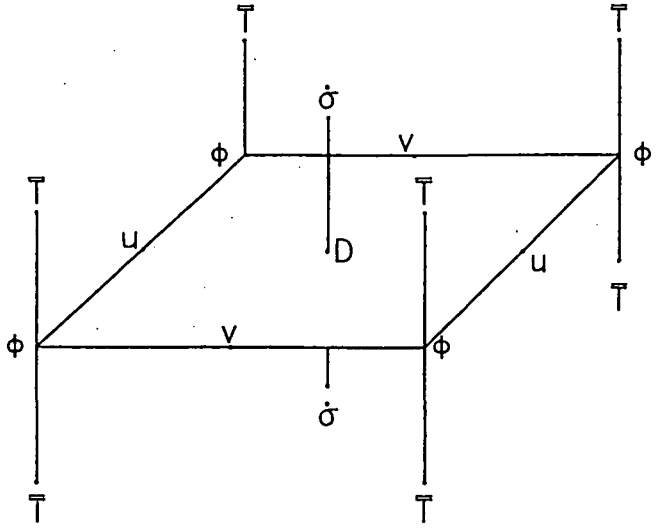

Fig. 1. The grid template for the variational assimilation model.

Chapter III

A Variational Assimilation Method for Satellite and Conventional Data: A Revised Basic Model IIB

Gary L. Achtemeier, Robert W. Scott, and J. Chen
Office of Climate and Meteorology
Division of Atmospheric Sciences
Illinois State Water Survey
Champaign, Illinois 61820

ABSTRACT

A variational objective analysis technique that modifies observations of temperature, height, and wind on the cyclone scale to satisfy the five "primitive" model forecast equations is presented. This analysis method overcomes all of the problems that hindered previous versions - problems such as over-determination, time consistency, solution method, and constraint decoupling. A preliminary evaluation of the method shows that it converges rapidly, the divergent part of the wind is strongly coupled in the solution, fields of height and temperature are well-preserved, and derivative quantities such as vorticity and divergence are improved. Problem areas are systematic increases in the horizontal velocity components, and large magnitudes of the local tendencies of the horizontal velocity components. The preliminary evaluation makes note of these problems but detailed evaluations required to determine the origin of these problems await future research.

1. Introduction

This study was designed to determine the feasibility of a constrained objective analysis based upon the variational methodology of Sasaki (1958, 1970). The method uses as dynamic constraints the five primitive equations for a dry, adiabatic, and non-viscous atmosphere: the two nonlinear horizontal momentum equations, the continuity equation, the hydrostatic equation and the thermodynamic equation. The method is diagnostic, however

given the similarities between the dynamic constraints and the hydrodynamical equations of numerical prediction models, there exists a potential for extension of the technique to the derivation of initial fields for numerical models.

The potential of the variational methods for multivariate objective analyses has been explored with many dynamic constraints. Some of the studies and the constraints used are: the geostrophic approximation (Sasaki, 1958), the continuity equation (O,Brien, 1970; Dickerson, 1978; Sherman, 1978; Ray et al., 1978), divergence and vorticity (Schaefer and Doswell, 1979), the balance equation (Stephens, 1970), the two horizontal momentum equations (Lewis and Grason, 1972; Bloom, 1983), the two horizontal momentum and hydrostatic equation (Lewis, 1972), and the two horizontal momentum, thermodynamic, and hydrostatic equations (Achtemeier, 1975).

Past attempts to develop a multivariate objective analysis based upon Sasaki's variational method with the five "primitive" equations as dynamical constraints have encountered several fundamental problems. Courant (1936) showed that the number of subsidiary conditions (dynamic constraints) must be at least one less than the number of adjustable dependent variables else the problem is overdetermined and a solution is not guaranteed. The over-specification problem must be solved as the five primitive equations form a closed set with five dependent variables.

The Euler-Lagrange operations yield local tendencies of the Lagrange multipliers if the local tendencies of the temperature or

the horizontal velocity components are explicit in the dynamic constraints. Boundary conditions for these terms are unknown. The problem of time consistency in variational problems has been explored by Lewis (1980, 1982) and Lewis et al (1983). More recently, the time consistency problem has been found more tractable through use of the adjoint method (Lewis and Derber, 1985; Talagrand and Courtier, 1987).

Achtemeier (1975) found that the Euler-Lagrange equations decoupled the divergent part of the wind from the remainder of the adjustment with the result that the continuity equation was not satisfied. Attempts to constrain the local tendencies of velocity and temperature to require exact solution of the continuity equation did not solve the coupling problem (Achtemeier, 1979).

The methodology to circumvent the above problems and the theoretical development of a primitive equation variational objective analysis is presented in the next section (mathematical details are presented in Appendices A, B,and C.) The method is evaluated in Section 3.

2. Theoretical Development

The objective analysis is designed for a terrain-following coordinate surface. We used a nonlinear vertical coordinate created from two functions that are piecewise continuous through the second derivatives. In this coordinate system, all coordinate surfaces above a reference pressure level are pressure surfaces.

The dynamical equations appear in their simplest form in pressure coordinates. Furthermore, hydrostatic truncation errors are confined to coordinate surfaces below the reference pressure level. The problems of reducing hydrostatic truncation error along terrain-following coordinate surfaces has been the subject of considerable investigation (Kurihara, 1968; Gary 1973; Sundqvist, 1975, 1976; Janjic, 1977, 1989, and Achtemeier, 1990). The vertical coordinate is described in Appendix A.1.

Subjecting the pressure gradient terms of the horizontal momentum equations written in terrain-following coordinates to the variational operations separates the two pressure gradient terms and combines the large, now uncompensated terms with terms from the other equations. These uncompensated terrain terms can dominate the adjustment. A test found that these terms generated large error that caused the variational method to diverge.

The pressure gradient problem was solved by nondimensionalizing the dynamic constraints (Charney, 1948; Haltiner, 1971) and partitioning the hydrostatic terms to isolate the terrain part so that the variational adjustment could be performed on the meteorological partition. Appendix A.2 presents details of this procedure.

As regards the time consistency problem, Fjortoft (1952) found that the local change in the winds could be approximated by the translation of a weather system along an advective or steering current, usually a smoothed middle tropospheric wind. Therefore, the local tendencies of the velocity components were partitioned

into advective components, represented by the steady part of a weather system moving within a steering current, and developmental components, represented by the development of a weather system. Appendix A.3 describes the partition. The developmental components of u and v were defined as dependent variables to be subjected to the variational adjustment.

Appendix A.4 gives the five dynamic constraints as modified. Abridged forms of these equations are as follows:

$$M_1 = -v + \phi_x + DTU + HAU + VAU + EXT(M_1) = 0 \qquad (1)$$

$$M_2 = u + \phi_y + DTV + HAV + VAV + EXT(M_2) = 0 \qquad (2)$$

$$M_3 = Q(u_x + v_y)\Delta\sigma + (\dot{\sigma} - \dot{\sigma}_o) + EXT(M_3) = 0 \qquad (3)$$

$$M_4 = -\phi_\sigma + \gamma T + EXT(M_4) = 0 \qquad (4)$$

$$M_5 = LTT + HAT + VAT + VVT + \dot{\sigma}\sigma_\sigma + EXT(M_5) = 0 \qquad (5)$$

Conventional symbols are used. Abridged terms are defined as follows:

DTU(V) = developmental component of local tendency of u or v.

LTT = local tendency of T.

HAU(V or T) = horizontal advection of u (v or T) relative to a moving weather system.

VAU(V or T) = vertical advection of u (v or T).

VVT = product of vertical velocity with perturbations of stability.

$EXT(M_i)$ = extra terms that arise from any of the following sources:

a) Lambert conformal map image projection,

b) conversion into the nonlinear vertical coordinate,

c) expansion of the Coriolis and/or map scale factors.

Q = a normalized pressure thickness weight that arises from (b) above. For pressure levels above 700 mb, Q = 1.

The fourth term on the right hand side of (5) is the product of the layer average static stability with the vertical velocity.

These equations have been nondimensionalized and terms expressed in powers of the Rossby number. All terms identified by three letters (eg., LTU or EXT) are higher order terms - either multiplied by the Rossby number or of order 0.1 or terms that involve unadjusted (observed) variables.

Dependent variables are u, v, Φ, σ, T, ϵ_u, and ϵ_v. The latter two variables are the developmental components of the local tendencies of u and v. This formulation leaves five constraints and seven variables to be adjusted.

Following Achtemeier (1975), a variational objective analysis was developed for adjustments of the seven dependent variables subject to exact satisfaction of the dynamic constraints (1)-(5). As expected, the addition of the two new dependent variables (the developmental components of u and v) was sufficient to overcome the over-specification problem. As regards the time consistency problem, recomposition of the local tendencies of u and v from the advective and developmental components yielded tendencies that

compared favorably with observed 3-h changes in u and v. However, the decoupling problem remained. Attempts to readjust the divergent part of the wind by requiring the adjusted horizontal velocity components to satisfy the continuity equation through a "variational adjustment within a variational adjustment" were unsuccessful in satisfying all five constraints.

An analysis of the growth of the divergent part of the adjusted wind was performed to determine how the variational solution decoupled from the continuity equation. It was found that the divergent part of the wind is determined by adjustments through the higher order terms (HOT) of (1) and (2). The divergent components can be made to satisfy the continuity constraint if these higher order terms are made to satisfy a particular solution of the vorticity theorem. Define

$$F_5 = HOT(M_1) \tag{6}$$

$$F_6 = HOT(M_2) \tag{7}$$

so that,

$$M_1 = -v + \phi_x + F_5 = 0 \tag{8}$$

$$M_2 = u + \phi_y + F_6 = 0 \tag{9}$$

Forming the divergence,

$$u_x+v_y+F_{6x}-F_{5y}=0 \tag{10}$$

The function that must integrate to zero is

$$\int (u_x+v_y)\, d\sigma-\int (F_{6x}-F_{5y})\, d\sigma=0 \tag{11}$$

for the vertical velocity to vanish at the top at the top of the domain. Therefore, (11) is a particular solution of the integrated vorticity theorem, the particular solution also requiring that the horizontal divergence integrate to zero, a requirement for satisfaction of the continuity equation.

It is necessary to build (11) into the dynamic constraints if the decoupling problem is to be eliminated from the variational objective analysis. Define F_5 and F_6 as dependent variables and revise the dynamic constraints as follows:

$$M_1=-F_5+DTU+HAU+VAU+EXT(M_1)=0 \tag{12}$$

$$M_2=F_6+DTV+HAV+VAV+EXT(M_2)=0 \tag{13}$$

$$M_3=Q(F_{6x}-F_{5y})\,\Delta\sigma+(\dot{\sigma}-\dot{\sigma}_o)+EXT(M_3)=0 \tag{14}$$

$$M_4=\phi_\sigma+\gamma T+EXT(M_4)=0 \tag{15}$$

$$M_4 = LTT + HAT + VAT + VVT + \dot{\sigma}\sigma_\sigma + EXT(M_5) = 0 \tag{16}$$

$$M_6 = -v + \phi_x + F_5 = 0 \tag{17}$$

$$M_7 = u + \phi_y + F_6 = 0 \tag{18}$$

The variational objective analysis is developed from these seven constraints. The nine adjustable variables include the original seven plus F_5 and F_6.

The dynamical constraints are written on centered differences on an Arakawa D-grid (Mesinger and Arakawa, 1976). The finite difference operators and finite averaging operators are defined following Anthes and Warner (1978). The conversion of the constraints from differential form into finite differences is given in Appendix B.

The gridded fields of meteorological data to be modified are meshed with the dynamical equations through Sasaki's (1970) variational operations. To simplify the derivations, the frictional terms in the horizontal momentum equations and the diabatic heating term in the thermodynamic equation were set to zero.

The finite difference analog of the adjustment functional is,

$$\tilde{F} = \Delta x \Delta y \sum_i \sum_j a_i b_j I_{i,j} \tag{19}$$

The integrand, $I_{i,j}$ is

$$
\begin{aligned}
I = & \pi_1 (u-u^o)^2 + \pi_1 (v-v^o)^2 + \pi_2 (\dot{\sigma}-\dot{\sigma}^o)^2 \\
& + \pi_3 (\phi-\phi^o)^2 + \pi_4 (T-T^o)^2 + \pi_5 (\phi_x-\phi_x^o)^2 \\
& + \pi_5 (\phi_y-\phi_y^o)^2 + \pi_6 (\phi_\sigma-\phi_\sigma^o)^2 + \pi_7 (\epsilon_u-\epsilon_u^o)^2 \\
& + \pi_7 (\epsilon_v-\epsilon_v^o)^2 + \pi_8 (\epsilon_T-\epsilon_T^o)^2 + \pi_9 (F_5-F_5^o)^2 \\
& + \pi_9 (F_6-F_6^o)^2 + 2\sum_{i-1}^{7} \lambda_i M_i
\end{aligned}
\tag{20}
$$

The weights, π_i, are Gauss' precision moduli (Whittaker and Robinson, 1926). The gridded initial variables (u^o, v^o, σ^o, Φ^o, T^o, $\epsilon_u{}^o$, $_v{}^o$, $F_5{}^o$, $F_6{}^o$) enter in a least squares formulation and receive π_i according to their relative accuracies. The strong constraints to be satisfied exactly are introduced through the Lagrangian multipliers, λ_i.

Objectively modified meteorological variables are determined by requiring the first variation on F to vanish. A necessary condition for the existence of a stationary set is that the functions are determined from the domain of admissible functions as solutions of the Euler-Lagrange equations. The variation is to be carried out at every point (r,s) within the grid. Thus, upon setting the weights $a_i = b_j = 1$ and differentiating the integrand (20) with respect to the arbitrary variable $\alpha_{r,s}$, the Euler-Lagrange operator in finite differences is

The Euler-Lagrange equations resulting from the operations

$$\frac{\partial I_{i,j}}{\partial \alpha_{r,s}} = I_{\alpha_{i,j}} \frac{\partial \alpha_{i,j}}{\partial \alpha_{r,s}} = I_{\alpha_{i,j}} \delta^{i}_{r} \delta^{j}_{s} = 0 \tag{21}$$

specified by (21) are given in Appendix C [(C.7)-(C.16)]. Including the seven dynamic constraints, these complete a closed set of 17 of linear and nonlinear partial differential and algebraic equations. Solutions are difficult to obtain by conventional methods. Achtemeier (1975) proposed a cyclical solution method that moves higher order terms and terms involving unadjusted (observed) variables into forcing functions. These forcing functions may be expressed with observed variables at the first cycle and with previously adjusted variables at higher cycles. Therefore the forcing functions are known at each cycle. This method of solution is valid for the latitudes and scales of motion for which the Rossby number is less than one.

Use of the cyclical solution method yields the following set of linear Euler-Lagrange equations:

$$M_3 = -q_5 (F_{6x} - F_{5y}) \Delta\sigma + (\dot{\sigma} - \dot{\sigma}_o) + q_5 F_7 \Delta\sigma = 0 \tag{22}$$

$$M_4 = \phi_\sigma + \gamma T + \beta = 0 \tag{23}$$

$$M_6 = -v + \phi_x + F_5 = 0 \tag{24}$$

$$M_7 - u + \phi_y + F_6 = 0 \tag{25}$$

$$\overline{\pi}_5^{xy}\nabla^2\phi + \overline{\pi}_6^{\sigma}\phi_{\sigma\sigma} + \pi_{5x}\overline{\phi}_x^x + \pi_{5y}\overline{\phi}_y^y + \pi_{6\sigma}\overline{\phi}_{\sigma}^{\sigma} - \pi_3\phi + \lambda_{5x} + \lambda_{6y} + \lambda_{4\sigma} + F_4 = 0 \tag{26}$$

$$\pi_1 u + \lambda_6 + F_1 = 0 \tag{27}$$

$$\pi_1 v - \lambda_5 + F_2 = 0 \tag{28}$$

$$\pi_2\dot{\sigma} + \lambda_3 + F_3 = 0 \tag{29}$$

$$\pi_4 T + \gamma\lambda_4 + F_8 = 0 \tag{30}$$

$$\pi_7(\epsilon_u - \epsilon_u^o) + R_o\lambda_1 = 0 \tag{31}$$

$$\pi_7(\epsilon_v - \epsilon_v^o) + R_o\lambda_2 = 0 \tag{32}$$

$$\pi_8(\epsilon_T - \epsilon_T^o) + R_o\lambda_7 = 0 \tag{33}$$

$$\pi_9(F_5 - F_5^o) - \lambda_1 + \lambda_5 - \Delta\sigma(q_5\overline{\lambda}_3^{\sigma})_y = 0 \tag{34}$$

$$\pi_9(F_6 - F_6^o) - \lambda_2 + \lambda_6 + \Delta\sigma(q_5\overline{\lambda}_3^{\sigma})_x = 0 \tag{35}$$

As shown in Appendix C, variables may be easily eliminated among the equations. There results three diagnostic equations in geopotential, vorticity, and divergence,

$$\left(\overline{\pi}_5^{xy} + \pi_1\frac{\pi_{11}}{\pi_{10}}\right)\nabla^2\phi + \left(\overline{\pi}_6^{\sigma} + \frac{\pi_4}{\gamma^2}\right)\phi_{\sigma\sigma} + \pi_{5x}\overline{\phi}_x^x + \pi_{5y}\overline{\phi}_y^y + \left(\pi_{6\sigma} + \frac{\pi_4}{\gamma^2}\right)\overline{\phi}_{\sigma}^{\sigma} - \pi_3\phi = -G_4 - \frac{\pi_1}{\pi_{10}}(G_{2y} - G_{3x}) \tag{36}$$

$$\pi_{10}\zeta - \pi_{11}\nabla^2\phi = G_{2y} - G_{3x} \tag{37}$$

$$\nabla^2 [(\Delta\sigma)^2 q_5^2 \pi_2 D] - \pi_{10} D = \nabla^2 G_1 + G_{2x} + G_{3y} \tag{38}$$

Details regarding symbol definition are found in Appendix C.

The variational theory specifies natural boundary conditions that are consistent with the Euler-Lagrange equations. If it is assumed that there are no adjustments in the data along the boundaries, then the boundary conditions may be specified. In the latter case, the Lagrange multipliers, λ_i, are zero at the boundaries and the initial unadjusted values are used for the boundary conditions.

Initially, the Euler-Lagrange equations were solved with specified boundary conditions. These boundary conditions forced high frequency waves into the solutions for the velocity components near the boundaries. Divergences calculated from these velocity components gave large erroneous vertical velocities. We therefore returned to the natural boundary conditions.

The Euler-Lagrange operator for natural boundary conditions is,

$$\frac{\partial I}{\partial\left(\frac{\partial f_i}{\partial x_j}\right)} = 0 \tag{39}$$

Performing the operation specified by (39) produces a set of Euler-Lagrange boundary equations in Φ, u, v, and D. Details of the derivations are given in Appendix D. The boundary conditions for Φ are,

$$\begin{aligned}(\pi_5+\frac{\pi_1\pi_9}{\pi_1+\pi_9})\phi_x-\pi_5\phi_x^o-\frac{\pi_1\pi_9}{\pi_1+\pi_9}(u^o-F_5^o)=0\\(\pi_5+\frac{\pi_1\pi_9}{\pi_1+\pi_9})\phi_y-\pi_5\phi_y^o+\frac{\pi_1\pi_9}{\pi_1+\pi_9}(u^o+f_6^o)=0\end{aligned} \tag{40}$$

The boundary conditions for u and v that are consistent with (40) are,

$$\begin{aligned}(\pi_5+\pi_1\frac{\pi_5+\pi_9}{\pi_9})v-\pi_5(\phi_x^o-F_5^0)-\pi_1\frac{\pi_5+\pi_9}{\pi_9}v^o=0\\(\pi_5+\pi_1\frac{\pi_5+\pi_9}{\pi_9})u+\pi_5(\phi_y^o+F_6^o)-\pi_1\frac{\pi_5+\pi_9}{\pi_9}u^o=0\end{aligned} \tag{41}$$

The derivation of (40) placed a constraint upon the boundary conditions for the divergence, namely, that the divergence must be specified along two rows or columns at the boundaries.

Subject to the boundary conditions and specification of the precision moduli, (36)-(38) may be solved for the geopotential, vorticity and divergence. Coefficients for the second order partial derivative terms are always positive, the equations are elliptic, and thus solutions by standard methods are assured. Then u and v must be retrieved from the vorticity and the divergence.

A number of investigators (Sangster, 1960; Hawkins and Rosenthal, 1965; Shukla and Saha, 1974; Schaefer and Doswell, 1979;

Lynch, 1988) have proposed methods for reconstruction of the velocity components from the vorticity and divergence (or streamfunction and velocity potential). After investigating several of these methods, including those of Endlich (1967) and Bjilsma et al. (1986), it was determined that the Lynch method could be best adapted to the Arakawa D-grid with a minimum of error in reconstructing the velocity components.

First, the field of divergence was modified by a small constant so that Gauss' theorem,

$$\iint_A D\,da = \oint_s V_n\,ds \tag{42}$$

was satisfied. Then the u-component was reconstructed through

$$\nabla^2 u = D_x - \zeta_y \tag{43}$$

subject to mixed boundary conditions in u (obtained from (41)) along the y-boundaries and u_y obtained along the x-boundaries from

$$u_y = v_x - \zeta \tag{44}$$

Then, beginning at the lower x-boundary with v from (41),

$$v_y = D - u_x \tag{45}$$

was solved to find v uniquely.

3. Case Study Description and Preprocessing of Data

The data used to test the variational objective analysis consisted of rawinsonde temperature, height, and wind data at standard National Weather Service reporting sites shown in Fig. 1 for a large part of the United States and parts of southern Canada on 12 GMT 10 April 1979 and 00 GMT 11 April 1979. This case was originally selected because microwave temperature soundings coexisted with special 3-hr rawinsonde data over a large area of the central United States (small dashed-line box in Fig. 1) during a major cyclogenesis. The 3-hr rawinsonde data were used as ground truth for the local tendencies of the velocity components and temperature diagnosed from the variational objective analysis.

The data at 12 GMT 10 April 1979 described a weak, dissipating short wave moving northward over the Central Plains in advance of a more vigorous short wave. At 00 GMT 11 April, an intense jet streak moved northeastward over Oklahoma and Texas and triggered a mesoscale convective system over northern Texas that produced a number of fatalities at Wichita Falls, Texas.

The data were gridded from the observations by a modification of the Barnes (1964) objective technique that is designed to minimize analysis error at the boundaries of the field of data (Achtemeier, 1986) and to provide accurate derivatives within the

interior of the domain (Achtemeier, 1989). The analyses were done for 10 levels from 1000 mb to 100 mb. The horizontal grid was a 40x25 array with a 100 km grid spacing. Then thermodynamic data were converted to the nonlinear vertical coordinate through a hydrostatically consistent interpolation downward from the reference pressure level of 700 mb to the terrain-following coordinate surfaces. In addition, a smoothed version of the 600 mb wind velocity components was obtained through a single pass of the objective interpolation designed to reproduce the long wavelength features inherent in the data. The smoothed wind field served as the advective wind in the calculation of the advective part of the local tendencies of the velocity components.

The above analyses produced gridded fields of temperature, height, and u and v wind components. The initial fields of vertical velocity, developmental components of the local tendencies and F_5 and F_6 must be estimated from these data. Letting

$$\epsilon_T = -km\left(u\frac{\partial T}{\partial x}+v\frac{\partial T}{\partial y}\right) \tag{46}$$

the adiabatic vertical velocity can be found by solving (B.10) for σ. Then an adjusted vertical velocity can be found by a variational formulation using the continuity equation (Chance, 1986) that is similar to the O'Brien (1970) method with the exception that compatibility between the divergence and the vertical velocity is forced at each level. The relative weight accorded to the adiabatic vertical velocity is directly

proportional to the static stability. Thus the adiabatic vertical velocity receives the greater weight in areas of higher stability such as the stratosphere. This procedure keeps large erroneous vertical velocities generated by divergence error from being transferred from the troposphere into the stratosphere where,in product with the static stability terms of (B.10), would produce large errors in the adjusted time derivatives of temperature.

We have no way of estimating the developmental components of the velocity component tendencies from data collected at a single time. Therefore, these fields were set to zero. An alternative, if available, would be local tendencies from a numerical model.

The forcing function variables, F_5 and F_6 are estimated by substituting the initial variables into (B.4) and (B.6). Then F_5 and F_6 were adjusted to satisfy (11) with the exception that the integral of the divergence was replaced by the adjusted vertical velocity.

The resulting fields (and selected derivative fields) of T, Φ, u, v, σ, ϵ_u, ϵ_v, F_5, and F_6 were designated as unadjusted fields and entered into the variational objective analysis through the functional integrand, I, given by (20). The unadjusted quantities were accorded precision modulus weights according to the formula,

$$\pi_i = \frac{G_i(x,y)}{2\sigma_i^2} \qquad (47)$$

where the σ_i is the root-mean-square (RMS) error of observation for the ith variable. G_i is in general a function of observation density but G≡1 for this study. However, since observational errors are available only for u, v, Φ, and T, only π_1, π_3, and π_4 can be obtained from (47). the σ_i for the remaining unadjusted quantities must be inferred from the known observational errors through the dynamic constraints or simplifications therefrom. These σ_i are given by,

$$\begin{aligned}
&\sigma_{\phi_x}=\sigma_{\phi_y}=\frac{\sqrt{2}\,\sigma_\phi}{\Delta S},\\
&\sigma_{\phi_\sigma}=\sigma_T\frac{\partial \ln(p)}{\partial\sigma},\\
&\sigma_{e_u}=\sqrt{2}\,\sigma_u\left[\frac{1}{(\Delta t)^2}-\frac{C^2}{(\Delta S)^2}+\frac{C}{\Delta t\Delta S}\right]^{\frac{1}{2}},\\
&\sigma_{\dot\sigma_k}=\frac{2\Delta\sigma}{\Delta S}\left[\sum_{j=1}^{k}(\sigma_{u_j})^2\right]^{\frac{1}{2}}
\end{aligned} \tag{48}$$

Here S is the average separation between observation sites.

In addition, $\pi_9 = \pi_1$ as terms such as the Taylor series expansion of the Coriolis parameter in product with the wind are considered equal in weight with the wind itself.

Table 1 shows the standard errors of observation for the winds, heights, and temperatures and the RMS errors for the other adjustable meteorological variables. Estimates for the scaler wind speed as functions of elevation angle of the balloon (Fuelberg, 1974) are given in the first two columns. The values for the 20

degree elevation angle compare favorably with the results from Hovermale's (1962) spectral decomposition of meteorological data. RMS values for heights and rawinsonde temperatures are from a composite of methods for estimating measurement error (Achtemeier, 1972).

Table 2 gives the nondimensional precision modulus weights calculated from the various functional relationships of the RMS errors from Table 1. The more accurately measured (estimated) variables receive larger values. Largest weights are accorded the geopotential height followed by the winds and temperatures. The developmental components of the local velocity tendencies receive the smallest weights.

Several modifications in the π_i given in Table 2 were made before the April 10-11 data were subjected to the variational objective analysis. First, the precision modulus weights for levels 9 and 10 of the vertical velocity were assigned large values to require the adjusted vertical velocity to vanish at the top of the domain. Second, the weights for the geopotential were reduced by a factor of 10 because prior studies gave solutions that were forced too strongly toward the geopotential. It is possible that, as a boundary condition, the geopotential has a greater impact upon the the solution than suggested by the magnitude of its precision modulus weight.

4. Evaluation of the Variational Assimilation Model

Three diagnostic criteria were used to evaluate the variational objective analysis. These criteria are, satisfaction of dynamical constraints, adjustment departures from observations, and pattern analysis.

a) Satisfaction of Dynamical Constraints

The method must converge regardless of how well the other criteria are satisfied. But some method must be developed that demonstrates that the analysis does converge. The Sasaki (1970) strong constraint formalism requires that the dynamical constraints; the nonlinear horizontal momentum equations, the hydrostatic equation, the continuity equation, and the thermodynamic equation be satisfied exactly (to within truncation). Recall that the cyclical solution method for solving the Euler-Lagrange equations required the substitution of observed or previously adjusted variables into the forcing functions. As a measure of progress toward convergence, at the end of each cycle, the adjusted variables were averaged with their respective values at the previous adjustment, reintroduced into the dynamical constraints and residuals calculated. It follows that the residuals decrease as the differences between adjusted variables at two successive cycles decrease. The residuals vanish (the

variational objective analysis converges) if the adjusted variables at two successive cycles are the same. A convenient measure of how rapidly the method is converging to a solution is the percent reduction of the initial unadjustment given by,

$$\Delta r(\%) = 100\left(1 - \frac{r^{o} - r^{\tau}}{r^{o}}\right) \qquad (49)$$

Fig. 2 shows how the reductions of the initial RMS differences for the two horizontal momentum equations varies for each pass through the cyclical solution sequence for the eight adjustable levels of the model. The residuals for the u-component momentum equation are approximately halved with each cycle through the fourth cycle. The solution stabilizes to near 99-100 percent reduction of the initial unadjustment except for a 97 percent reduction at the 9th level after eight cycles. The RMS differences for the v-component equation decrease at the first cycle and level off at the second cycle. These differences increase slightly at level 7. Then the residuals decrease monotonically through the eighth cycle with reductions of the initial unadjustment of from 98-99 percent (96 percent at level 9).

There were two reasons why the analysis was done through eight cycles. First, the objective of obtaining near 100 percent reduction in the RMS differences was accomplished for most levels. Second, regardless of the care taken in formulating consistent boundary conditions, there remained deleterious boundary effects that were drawn into the interior of the domain one grid space for

each cycle. The outer three rows of grid points were deleted from the evaluation statistics (see large dashed rectangle in Fig. 1). Therefore, the effects of the boundary conditions entered the evaluation area beginning at the fourth cycle.

The reductions of the initial unadjustment for the integrated continuity equation are shown in the left panel of Fig. 3. The rate of percentage reductions drops off after a large decline at the first pass but still reductions by the eighth pass were mostly between 97-99 percent. The slower convergence at level 9 (92 percent after 8 cycles) and also at level 9 for the horizontal momentum equations may have been the result of large adjustments of the divergent part of the wind required for mass consistency with small vertical velocities in the stratosphere.

The initial unadjustments for the hydrostatic and thermodynamic equations (middle and right panels of Fig. 3) monotonically decreased by about one half at each cycle. The percentage reductions of the RMS differences were mostly near 100 percent at all levels by the eighth cycle.

The satisfaction of constraints test shows that convergence toward a solution was obtained for all levels and for all five dynamic constraints. Therefore, MODEL IIB represents a significant advancement over the MODEL II.

b) Adjustment Departures from Observations

The transferral of the observations to the grid and the modification of the gridded data to satisfy the dynamical constraints is a two-step process. Information from the observations is not available to the second step. Therefore, there is an implicit assumption that the initial gridded fields correctly carry the phenomena described by the observations. This assumption is not strictly true and it is necessary to grid the data with sufficient accuracy so that analysis error does not dominate the first and second derivatives. We have modified the widely used Barnes (1964, 1973) method for gridding meteorological data to yield significant improvement in the accuracy of the gridded data and its derivatives (Achtemeier, 1986, 1989).

In the section under a) above, we showed that the variational objective analysis converges to a solution. Now we seek to find whether the variational method improved upon the unadjusted analysis by adjusting the fields to better fit the original observations.

Consider an "accuracy index" given by the solid lines in Fig. 4. We first calculated two sets of RMS differences, one between values from the unadjusted fields at observation locations and the observations and the second between the adjusted fields and the observations. Then we subtracted from these RMS differences the standard errors of observation for wind components, height, and

temperature listed in Table 1. This means that if the results are zero, the objective analysis has gridded the data to within the standard error of observation for the data. If the results are negative, then the objective analysis has produced a better fit to the observations. Positive values mean that the adjustments have, on the whole, departed farther from the observations than expected. In interpreting these results, it must be kept in mind that the mean winter standard observational error estimates taken from Hovermale's (1962) results do not exactly express the true observational error for this case. Thus, some small departure of either sign from given values should be expected.

The accuracy index for the unadjusted and adjusted heights and temperatures (Figs. 4a and 4b) were within acceptable limits. The index for the adjusted heights was displaced toward the positive, an indication that adjustments away from the observations were necessary to bring the fields into constraint satisfaction. The unadjusted fields of the horizontal velocity components were also within acceptable limits (Figs. 4c and 4d). However, above 800 mb, large positive values for the adjusted velocity components show that the variational analysis produced wind fields that were significantly different from the observations.

The dashed lines in Fig. 4 are the means of the differences between the unadjusted (adjusted) fields interpolated to the observation sites and the observations. Means near zero are expected unless systematic adjustment is required to achieve solution of the variational equations. Means were near zero for

the heights and the temperatures, except for temperatures near the tropopause between 300 mb and 200 mb where systematic adjustments were expected. The means were also near zero for the unadjusted velocity components. However, large systematic adjustments were found for the variationally adjusted velocity components (Figs. 4c and 4d). The u-components were increased on the average 6 m s^{-1} between 500 mb and 300 mb. The v-component systematic reduction was a linear function of pressure. The v-component was on the average decreased by approximately 8 m s^{-1} between 300 mb and 200 mb.

There was no systematic modification of the height fields that could be called upon to explain the adjustments in the velocity fields. An error in the mathematical derivation of the dynamic constraints or in the programming is suspected in these cases. The pattern analysis should provide further insight into the origin of these large systematic adjustments.

c) Pattern Analysis: 00 GMT 11 April 1979

Maps of heights, wind vectors, and temperatures were taken from selected levels within the domain of the variational objective analysis for 00 GMT, 11 April 1979, in order to interpret the statistical results presented in subsections a) and b). Comparisons were made between patterns in the unadjusted initial fields and the adjusted fields. The analyses were done on the synoptic scale however, we note that a mesoscale convective system was located within the high frequency observation area over parts of Texas and Oklahoma.

Heights at 60 m intervals and wind vectors at 300 km intervals are shown in Fig. 5 for 800 mb, 500 mb, and 300 mb. The convention for wind speed is: flag (25 m s^{-1}), barb (5 m s^{-1}), and short barb (2.5 m s^{-1}). At 800 mb, the circulation center has been displaced from its unadjusted location over northwestern Colorado to its adjusted location over eastern Colorado in better agreement with the center of lowest heights. Elsewhere, adjustments in both heights and winds at 800 mb were small (Fig. 6). At 500 mb (Fig. 5), the unadjusted analysis placed a weak short wave trough oriented eastward into Kansas from the parent trough. No trough appears in the wind field over Kansas. Thus, winds blow from high to low heights over Texas and Oklahoma and from low to high heights over Nebraska. The adjusted winds have been turned to more westerly in better agreement with the heights over Texas and

Oklahoma however, east of the Great Plains, the adjusted winds turn to blow toward higher heights. The same pattern of adjustment is also evident at the 300 mb jet stream level. The unadjusted analysis fits the winds with the height field. The adjusted analysis increases the wind speeds and turns the winds more westerly to blow toward higher heights.

The differences between the adjusted and unadjusted fields are shown in Fig. 6 for 500 mb and 300 mb. In general, the variational objective analysis decreased the heights over the northern states and increased the heights over the southern states. The 10 m adjustment over Oklahoma at 500 mb tended to lessen the sharpness of the short wave trough there. Elsewhere, heights were lowered 15-20 m over Montana.

Fig. 6 also shows that an average 5 m s^{-1} westerly component was added to the wind field at 500 mb and an average 10 m s^{-1} northwesterly component was added to the 300 mb wind field. This broad scale adjustment has no apparent relationship to either the height field adjustment or the synoptic weather pattern.

Fig. 7 shows fields of unadjusted and adjusted mean layer temperatures for 750 mb, 450 mb, and 250 mb. The unadjusted patterns at all levels have been preserved by the variational objective analysis. Temperature adjustments were less than one degree at 750 mb and 450 mb. The variational analysis cooled the 250 mb layer by an average of 2C. The unadjusted layer average temperature was too warm across the tropopause and the change was made to make the temperatures consistent with the heights.

The variational objective analysis modified height, temperature, and wind velocity for satisfaction of the dynamic constraints. We now assess how these adjustments have impacted upon derivative quantities such as vorticity, divergence, and vertical velocity that are derived from these basic fields. In addition, the local tendencies of the velocity components and temperature are determined from arithmetic sums of adjusted terms. Patterns of these sensitive variables must be physically realistic when compared with other data sets such as cloud fields, precipitation, and independent measurements of the variable.

Patterns of relative vorticity for the unadjusted and adjusted wind fields are shown in Fig. 8 for 500 mb. The variational objective analysis shifted the vorticity gradient, identifying the area of positive vorticity advection and upward vertical velocity, from over the Texas panhandle to over Oklahoma and Kansas, locations coincident with the mesoscale convective system. Elsewhere, there were only small differences between the unadjusted and adjusted vorticities.

A comparison of the 500 mb vertical velocity patterns (Fig. 9) shows that the variational objective analysis shifted the center of maximum vertical velocity eastward from the Texas panhandle to western Oklahoma in better agreement with the location of the mesoscale convective system located over central Oklahoma and north Texas. The variational analysis also weakened the subsidence area over Nebraska by 2 cm s^{-1}. The subsidence area over Louisiana and eastern Texas in the unadjusted vertical velocities was replaced by

2-4 cm s^{-1} rising motion in the adjusted field. Deep convective precipitation was located within this area (see shaded area in Fig. 9).

Once the variational objective analysis was completed, the developmental components of the local tendencies of velocity components and temperature were recombined with the advective components, redimensionalized, and expressed as 3-hr changes. These 3-hr "adjustment" tendencies were compared with tendencies calculated from 3-hr rawinsonde data collected over the central part of the United States as part of the NASA AVE/SESAME project (see fine dashed grid in Fig. 1). Then "unadjusted" 3-hr tendencies were calculated upon substitution of unadjusted variables into the dynamical constraints and solving for the tendency terms. Inherent in these comparisons is an assumption that the observed 3-hr tendencies are "ground truth". This assumption is not strictly valid for the following reasons. First, it is likely that some of the observations, either at 0000 GMT or at 0300 GMT, were influenced by the mesoscale phenomena within the analysis areas. Second, the unadjusted and adjusted 3-hr tendencies were calculated from 0000 GMT data and are therefore centered at 0000 GMT. These tendencies were compared with the ground truth tendencies that were calculated from observations taken at both 0000-0300 GMT and are therefore centered at 0130 GMT. And third, extrapolation of the local tendencies calculated from the unadjusted and adjusted data has validity only if the time scales of the passage of the weather systems are much greater than

three hours.

Fig. 10 shows fields of the 3-hr u-component tendencies at 800 mb and 500 mb. The observed tendencies show increases in u over Oklahoma and decreases in u over northern Missouri and Iowa. Both unadjusted and adjusted tendencies show similar features but they are shifted to the southwest by about 500 km. Note also that the unadjusted and adjusted tendencies have approximately the same pattern and the centers from the variational objective analysis tend to be slightly larger in magnitude.

The v-component tendencies at 800 mb and 500 mb are shown in Fig 11. Unlike the u-component tendencies, the centers for unadjusted and adjusted tendencies are approximately collocated with the observed centers. The magnitudes of the positive center over Arkansas compare well at 800 mb however the adjusted field shows little correlation with the observed v-tendencies in the western half of the grid. At 500 mb, the centers were mostly collocated however the magnitudes for both the unadjusted and adjusted v-component tendencies were much greater than the observed 3-hr magnitudes - the magnitudes of the adjusted v-component being the largest.

At 300 mb, Fig. 12, both unadjusted velocity component tendencies departed considerably from the observed fields. The adjusted tendencies appeared to be no more correct.

Table 3 gives correlation coefficients between the unadjusted (initial) and observed tendencies and between the adjusted (variational) and observed tendencies for the eight interior levels

of the analysis domain. Somewhat surprisingly, the adjusted correlations were higher than the unadjusted correlations for most levels below 500 mb. In calculating the correlation coefficients that appear in Table 4, we shifted the adjusted and unadjusted tendency fields to the northeast approximately 150 km to account for the 1.5 hr translation of the weather system. The correlations for the shifted tendencies were larger. The variational objective analysis gave improvement over the unadjusted u and v tendencies however, in general the correlations for the adjusted fields were in the range from 0.5-0.8 below 500 mb and were still negative above 400 mb. Results for the temperature tendencies in both tables showed no clear indication of superiority of the adjusted temperatures over the unadjusted temperatures.

5. Discussion

Based upon our experience with developing a basic variational objective analysis technique (Achtemeier et al., 1986) we have derived a new variational objective analysis method that appears to solve all of the problems encountered with earlier versions. These problems included the problem of over-determination noted by Courant (1936), the problem of time consistency that arose upon applying the direct variational method to local tendencies of wind velocity components and temperature, the problem of solving a set of complicated nonlinear partial differential equations, and the problem of decoupling the divergence equation constraint from the

remaining dynamical constraints. This version of the objective analysis contains more equations and requires more complicated solution methods than were necessary for the 1986 version.

The evaluation presented in this report is only preliminary in that it identifies problems with the method but does not determine whether the problems are endemic to the method and therefore degrade data assimilation or whether the problems arise because of correctable errors in the mathematical derivations or the programming.

The satisfactory results of the evaluation are as follows.

1) The method converges for all five dynamic constraints. The divergent part of the wind is strongly coupled in the solution. Convergence after only eight cycles ranged mostly between 98-100 percent of the initial unadjustment with the poorest convergence at the 9th level still at an acceptable 92 percent.

2) The method gave reasonable adjusted fields of heights and temperatures from the standpoint of pattern recognition. The major synoptic weather systems were retained from an accurate initial objective interpolation to the analysis grid. Smaller features such as short waves were also retained. The method did not introduce erroneous wavelengths into the adjusted fields.

3) Sensitive derivative fields such as vorticity and vertical velocity were better located with respect to important

precipitation producing weather systems relative to the unadjusted fields. Gradients of positive vorticity advection were collocated with upward vertical velocity centers.

The unsatisfactory results from the evaluation are as follows.

1) The variational objective analysis systematically increased the zonal component of the wind in a way that caused significant departures from the original observations. These departures appeared to be a function of elevation and of latitude from the grid origin (the largest increases were found in the eastern part of the grid). These departures systematically turned the winds east of the Great Plains to blow from low to high heights.

2) Though at many levels, the patterns were similar, the variational objective analysis greatly overestimated the magnitudes of the local tendencies of the wind components and temperature. Correlations between verification 3-hr tendencies and 3-hr tendencies derived from adjusted data ranged from about 0.5 to 0.8 at levels below 500 mb. Correlations were mostly very small or negative at 200 mb and 300 mb.

The reasons for the unsatisfactory results await a more thorough analysis of the method. The systematic increases in the adjusted wind velocity are suggestive of an error embedded within the mathematical formulas or coding of the programs. We were able

to trace the vary large magnitudes of the tendencies to the advective components. These are relative simple formulations and it has yet to be determined why large advective changes in velocity were found in both the unadjusted and adjusted fields but were not observed.

It could be argued that the large tendencies of the adjusted fields should have been expected given that a mesoscale convective system was within the analysis area during the period 0000-0300 GMT. The variational objective analysis was rerun for 1200 GMT 10 April 1979 data set to test this argument. This period was characterized by the same general synoptic scale long wave trough over the western United States. There were no significant precipitation systems active however. The results showed large magnitude centers of the local tendencies of u and v in both the unadjusted and adjusted fields. Therefore, the finding of large magnitude tendencies within the 0000 GMT 11 April variational analysis was not coincidental with severe weather.

In conclusion, the variational objective analysis represents a mammoth effort in mathematical development and programming. One must question whether, if the problems encountered thus far are solved, the difficulty of the method would limit its use in routine analysis of meteorological data given that there are other nonvariational techniques for blending meteorological data that are being used with success. The answer to the question will in part be delayed until the methods currently in use have been fully applied and evaluated.

Acknowledgments.

This work was supported by the National Aeronautics and Space Administration (NASA) under Grant NAG8-059. The programming efforts of Mrs. Julia Chen are gratefully acknowledged. Mr. Robert Scott prepared the figures.

Appendix A: The Dynamic Constraints

Following Shuman and Hovermale (1968), the horizontal momentum equations and the continuity equation that form the basis of the numerical variational objective analysis/assimilation method are written below as they appear in an arbitrary vertical coordinate and cartesian on a conformal projection of the earth:

$$\frac{\partial u}{\partial t}+m\left(u\frac{\partial u}{\partial x}+v\frac{\partial u}{\partial y}\right)+\dot{\sigma}\frac{\partial u}{\partial \sigma}-fv+m\left(\frac{\partial \phi}{\partial p}\frac{\partial p}{\partial x}+\frac{\partial \phi}{\partial x}\right)+f_u=0 \qquad \text{(A.1)}$$

$$\frac{\partial v}{\partial t}+m\left(u\frac{\partial v}{\partial x}+v\frac{\partial v}{\partial y}\right)+\dot{\sigma}\frac{\partial v}{\partial \sigma}+fu+m\left(\frac{\partial \phi}{\partial p}\frac{\partial p}{\partial y}+\frac{\partial \phi}{\partial y}\right)+f_v=0 \qquad \text{(A.2)}$$

$$\frac{d}{dt}\ln\left(\frac{\partial p}{\partial \sigma}\right)+m\left(\frac{\partial u}{\partial x}+\frac{\partial v}{\partial y}\right)+\frac{\partial \dot{\sigma}}{\partial \sigma}-\left(u\frac{\partial m}{\partial x}+v\frac{\partial m}{\partial y}\right)=0 \qquad \text{(A.3)}$$

The hydrostatic equation is,

$$\frac{\partial \sigma}{\partial p}\frac{\partial \phi}{\partial \sigma}+\frac{RT}{p}=0 \qquad \text{(A.4)}$$

and the thermodynamic equation,

$$\frac{\partial T}{\partial t}+m\left(u\frac{\partial T}{\partial x}+v\frac{\partial T}{\partial y}\right)+\dot{\sigma}\frac{\partial T}{\partial \sigma}-\frac{RT\omega}{c_p p}-\frac{Q}{c_p}=0 \qquad \text{(A.5)}$$

These equations must be subject to several transformations before they can be used in a successful variational method. These transformations are described in the following sections.

A.1 A Nonlinear Vertical Coordinate System

The vertical coordinate is designed to concentrate horizontal variations with the lower coordinate surface to levels below a reference pressure level p^*. The coordinate surfaces above p^* are constant pressure surfaces. The transformation into a nonlinear vertical coordinate was done for the following reasons:

(1) The dynamical equations appear in their simplest form on pressure surfaces. The complex, compensatory terms are confined to levels below p^*.

(2) Vertical interpolation of meteorological observations to coordinate surfaces is not required for pressure surfaces. Further, there is no need to interpolate from sigma coordinates back to pressure surfaces for purposes of interpretation of the variationally adjusted fields of data.

(3) Hydrostatic truncation error and pressure gradient force errors are eliminated on the pressure levels above p^*. The problems of reducing hydrostatic truncation error along

sloping coordinate surfaces are well known (Achtemeier, 1990).

Two curves that are piece wise continuous through the second derivatives make up the nonlinear vertical coordinate. The upper layer relates to pressure by a straight line. Boundary conditions are $\sigma = 0$ at $p = p_u$ and $\sigma = \sigma^*$ at $p = p^*$. This equation is,

$$\sigma=\sigma^*\frac{p-p_u}{p^*-p_u} \tag{A.6}$$

Boundary conditions for the lower curve are $\sigma = 1.0$ at $p = p_s$ and

$$\begin{aligned}\sigma&=\sigma^*\\ \frac{\partial\sigma}{\partial p}&=\frac{\sigma^*}{(p_s-p_u)}\\ \frac{\partial^2\sigma}{\partial p^2}&=0\end{aligned} \tag{A.7}$$

at $p = p^*$. The lower curve, a cubic polynomial, is,

$$\sigma=\beta\,(p-p^*)^3+\sigma^*\frac{p-p_u}{p^*-p_u}, \tag{A.8}$$

where

$$\beta=(1-\sigma^*\frac{p_s-p_u}{p^*-p_u})\,(p_s-p^*)^{-3}. \tag{A.9}$$

Fig. A.1 shows the distribution of coordinate surfaces below 600 mb for the approximate range of surface pressures (800 to 1025 mb) for the smoothed orography of the variational analysis. The reference pressure p^* is 700 mb. These coordinate surfaces tend to

follow constant pressure surfaces at locations away from areas of high elevation. The compression of the coordinate surfaces over higher elevation is clearly evident.

Other variables that are an outcome of the nonlinear vertical coordinate appear elsewhere in the transformation of the dynamic equations. These are:

$$
\begin{aligned}
q_1 &= \frac{-6\beta\,(p-p^*)}{J^2}, \\
q_2 &= \frac{2\alpha J_s}{J}\left(\frac{p-p^*}{p_s-p^*}\right)^3, \\
q_3 &= \frac{1}{Jp}, \\
q_4 &= \frac{J_s}{Jp}\left(\frac{p-p^*}{p_s-p^*}\right)^3, \\
q_5 &= \int_{\sigma_1}^{\sigma_2} q_1\, d\sigma = \frac{J_1}{J_2}.
\end{aligned}
\qquad \text{(A.10)}
$$

where,

$$
\begin{aligned}
\alpha &= \frac{\sigma^*}{p^*-p_u}, \\
J &= 3\beta\,(p-p^*)^2+\alpha, \\
J_s &= 3\beta\,(p_s-p^*)^2+\alpha.
\end{aligned}
$$

It is understood that if $p - p^* < 0$, then $p - p^* \equiv 0$.

Terms in the dynamic equations that must be transformed are as follows:

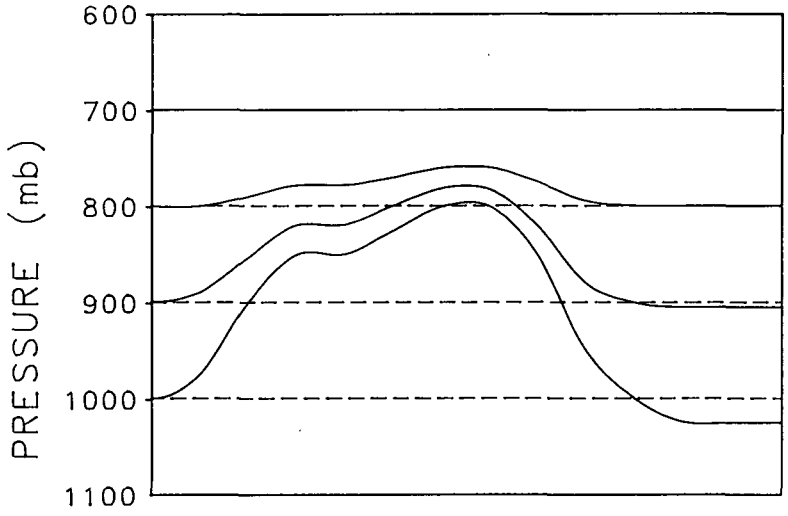

Fig. A.1 Distribution of coordinate surfaces below 800 mb.

(1) The pressure gradient force terms of the horizontal momentum equations (A.1 and A.2) take the form,

$$m\left(\frac{\partial \phi}{\partial p}\frac{\partial p}{\partial x}+\frac{\partial \phi}{\partial x}\right)=m\left(RT\frac{\partial \ln p}{\partial x}+\frac{\partial \phi}{\partial x}\right) \qquad \text{(A.11)}$$

(2) The first term of the continuity equation transforms into

$$\frac{d}{dt}\ln\frac{\partial p}{\partial \sigma}=q_1\dot{\sigma}+q_2\omega_s \qquad \text{(A.12)}$$

(3) The hydrostatic equation transforms to,

$$\frac{\partial \phi}{\partial \sigma}+T\frac{\partial \ln p}{\partial \sigma}=0 \qquad \text{(A.13)}$$

(4) The fourth term of the thermodynamic equation (5) becomes,

$$\frac{RT\omega}{c_p p}=\frac{RT}{c_p}\left(q_3\dot{\sigma}+q_4\omega_s\right) \qquad \text{(A.14)}$$

A.2 Reduction of Terrain Impacts upon Analysis

Small hydrostatic residuals and related pressure gradient force errors that plague numerical models written in terrain-following coordinates have been well documented. Much larger errors can be generated upon subjecting the pressure gradient terms of the horizontal momentum equations to the variational operations. The variational operator separates the two pressure gradient terms and combines the large now uncompensated terms with terms from the other equations. The terrain terms, for which the nonmeteorological part may exceed 90 percent of the magnitude of

the term, can dominate the adjustment. A test found that these terms generated large error that caused the variational method to diverge.

The above problem may be avoided if the hydrostatic terms are partitioned to isolate the terrain part so that the variation can be applied to only the meteorological "signal". Note that a partition not a transforation is done. There is no change in the vertical coordinate.

The equations were nondimensionalized following the methodology of Charney (1948) and Haltiner (1971). The resulting nondimensional variables contain the "whole" signal. The geopotential height and temperature are partitioned into terrain, reference, meteorological, and residual categories according to,

$$( )_w = ( )_T + ( )_R + ( )^o + [( ) - ( )^o] \qquad \text{(A.15)}$$

In addition, the "whole" pressure is partitioned into terrain and reference parts according to

$$p_w = p_T + p_R \qquad \text{(A.16)}$$

The hydrostatic equation is partitioned into four groups of terms. These are:

Terrain,

$$[(\frac{p_w}{p_R} - 1) \frac{\partial \phi_w^o}{\partial \sigma} + \frac{\partial \phi_T}{\partial \sigma} + \frac{T_w^o}{p_R} \frac{\partial \ln p_T}{\partial \sigma}] \qquad \text{(A.17)}$$

Reference,

$$[\frac{\partial \phi_R}{\partial \sigma} + \gamma T_R] \tag{A.18}$$

Meteorological,

$$[\frac{\partial \phi}{\partial \sigma} + \gamma T] \tag{A.19}$$

Residual,

$$[(\frac{p_w}{p_R} - 1)\frac{\partial}{\partial \sigma}(\phi - \phi^o) + \frac{T - T^o}{p_R}\frac{\partial \ln p_T}{\partial \sigma}] \tag{A.20}$$

where,

$$\gamma = \frac{\partial \ln p_R}{\partial \sigma}$$

Non-derivative p_w and p_R in (A.17) and (A.20) are layer mean pressures which must be accurately known for the partition to be successful. After some experimentation, it was found that, given the pressures at the top and the bottom of the layer, the average of the arithmetic mean plus twice the geometric mean,

$$p = \frac{0.5(p_t + p_b) + 2\sqrt{p_t p_b}}{3}$$

yields accurate layer mean pressure. The superscript zero identifies observed variables. These are not subject to the variational operations.

Upon specification of p_R (p_R = 1000, 900, 800 mb), p_T is known through (A.16). Therefore, (A.17) can be solved for the terrain

height ϕ_T. ϕ_R is found from the level average of height after the removal of ϕ_T. Remaining reference variables are obtained through (A.18) and the meteorological variables are found from (A.15). The residual group (A.20) exist through small modifications in ϕ that result from the variational operation. These terms are typically two orders of magnitude smaller than the meteorological terms. If these terms are represented by β, then the hydrostatic equation that is subject to the variational operation is,

$$\frac{\partial \phi}{\partial \sigma} + \gamma T + \beta = 0 \qquad \text{(A.21)}$$

Now the pressure gradient terms of the horizontal momentum equations can be partitioned to separate the terrain part from the meteorological part that is subject to the variational operations. The modified nondimensional pressure gradient term is,

$$\frac{\partial \phi}{\partial x} + T\frac{\partial \ln p}{\partial x} = \frac{\partial \phi}{\partial x} + \eta_x \qquad \text{(A.22)}$$

where,

$$\eta_x = (T - T^o)\frac{\partial \ln p_T}{\partial x} + \frac{\partial \phi_T}{\partial x} + T_w^o \frac{\partial \ln p_T}{\partial x}$$

A.3 Partition of the Local Tendencies of u and v

Local changes in the horizontal velocity components result from translation of existing disturbances and development.

Consider that the local change in the u-component of the wind for a moving weather system is,

$$\frac{\partial u}{\partial t} = -c\cdot\nabla u + \frac{du}{dt} \qquad \text{(A.23)}$$

where c is the velocity of an advective or steering current (Fjortoft, 1952) usually a smoothed middle tropospheric wind. Let $u = u_0 + u'$ where u_0 is the u-component of the steady part of the circulation and u' arises from development. Then,

$$\frac{\partial u}{\partial t} = -c\cdot\nabla u_o + \left(\frac{du'}{dt} - c\cdot\nabla u'\right)$$

The first term is the local change in u caused by translation of the steady part of a disturbance. The second term is the local change of u from development. Note that the vertical advection of u is considered part of development.

The use of the advective current throughout the troposphere is valid because most synoptic systems tend to maintain vertical structure. Any changes in vertical structure are assumed to be the result of development. However, the variational operations require that the adjustments be done on total velocity components. Therefore, we represent the local tendency of u by (A.23). The total derivative, an approximate developmental component, is defined as a new dependent variable, $\epsilon_u = du/dt$ ($\epsilon_v = dv/dt$).

A.4 The Dynamic Constraints

Subjecting the dynamic equations (A.1) - (A.5) to the required transformations yields the following constraints: For the horizontal momentum equations,

$$R_o[\epsilon_u + m(u-c_x)\frac{\partial u}{\partial x} + m(v-c_y)\frac{\partial u}{\partial y} + R_o\dot{\sigma}\frac{\partial u}{\partial \sigma}] - (1+R_1C)v + (1+R_1K)(\frac{\partial \phi}{\partial x} + \eta_x) + f_u = 0 \quad \text{(A.24)}$$

$$R_o[\epsilon_v + m(u-c_x)\frac{\partial v}{\partial x} + m(v-c_y)\frac{\partial v}{\partial y} + R_o\dot{\sigma}\frac{\partial v}{\partial \sigma}] + (1+R_1C)u + (1+R_1K)(\frac{\partial \phi}{\partial y} + \eta_y) + f_v = 0 \quad \text{(A.25)}$$

As part of the nondimensionalization, the Coriolis parameter and the map scale factor have been expanded into a Taylor series. Thus, $f = 1 + R_1C$ and $m = 1 + R_1K$ where $R_1 = 0.1$.

The continuity equation will become an integrated constraint,

$$\int q_5(\frac{\partial u}{\partial x} + \frac{\partial v}{\partial y})\,d\sigma + (\dot{\sigma} - \dot{\sigma}_0) + \int q_5[\frac{Lh}{Hl}q_2\omega_s + R_1K(\frac{\partial u}{\partial x} + \frac{\partial v}{\partial y}) - R_1(u\frac{\partial K}{\partial x} + v\frac{\partial K}{\partial y})]\,d\sigma = 0 \quad \text{(A.26)}$$

The hydrostatic and thermodynamic equations are,

$$\frac{\partial \phi}{\partial \sigma} + \gamma T + \beta = 0 \quad \text{(A.27)}$$

$$R_o\left[\epsilon_T+m\left(u\frac{\partial T}{\partial x}+v\frac{\partial T}{\partial y}\right)+\dot{\sigma}\left(\frac{\partial T}{\partial \sigma}-\kappa q_3 T\right)\right.$$
$$\left.-\kappa q_4 \omega_s\left(\frac{R_o}{F}T_R+T\right)\right]+\dot{\sigma}\sigma_\sigma-\frac{Q^*}{C_p}=0 \qquad \text{(A.28)}$$

where,

$$\sigma_\sigma=\frac{R_o^2}{F}\left(\frac{\partial T_R'}{\partial \sigma}-\kappa q_3 T_R'\right)$$

is the static stability. Here F is the Froude number and Q^* carries nondimensionalization constants. In addition,

$$\kappa=\frac{R}{C_p}$$

$$\epsilon_T=\frac{dT}{dt}$$

where the latter is introduced as a dependent variable.

Appendix B: Finite Difference Equations for the Dynamic Constraints

The dynamic equations will be written in centered differences on an Arakawa D grid (Mesinger and Arakawa, 1976). Fig. B1 shows the distribution of variables on the staggered grid. Anthes and Warner (1978) define the horizontal finite difference operators and the finite averaging operators as

$$\begin{aligned} \alpha_x &\equiv (\alpha_{i+1/2,j}-\alpha_{i-1/2,j})/\Delta x \\ \alpha_y &\equiv (\alpha_{i,j+1/2}-\alpha_{i,j-1/2})/\Delta y \\ \overline{\alpha}^x &\equiv (\alpha_{i+1/2,j}+\alpha_{i-1/2,j})/2 \\ \overline{\alpha}^y &\equiv (\alpha_{i,j+1/2}+\alpha_{i,j-1/2})/2 \end{aligned} \tag{B.1}$$

The i are the east-west indices, the j are the north-south indices as defined at the grid origin located at the lower left corner of the grid. In addition, the vertical differences and averages are defined by

$$\begin{aligned} \alpha_\sigma &\equiv (\alpha_{k+1/2}-\alpha_{k-1/2})/\Delta\sigma \\ \overline{\alpha}^\sigma &\equiv (\alpha_{k+1/2}+\alpha_{k-1/2})/2 \end{aligned} \tag{B.2}$$

The finite difference equations for the horizontal momentum equations are,

$$M_6 = -v+\phi_x+F_5=0 \tag{B.3}$$

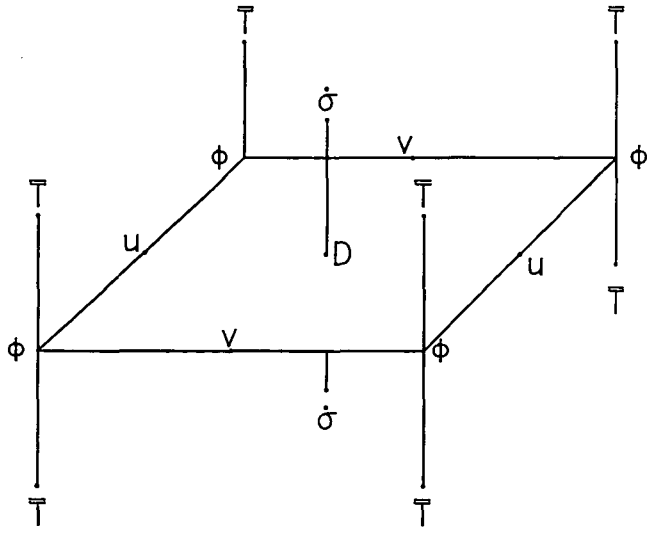

Fig B1. The grid template for the variational assimilation model.

$$M_1 = -F_5 + R_o [\overline{\epsilon_u}^{xy} + \overline{m}^x (\overline{u - c_x})^{xy} \overline{u}_x^y + \overline{m}^x (v - c_y) \overline{u}_y^x + R_o \overline{\sigma}^{y\sigma} \overline{u}_\sigma^{xy\sigma}] - R_1 \overline{C}^x v + R_1 \overline{K}^x \phi_x + (1 + R_1 \overline{K}^x) \eta_x + f_u = 0 \quad \text{(B.4)}$$

$$M_7 = u + \phi_y + F_6 = 0 \quad \text{(B.5)}$$

$$M_2 = -F_6 + R_o [\overline{\epsilon_v}^{xy} + \overline{m}^y (u - c_x) \overline{v}_x^y + \overline{m}^y (\overline{v - c_y})^{xy} \overline{v}_y^x + R_o \overline{\sigma}^{x\sigma} \overline{v}_\sigma^{xy\sigma}] + R_1 \overline{C}^y u + R_1 \overline{K}^y \phi_y + (1 + R_1 \overline{K}^y) \eta_y + f_v = 0 \quad \text{(B.6)}$$

The continuity equation is

$$M_3 = \int q_5 (u_x + v_y) \, d\sigma + (\dot{\sigma} - \dot{\sigma}_o) + \int q_5 F_7 \, d\sigma = 0 \quad \text{(B.7)}$$

$$F_7 = \int [\frac{Lh}{Hl} q_2 \omega_s + R_1 \overline{K}^{xy} (u_x + v_y) - R_1 (\overline{u}^x \overline{K}_x^y + \overline{v}^y \overline{K}_y^x)] \, d\sigma \quad \text{(B.8)}$$

The hydrostatic and thermodynamic equations are,

$$M_4 = \phi_\sigma + \gamma T + \beta = 0 \quad \text{(B.9)}$$

$$M_5 = R_o [\epsilon_T + \overline{m}^{xy} \overline{u}^{x\sigma} \overline{T}_x^y + \overline{m}^{xy} \overline{v}^{y\sigma} \overline{T}_y^x + \dot{\sigma} (\overline{T}_\sigma^{xy\sigma} - \kappa \overline{q_3}^{xy} \overline{T}^{xy}) - \kappa \overline{q_4}^{xy} \omega_s (\frac{R_o}{F} T_R + \overline{T}^{xy})] + \dot{\sigma} \sigma_\sigma - \frac{Q^*}{c_p} = 0 \quad \text{(B.10)}$$

The seven dynamic equations are referenced at, respectively, M_1 and M_6 at v, M_2 and M_7 at u, M_3 at D, M_4 at T, and M_5 at the vertical velocity.

Appendix C: The Euler-Lagrange Equations

The gridded fields of meteorological data to be modified are meshed with the dynamical equations through Sasaki's (1970a) variational operations. To simplify the derivations, the frictional terms in the horizontal momentum equations and the diabatic heating term in the thermodynamic equation were set to zero.

Early experiments with this method found that the divergent part of the wind was decoupled from the adjustment with the result that the continuity equation was not satisfied. Attempts to readjust the winds through a subsidiary variational formulation that satisfied the continuity equation were not successful. The vertical velocity tended to "drift" with the result that the thermodynamic equation was not satisfied.

Analysis of the problem revealed that the divergent part of the wind could be coupled with the variational adjustment if an additional constraint was satisfied. The adjusted variables must satisfy a particular solution of the integrated vorticity equation. The integrated divergence and the integrated vorticity theorem must vanish at the top of the model domain. This requirement is met if F_5 and F_6 are made dependent variables and M_3 is modified to

$$M_3 = -q_5 (F_{6x} - F_{5y}) \Delta\sigma + (\dot{\sigma} - \dot{\sigma}_o) + q_5 F_7 \Delta\sigma = 0 \qquad \text{(C.1)}$$

In addition,

$$M_6 = -v + \phi_x + F_5 = 0 \tag{C.2}$$

$$M_7 = u + \phi_y + F_6 = 0 \tag{C.3}$$

The finite difference analog of the adjustment functional is,

$$\tilde{F} = \Delta x \Delta y \sum_i \sum_j a_i b_j I_{i,j} \tag{C.4}$$

The integrand, $I_{i,j}$ is

$$\begin{aligned} I = & \pi_1 (u-u^o)^2 + \pi_1 (v-v^o)^2 + \pi_2 (\dot{\sigma}-\dot{\sigma}^o)^2 \\ & + \pi_3 (\phi-\phi^o)^2 + \pi_4 (T-T^o)^2 + \pi_5 (\phi_x-\phi_x^o)^2 \\ & + \pi_5 (\phi_y-\phi_y^o)^2 + \pi_6 (\phi_\sigma-\phi_\sigma^o)^2 + \pi_7 (\epsilon_u-\epsilon_u^o)^2 \\ & + \pi_7 (\epsilon_v-\epsilon_v^o)^2 + \pi_8 (\epsilon_T-\epsilon_T^o)^2 + \pi_9 (F_5-F_5^o)^2 \\ & + \pi_9 (F_6-F_6^o)^2 + 2 \sum_{i-1}^{7} \lambda_i M_i \end{aligned} \tag{C.5}$$

The weights, π_i, are Gauss' precision moduli (Whittaker and Robinson, 1926). The gridded initial variables (u^o, v^o, σ^o, Φ^o, T^o, ϵ_u^o, $_v^o$, F_5^o, F_6^o) enter in a least squares formulation and receive π_i according to their relative accuracies. The strong constraints to be satisfied exactly are introduced through the Lagrangian multipliers λ_i.

Objectively modified meteorological variables are determined by requiring the first variation on F to vanish. A necessary condition for the existence of a stationary set is that the functions are determined from the domain of admissible functions as solutions of the Euler-Lagrange equations. The variation is to be

carried out at every point (r,s) within the grid. Thus, upon setting the weights $a_i = b_j = 1$ and differentiating the integrand (C.5) with respect to the arbitrary variable $\alpha_{r,s}$, the Euler-Lagrange operator in finite differences is

$$\frac{\partial I_{i,j}}{\partial \alpha_{r,s}} - I_{\alpha_{i,j}} \frac{\partial \alpha_{i,j}}{\partial \alpha_{r,s}} - I_{\alpha_{i,j}} \delta_r^i \delta_s^j = 0 \qquad \text{(C.6)}$$

Each term in $I_{i,j}$ that contains an overbar term, that is, each term in M_i [(B.4), (B.6), (B.9), (B.10), (C.1) - C.3)] produces an overbar term when subjected to the operations specified by (C.6). Multiplicate overbar terms such as $(\bar{xy})$ are treated having no overbar so that fewer grid points are required to express these terms in the Euler-Lagrange equations.

The Euler-Lagrange equations resulting from the operations specified by (C.6) are

$$\pi_1 u + \lambda_6 + F_1 = 0 \qquad \text{(C.7)}$$

$$\pi_1 v - \lambda_5 + F_2 = 0 \qquad \text{(C.8)}$$

$$\pi_2 \dot{\sigma} + \lambda_3 + F_3 = 0 \qquad \text{(C.9)}$$

$$\overline{\pi}_5^{xy}\nabla^2\phi+\overline{\pi}_6^{\sigma}\phi_{\sigma\sigma}+\pi_{5x}\overline{\phi}_x^x+\pi_{5y}\overline{\phi}_y^y+\pi_{6\sigma}\overline{\phi}_{\sigma}^{\sigma}$$
$$-\pi_3\phi+\lambda_{5x}+\lambda_{6y}+\lambda_{4\sigma}+F_4=0 \qquad \text{(C.10)}$$

$$\pi_4 T+\gamma\lambda_4+F_8=0 \qquad \text{(C.11)}$$

$$\pi_7(\epsilon_u-\epsilon_u^o)+R_o\lambda_1=0 \qquad \text{(C.12)}$$

$$\pi_7(\epsilon_v-\epsilon_v^o)+R_o\lambda_2=0 \qquad \text{(C.13)}$$

$$\pi_8(\epsilon_T-\epsilon_T^o)+R_o\lambda_7=0 \qquad \text{(C.14)}$$

$$\pi_9(F_5-F_5^o)-\lambda_1+\lambda_5-\Delta\sigma(q_5\overline{\lambda}_3^{\sigma})_y=0 \qquad \text{(C.15)}$$

$$\pi_9(F_6-F_6^o)-\lambda_2+\lambda_6+\Delta\sigma(q_5\overline{\lambda}_3^{\sigma})_x=0 \qquad \text{(C.16)}$$

Variation on the Lagrange multipliers restores the original constraints [(B.4), (B.6), (B.9), (B.10), (C.1) - C.3)].

The forcing functions, F_1 - F_4 contain the following:

$$F_1=-\pi_1 u^o-\Delta\sigma\lambda_{3x}+R_1\overline{C}^y\lambda_2+R_o\{\overline{m}^y\overline{\lambda}_1^{xy}\overline{u}_x^x+\overline{m}^y\lambda_2\overline{v}_x^y$$
$$-[\overline{m}^{xy}\overline{\lambda}_1^y(\overline{u-c_x})^x]_x-[\overline{m\lambda_1(v-c_y)}^x]_y-R_o(\overline{\sigma}^x\overline{\lambda}_1^{xy\sigma})_{\sigma} \qquad \text{(C.17)}$$
$$+\overline{m}^y(\overline{\lambda_7 T_x^y})^{x\sigma}\}-R_1[(\lambda_3\overline{K}^{xy})_x+\lambda_3\overline{K}_x^{xy}]$$

$$F_2 = -\pi_1 V^{o} - \Delta\sigma\lambda_{3y} - R_1\overline{C}^{x}\lambda_1 + R_o\{\overline{m}^{x}\lambda_1\overline{u}_y^{x} + \overline{m}^{x}\overline{\lambda}_2^{xy}\overline{v}_y^{y}$$
$$- [m\overline{\lambda_2(u-c_x)}^{y}]_x - [\overline{m}^{xy}\overline{\lambda}_2^{x}(\overline{v-c_y})^{y}]_y - R_o(\overline{\sigma}^{y}\overline{\lambda}_2^{xy\sigma})_\sigma \quad (C.18)$$
$$+\overline{m}^{x}\overline{(\lambda_7\overline{T}_y^{x})}^{y\sigma}\} - R_1[(\lambda_3\overline{K}^{xy})_y + \lambda_3\overline{K}_y^{xy}]$$

$$F_3 = -\pi_2\dot{\sigma}^{o} + \lambda_5\sigma_\sigma + R_o\lambda_5(\overline{T}_\sigma^{xy\sigma} - \kappa\overline{q}_3^{xy}\overline{T}^{xy}) + R_o^2(\overline{\lambda}_1^{y\sigma}\overline{u}_\sigma^{x} + \overline{\lambda}_2^{x\sigma}\overline{v}_\sigma^{y}) \quad (C.19)$$

$$F_4 = \pi_3\phi_o - \pi_5\nabla^2\phi^{o} - \pi_6\phi_{\sigma\sigma}^{o} - \pi_{5x}\overline{\phi}_x^{ox} - \pi_{5y}\overline{\phi}_y^{oy} - \pi_{6\sigma}\overline{\phi}_\sigma^{o\sigma} + R_1K(\lambda_{1x} + \lambda_{2y}) \quad (C.20)$$

In addition, the forcing function F_8 is,

$$F_8 = -\pi_4 T^{o} - R_o[(\overline{m}^{x}\overline{u}^{x}\overline{\lambda_7^\sigma})_x^y + (\overline{m}^{y}\overline{v}^{y}\overline{\lambda_7^\sigma})_y^x + (\overline{\sigma\lambda_7})_\sigma^{xy\sigma} + \kappa q_3(\overline{\sigma\lambda_7})^{xy}$$
$$+\kappa q_4(\overline{\omega_s\lambda_7})^{xy}] \quad (C.21)$$

We observe that the forcing functions contain the nonlinear terms of their respective equations. Further, the forcing functions consist of terms that are either observed and therefore not adjusted, or are multiplied by R_o or R_1. These equations may be therefore linearized and a solution obtained through a cyclical method as follows. Terms multiplied by R_o or R_1 are expressed with observed variables at the first cycle, and are expressed by previously adjusted variables at higher cycles. Therefore the forcing functions are known at each cycle. This solution method is valid for the latitudes and motion scales for which the Rossby number is less than one.

The set of equations [(B.4), (B.6), (B.9), (B.10), (C.1) - C.3), (C.7) - (C.16)] are the linear algebraic and partial differential equations to be solved. Variables may be eliminated to reduce the number of equations to three diagnostic equations in vorticity, divergence, geopotential. Eliminate λ_4, λ_5, λ_6, and T between, respectively, (B.9), (C.10) and (C.11); (C.8) and (C.15), and (C.7) and (C.16). Next, eliminate $_3$ between (C.9) and (C.15) and (C.16). Then, λ_1 and λ_2 may be eliminated between (C.12) and (C.13) and (C.10), (C.15) and (C.16). If M_1 and M_2 are rewritten, pulling out the ϵ_u and ϵ_v terms and designating the remaining terms as f_5 and f_6, respectively, then ϵ_u and ϵ_v may be eliminated by substituting (C.12) and (C.13) into (C.15) and (C.16). Finally, letting $D = u_x + v_y$, the vertical velocity can be eliminated between (C.1) and (C.15) and (C.16). Performing the above operations reduces the Euler-Lagrange equation set to the following five equations:

$$-v+\phi_x+F_5=0 \tag{C.22}$$

$$u+\phi_y+F_6=0 \tag{C.23}$$

$$\pi_1 v+(\pi_9+\frac{\pi_7}{R_o^2})F_5-(\Delta\sigma)^2[\overline{(Q_5^2\pi_2)^{\sigma}D}]_y+G_{1y}+G_3=0 \tag{C.24}$$

C-2

$$-\pi_1+(\pi_9+\frac{\pi_7}{R_o^2})F_6+(\Delta\sigma)^2[\overline{(q_5^2\pi_2)^{\sigma}D}]_x-G_{1x}-G_2=0 \qquad (C.25)$$

$$\begin{aligned}&\overline{\pi}_5^{xy}\nabla^2\phi+\overline{\pi}_6^{\sigma}\phi_{\sigma\sigma}+\pi_{5x}\overline{\phi}_x^x+\pi_{5y}\overline{\phi}_y^y+\pi_{6\sigma}\overline{\phi}_{\sigma}^{\sigma}\\&-\pi_3\phi+(\pi_1 v)_x-(\pi_1 u)_y+G_4=0\end{aligned} \qquad (C.26)$$

where the forcing functions, G_1 - G_4 are given by:

$$G_1=\Delta\sigma[q_5\overline{F}_3^{\sigma}+q_5\pi_2\dot{\sigma}^{o}-q_5\overline{\pi}_2^{\sigma}F7\Delta\sigma]$$

$$G_2=\pi_9F_6^{o}+\frac{\pi_7}{R_o^2}(f_6+R_o\varepsilon_v^{o})+F_1$$

$$G_3=-\pi_9F_5^{o}-\frac{\pi_7}{R_o^2}(f_5+R_o\varepsilon_u^{o})+F_2$$

$$G_4=F_{2x}-F_{1y}+(\frac{\pi_4\beta}{\gamma^2}+\frac{\pi_4T^{o}}{\gamma})_{\sigma}+F_4$$

We are now in a position to substitute (C.22) and (C.23) into (C.24) and (C.25) to eliminate F_5 and F_6. We make note that the substitution generates the following combination of precision modulus weights,

Further, we note that all of these precision moduli vary horizontally with horizontal variations in π_1. Thus, if,

$$\pi_{10}=\pi_1+\pi_9+\frac{\pi_7}{R_o^2}; \quad \pi_{11}=\pi_9+\frac{\pi_7}{R_o^2}.$$

$\pi_1(x,y,\sigma)=\pi_1(\sigma)f(x,y)$, and the horizontal variations of π_7 and π_9 also vary as $f(x,y)$, then by dividing all precision moduli by $f(x,y)$, the horizontal variations of π_{10} and π_{11} may be removed without changing the relative relationships between the weights. With these modifications, the Euler-Lagrange equations (C.24) and (C.25) may be combined to form a divergence equation,

$$\nabla^2[(\Delta\sigma)^2 q_5^2 \pi_2 D]-\pi_{10}D=\nabla^2 G_1+G_{2x}+G_{3y} \tag{C.27}$$

The vorticity formed from (C.24) and (C.25) is,

$$\pi_{10}\zeta-\pi_{11}\nabla^2\phi=G_{2y}-G_{3x} \tag{C.28}$$

Substitution of the vorticity between (C.26) and (C.28) leaves a diagnostic equation in geopotential,

$$\left(\overline{\pi}_5^{xy}+\pi_1\frac{\pi_{11}}{\pi_{10}}\right)\nabla^2\phi+\left(\overline{\pi}_6^{\sigma}+\frac{\pi_4}{\gamma^2}\right)\phi_{\sigma\sigma}+\pi_{5x}\overline{\phi}_x^x+\pi_{5y}\overline{\phi}_y^y+\left(\pi_{6\sigma}+\frac{\pi_4}{\gamma^2}\right)\overline{\phi}_\sigma^\sigma-\pi_3\phi$$
$$=-G_4-\frac{\pi_1}{\pi_{10}}(G_{2y}-G_{3x}) \tag{C.29}$$

Equations (C.27) - (C.29) form the three diagnostic equations that must be solved for a successful variational adjustment. All terms to the right of the equal sign are forcing functions that contain either unadjusted initial variables and/or variables that have been adjusted at the last iteration. (C.29) is solved first to get the geopotential height. Then the divergence and vorticity are

obtained through (C.27) and (C.28).

Appendix D: Boundary Conditions

The variational theory specifies natural boundary conditions that are consistent with the Euler-Lagrange equations. If it is assumed that there are no adjustments in the data along the boundaries, then the boundary conditions may be specified. In the latter case, the Lagrange multipliers, λ_i, are zero at the boundaries and the initial unadjusted values are used for the boundary conditions.

Initially, the Euler-Lagrange equations were solved with specified boundary conditions. These boundary conditions forced high frequency waves into the solutions for the velocity components near the boundaries. Divergences calculated from these velocity components gave large erroneous vertical velocities. We therefore returned to the natural boundary conditions.

The Euler-Lagrange operator for natural boundary conditions is,

$$\frac{\partial I}{\partial\left(\frac{\partial f_i}{\partial x_j}\right)}=0 \qquad \text{(D.1)}$$

Performing the operation specified by (D.1) yields the following expressions for the boundary conditions on Φ

$$\pi_5(\phi_x-\phi_x^{\circ})+\lambda_5+R_1K\lambda_1=0 \qquad \text{(D.2)}$$

$$\pi_5(\phi_y-\phi_y^o)+\lambda_6+R_1K\lambda_2=0 \tag{D.3}$$

$$\pi_6(\phi_\sigma-\phi_\sigma^o)+\lambda_4=0 \tag{D.4}$$

The terms multiplied by R_1 come from the constraints, M_1 and M_2. These equations can be solved for the Φ boundary conditions subject to substitutions for the λ_i through the Euler-Lagrange equations (22)-(35) in the text. The lateral boundary conditions for the x- and y-boundaries are, respectively,

$$\begin{aligned}(\pi_{10}\pi_5+\pi_{13})\phi_x-\pi_{10}\pi_5\phi_x^o+\frac{\pi_{13}}{\pi_1}F_2+\pi_9\pi_{12}F_5^o+\pi_{12}\Delta\sigma(Q\lambda_3)_y\\ +\frac{\pi_7}{R_o}(1+\pi_{12})\left(\frac{f_5}{R_o}+\epsilon_u^o\right)=0\end{aligned} \tag{D.5}$$

$$\begin{aligned}(\pi_{10}\pi_5+\pi_{13})\phi_y-\pi_{10}\pi_5\phi_y^o-\frac{\pi_{13}}{\pi_1}F_1+\pi_9\pi_{12}F_6^o-\pi_{12}\Delta\sigma(Q\lambda_3)_x\\ +\frac{\pi_7}{R_o}(1+\pi_{12})\left(\frac{f_6}{R_o}+\epsilon_v^o\right)=0\end{aligned} \tag{D.6}$$

where,

$$\pi_{10}=\frac{\pi_9+\pi_1+\frac{\pi_7}{R_o}}{\pi_1},$$

$$\pi_{11}=\pi_9+\frac{\pi_7}{R_o},$$

$$\pi_{12}=1-\frac{R_1K}{R_o}\frac{\pi_7}{\pi_1},$$

$$\pi_{13}=\pi_{11}\pi_{12}+\frac{\pi_7}{R_o}\pi_{10}.$$

Several observations may be made with regard to (D.5) and (D.6).

(1) F_1, F_2, λ_3, f_5, and f_6 all contain terms that are updated at each cycle. Thus it is possible to update the boundary conditions as the interior fields are being adjusted.

(2) These forcing functions contain nonlinear terms that cannot be calculated at the boundaries unless derivatives are extrapolated across the boundaries. Therefore, the boundary equations may be simplified by setting $\lambda_1 = \lambda_2 = \lambda_3 = 0$ at the boundaries. It follows therefore, that

$$F_1 = -\pi_1 u^o, \quad F_2 = -\pi_1 v^0, \quad F_3 = -\pi_2 \dot{\sigma}^o$$

(3) From (22) and (29),

$$Q\Delta\sigma\,(D+F_7) + \frac{\lambda_3}{\pi_2} + \dot{\sigma}^o - \dot{\sigma}_0 = 0 \qquad \text{(D.7)}$$

Given that it is the gradient of λ_3 that appears in (D.5) and (D.6) it follows from (D.7) that gradient of the divergence must be specified, or in other words, the divergence must be specified along at least two boundary grid rows or columns in order that the gradient of λ_3 vanish in the Φ boundary equations.

(4) π_7 is at least two orders of magnitude smaller than the remaining precision moduli. Neglecting π_7 leads to the following simplifications,

The equations for the lateral boundary conditions on Φ are thus,

$$\pi_{10}=\frac{\pi_9+\pi_1}{\pi_1},\quad \pi_{11}=\pi_{13}=\pi_9,\quad \pi_{12}=1$$

$$\begin{aligned}(\pi_5+\frac{\pi_1\pi_9}{\pi_1+\pi_9})\phi_x-\pi_5\phi_x^o-\frac{\pi_1\pi_9}{\pi_1+\pi_9}(u^o-F_5^o)=0\\(\pi_5+\frac{\pi_1\pi_9}{\pi_1+\pi_9})\phi_y-\pi_5\phi_y^o+\frac{\pi_1\pi_9}{\pi_1+\pi_9}(u^o+F_6^o)=0\end{aligned}\qquad (D.8)$$

The boundary conditions for u and v may be found by solving the same set of equations used for finding the Φ boundary conditions but for u and v. The results are,

$$\begin{aligned}(\pi_5+\pi_1\frac{\pi_5+\pi_9}{\pi_9})v-\pi_5(\phi_x^o-F_5^0)-\pi_1\frac{\pi_5+\pi_9}{\pi_9}v^o=0\\(\pi_5+\pi_1\frac{\pi_5+\pi_9}{\pi_9})u+\pi_5(\phi_y^o+F_6^o)-\pi_1\frac{\pi_5+\pi_9}{\pi_9}u^o=0\end{aligned}\qquad (D.9)$$

REFERENCES

Achtemeier, G. L., 1990: Reducing hydrostatic truncation error in a meso-beta boundary layer model. (Accepted for publication in Mon. Wea. Rev.)

Achtemeier, G. L., 1989: Modification of a Successive Corrections Objective Analysis for Improved Higher Order Calculations. Mon. Wea. Rev., 117, 78-86.

Achtemeier, G. L., 1986: The impact of data boundaries upon a successive corrections objective analysis of limited-area data sets. Mon. Wea. Rev., 114, 40-49.

Achtemeier, G. L., 1979. Evaluation of operational objective streamline methods. Mon. Wea. Rev. 107, 198-206.

Achtemeier, G. L., 1975: On the Initialization problem: A variational adjustment method. Mon. Wea. Rev., 103, 1090-1103.

Achtemeier, G. L., 1972: Variational initialization of atmospheric fields - a quasi-geostrophic diagnostic model. Ph.D. Dissertation, Tallahassee, Florida State University, 101-103.

Achtemeier, G. L., H. T. Ochs, III, S. Q. Kidder, R. W. Scott, J. Chen, D. Isard, and B. Chance, 1986: A variational assimilation method for satellite and conventional data: Development of basic model for diagnosis of cyclone systems. NASA Con. Report. 3981, 223 pp.

Anthes, R. A., and T. T. Warner, 1978: Development of hydrodynamic models suitable for air pollution and other mesometeorological studies. Mon. Wea. Rev., 106, 1045-1078.

Barnes, S. L., 1973: Mesoscale objective analysis using weighted time-series observations. NOAA Tech. Memo. ERL NSSL-62, National Severe Storms Laboratory, Norman, OK 73069, 60 pp. (NTIS COM-73-10781).

Barnes, S. L., 1964: A technique for maximizing details in numerical weather map analysis. J. Appl. Meteor., 3, 396-409.

Bjilsma, S. J., L. M. Hafkenscheid and P Lynch, 1986: Computation of the streamfunction and velocity potential and reconstruction of the wind field. Mon. Wea. Rev., 114, 1547-1551.

Bloom, S. C., 1983: The use of dynamical constraints in the analysis of mesoscale rawinsonde data. Tellus, 35, 363-378.

Chance, B. A., 1986: Application of satellite data to the variational analysis of the three dimensional wind field. NASA Con. Rept. 4022, 86 pp.

Charney, J. G., 1948: On the scale of atmospheric motion. Geofys. Publikas., 17, 1-17.

Courant, R., 1936: Differential and Integral Calculus, Vol. 2, (E. J. McShane, translator), Wiley - Interscience, p198.

Dickerson, M. H., 1978: MASCON - A mass consistent atmospheric flux model for regions with complex terrain. J. Appl. Meteor., 17, 241-253.

Endlich, R. M., 1967: An iterative method for altering the kinematic properties of wind fields. J. Meteor., 6, 837-844.

Fjortoft, R., 1952: On a numerical method of integrating the barotropic vorticity equation. Tellus, 4, 179-194.

Fuelberg, H. E., 1974: Reduction and error analysis of the AVE II pilot experiment data. NASA CR-120496, Marshall Space Flight Center, Alabama, p. 60.

Gary, J. M., 1973: Estimate of truncation error in transformed coordinate primitive equation atmospheric models. J. Atmos. Sci., 30, 223-233.

Haltiner, G. J., 1971: Numerical Weather Prediction, Wiley and Sons, USA, 46-61.

Hawkins, H. F., and S. L. Rosenthal, 1965: On the computation of stream functions from the wind field. Mon. Wea. Rev., 93, 245-253.

Hovermale, J. B., 1962: A comparison of data accuracy in the troposphere and in the stratosphere. Dept. Meteorology, Penn. State Univ., Contract AF 19-(604)-6261, Rept. No. 2.

Janjic, Z. I., 1977: Pressure gradient force and advection scheme used for forecasting with steep and small scale terrain. Beitr. Phys. Atmos., 50, 186-199.

Janjic, Z. I., 1989: On the pressure gradient force error in σ-coordinate spectral models. Mon. Wea. Rev., 117, 2285-2292.

Kurihara, Y., 1968: Note on finite difference expressions for the hydrostatic relation and pressure gradient force. Mon. Wea. Rev., 96, 654-656.

Lewis, J. M., 1982: Adaptation of P.D. Thompson's scheme to the constraint of potential vorticity conservation. Mon. Wea. Rev., 110, 1618-1634.

Lewis, J. M., 1980: Dynamical adjustment of 500 mb vorticity using P.D. Thompson's scheme - a case study. Tellus, 32, 511-514.

Lewis, J. M., 1972: The operational upper air analysis using the variational method. Tellus, 24, 514-530.

Lewis, J. M., and T.H. Grayson, 1972: The adjustment of surface wind and pressure by Sasaki's variational matching technique. J. Appl. Meteor., 11, 586-597.

Lewis, J. M., C. M. Hayden and A. J. Schreiner, 1983: Adjustment of VAS and RAOB geopotential analysis using quasi-geostrophic constraints. Mon. Wea. Rev., 111, 2058-2067.

Lewis, J. M., and J. C. Derber, 1985: The use of adjoint equations to solve a variational adjustment problem with advective constraints. Tellus, 37A, 309-322.

Lynch, P., 1988: Deducing the wind from vorticity and divergence. Mon. Wea. Rev., 116, 86-93.

Mesinger, G., and A. Arakawa, 1976: Numerical methods used in atmospheric models. Vol. 1, GARP Publications Series No. 17, p47.

O'Brien, J.J., 1970: Alternative solutions to the classical vertical velocity problem. J. Appl. Meteor., 9, 197-203.

Ray, P. S., K. K. Wagner, K. W. Johnson, J. J. Stephens, W. C. Bumgarner, and E. A. Mueller, 1978: Triple-Doppler observations of a convective storm. J. Appl. Meteor., 17, 1201-1212.

Sangster, W. E., 1960: A method of representing the horizontal pressure force without reduction of pressures to sea level. J. Meteor., 17, 166-176.

Sasaki, Y., 1958: An objective analysis based upon the variational method. J. Meteor. Soc. Japan, 36, 77-88.

Sasaki, Y., 1970: Some basic formalisms in numerical variational analysis. Mon. Wea. Rev., 98, 875-883.

Schaefer, J. T., and C. A. Doswell III, 1979: On the interpolation of a vector field. Mon. Wea. Rev., 107, 458-476.

Sherman, C. A., 1978: A mass consistent model for wind fields over complex terrain. J. Appl. Meteor., 17, 312-319.

Shuman, F., and J. B. Hovermale, 1968: An operational six-layer primitive equation model. J. Appl. Meteor., 7, 525-547.

Shukla, J., and K. R. Saha, 1974: Computation of non-divergent stream function and irrotational velocity potential from the observed winds. Mon. Wea. Rev., 102, 419-425.

Sundqvist, H., 1975: On truncation errors in sigma-system models. Atmosphere, 13, 81-95.

Sundqvist, H., 1976: On vertical interpolation and truncation in conexion with use of sigma system models. Atmosphere, 14, 37-52.

Whittaker, E., and G. Robinson, 1926: The Calculus of Observations, (2nd Edition). London, Blackie and Son, Ltd., p.176.

Table 1

Nondimensional standard errors of observation for wind, height, and temperature and RMS errors for other adjustable meteorological variables.

Model Level	Pressure (mb)	VARIABLE u_{20}	u_{40}	Φ	$\Delta\Phi/\Delta x$	$\Delta\Phi/\Delta\sigma$	Mean Temp	σ	ϵ_u
								0.00	
10	100	0.45	0.23	0.25	0.71				
							3.68	0.59	2.13	6.98
9	200	0.45	0.23	0.20	0.56				
							3.21	0.88	1.88	6.98
8	300	0.42	0.21	0.18	0.51				
							2.28	0.88	1.64	6.51
7	400	0.36	0.18	0.15	0.42				
							1.53	0.76	1.43	5.58
6	500	0.32	0.16	0.12	0.33				
							0.97	0.59	1.24	4.65
5	600	0.30	0.15	0.09	0.26				
							0.61	0.44	1.04	4.34
4	700	0.28	0.14	0.08	0.22				
							0.53	0.44	0.84	3.72
3	800	0.24	0.12	0.07	0.20				
							0.47	0.44	0.64	3.26
2	900	0.21	0.11	0.06	0.18				
							0.42	0.44	0.44	3.10
1	1000	0.20	0.10	0.06	0.17				

Table 2

Nondimensional precision modulus weights for variational objective analysis.

Model Level	Pressure (mb)	VARIABLE u_{20}	Φ	$\Delta\Phi/\Delta x$	$\Delta\Phi/\Delta\sigma$	Mean Temp	σ	ϵ_u
							100	
10	100	2.5	8.0	1.0				
					0.04	1.4	10	0.01
9	200	2.5	12.5	1.6				
					0.05	0.6	0.14	0.01
8	300	2.8	15.4	1.9				
					0.10	0.6	0.19	0.01
7	400	3.9	22.2	2.8				
					0.21	0.9	0.24	0.02
6	500	4.9	34.7	4.6				
					0.53	1.4	0.33	0.02
5	600	5.6	61.7	7.4				
					1.34	2.6	0.46	0.03
4	700	6.4	78.1	10.3				
					1.78	2.6	0.71	0.04
3	800	8.7	102.0	12.5				
					2.26	2.6	1.22	0.05
2	900	11.3	138.9	15.4				
					2.83	2.6	2.58	0.05
1	1000	12.5	138.9	17.3				

Table 3. Correlation coefficients for a 216-point subset of initial (i) and variational (v) u, v, and T 3-h forward tendencies at 0000 UTC compared with observed 3-h tendencies centered at 0130 UTC.

p lev	u_i	u_v	v_i	v_v	T_i	T_v
200	-0.34	-0.08	-0.27	-0.25	0.17	0.07
300	-0.10	-0.24	0.43	0.10	-0.36	0.17
400	-0.24	0.12	0.53	0.35	0.24	0.59
500	-0.26	0.31	0.43	0.71	0.75	0.65
600	0.36	0.56	0.01	0.35	0.42	0.75
700	0.66	0.71	0.15	0.61	0.55	0.72
800	0.55	0.59	0.54	0.79	0.48	0.17
900	0.65	0.60	0.31	0.37	0.25	0.22

Table 4. Same as Table 1 but with 0000 UTC 3-h forward tendencies shifted by weather system translation to approximate 0130 UTC observed tendencies.

p lev	u_i	u_v	v_i	v_v	T_i	T_v
200	-0.35	-0.06	-0.31	-0.25	0.12	0.02
300	0.01	-0.04	0.56	0.23	-0.31	0.14
400	-0.27	0.20	0.45	0.30	0.35	0.67
500	-0.03	0.57	0.54	0.73	0.83	0.64
600	0.56	0.69	0.02	0.45	0.57	0.76
700	0.79	0.83	0.22	0.73	0.66	0.71
800	0.72	0.75	0.60	0.87	0.55	0.23
900	0.82	0.78	0.35	0.48	0.32	0.49

FIGURE CAPTIONS

Fig. 1. The distribution of rawinsonde stations over the analysis grid (solid rectangle), evaluation grid (large dashed rectangle), and SESAME I network (small dashed rectangle).

Fig. 2. Residual reduction as a function of cycle for the u-component (left panel) and v-component (right panel) dynamic constraints.

Fig. 3. Residual reduction as a function of cycle for the integrated continuity equation (left panel), the hydrostatic equation (middle panel), and the thermodynamic equation (right panel).

Fig. 4. RMS differences between unadjusted (adjusted) fields and observations after removal of standard observation error (solid lines) and means of differences between unadjusted (adjusted) fields and observations (dashed lines) for a) heights, b) temperatures, c) u-comp, and d) v-comp.

Fig. 5. Heights and wind vectors at 800 mb, 500 mb, and 300 mb for a) unadjusted and b) adjusted fields.

Fig. 6. Differences between adjusted and unadjusted heights and vector winds at 800 mb, 500 mb, and 300 mb.

Fig. 7. Same as Fig. 5 but for temperature.

Fig. 8. Relative vorticities at 500 mb, a) unadjusted and b) adjusted.

Fig. 9. a) unadjusted, b) adjusted vertical velocities (cm sec^{-1}) at 500 mb. Precipitation areas are stippled.

Fig. 10. u-component tendencies for 800 mb (left panels) and 500 mb (right panels) for a) observed, b) unadjusted, and c) adjusted fields in m sec^{-1} 3-hr^{-1}.

Fig. 11. Same as Fig. 10 but for the v-component.

Fig. 12. u-component tendencies (left panels) and v-component tendencies (right panels) at 300 mb for a) observed, b) unadjusted, and c) adjusted fields in m sec^{-1} 3-hr^{-1}.

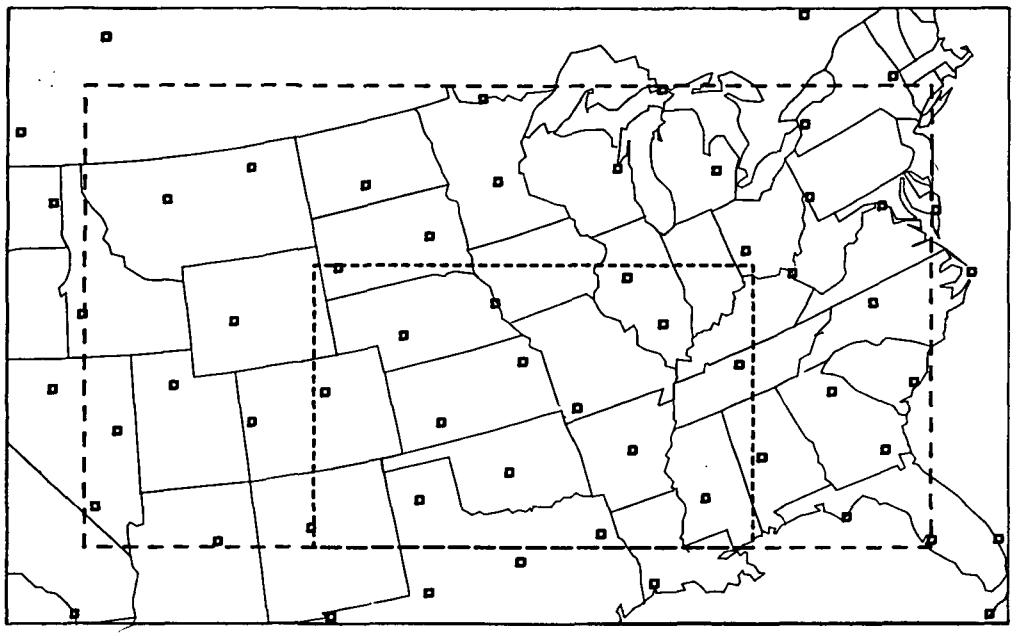

Fig. 1. The distribution of rawinsonde stations over the analysis grid (solid rectangle), evaluation grid (large dashed rectangle), and SESAME I network (small dashed rectangle).

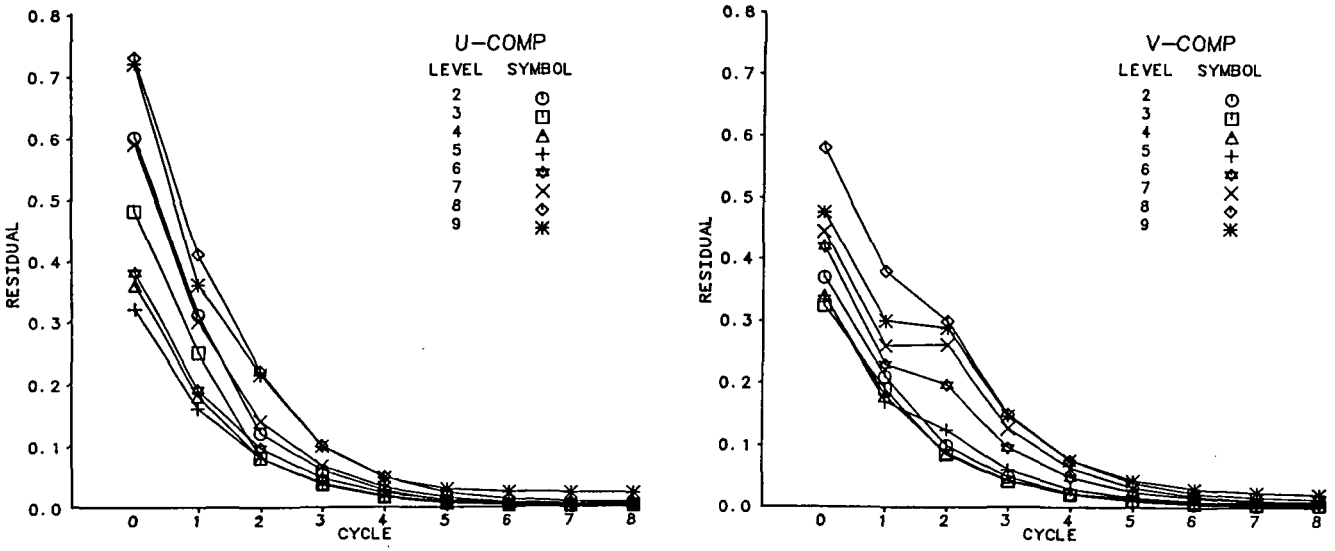

Fig. 2. Residual reduction as a function of cycle for the u-component (left panel) and v-component (right panel) dynamic constraints.

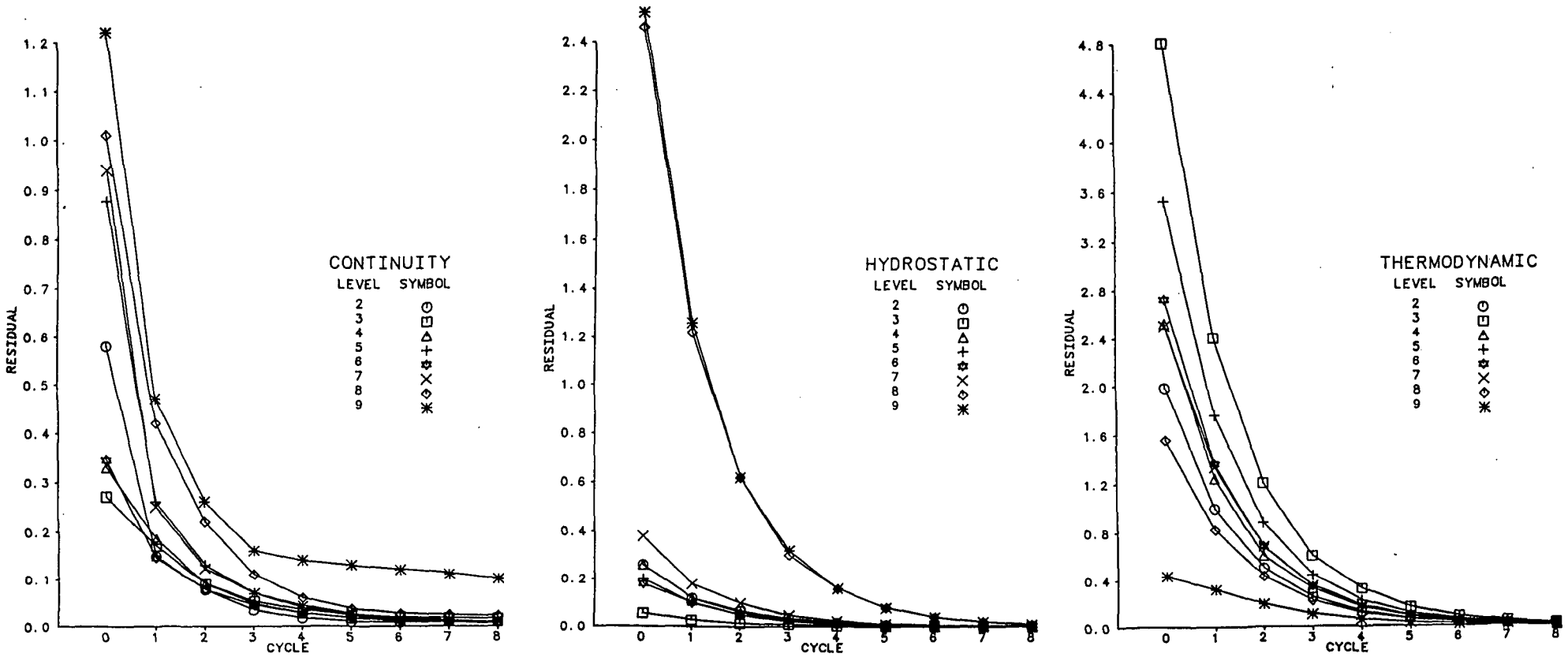

Fig. 3. Residual reduction as a function of cycle for the integrated continuity equation (left panel), the hydrostatic equation (middle panel), and the thermodynamic equation (right panel).

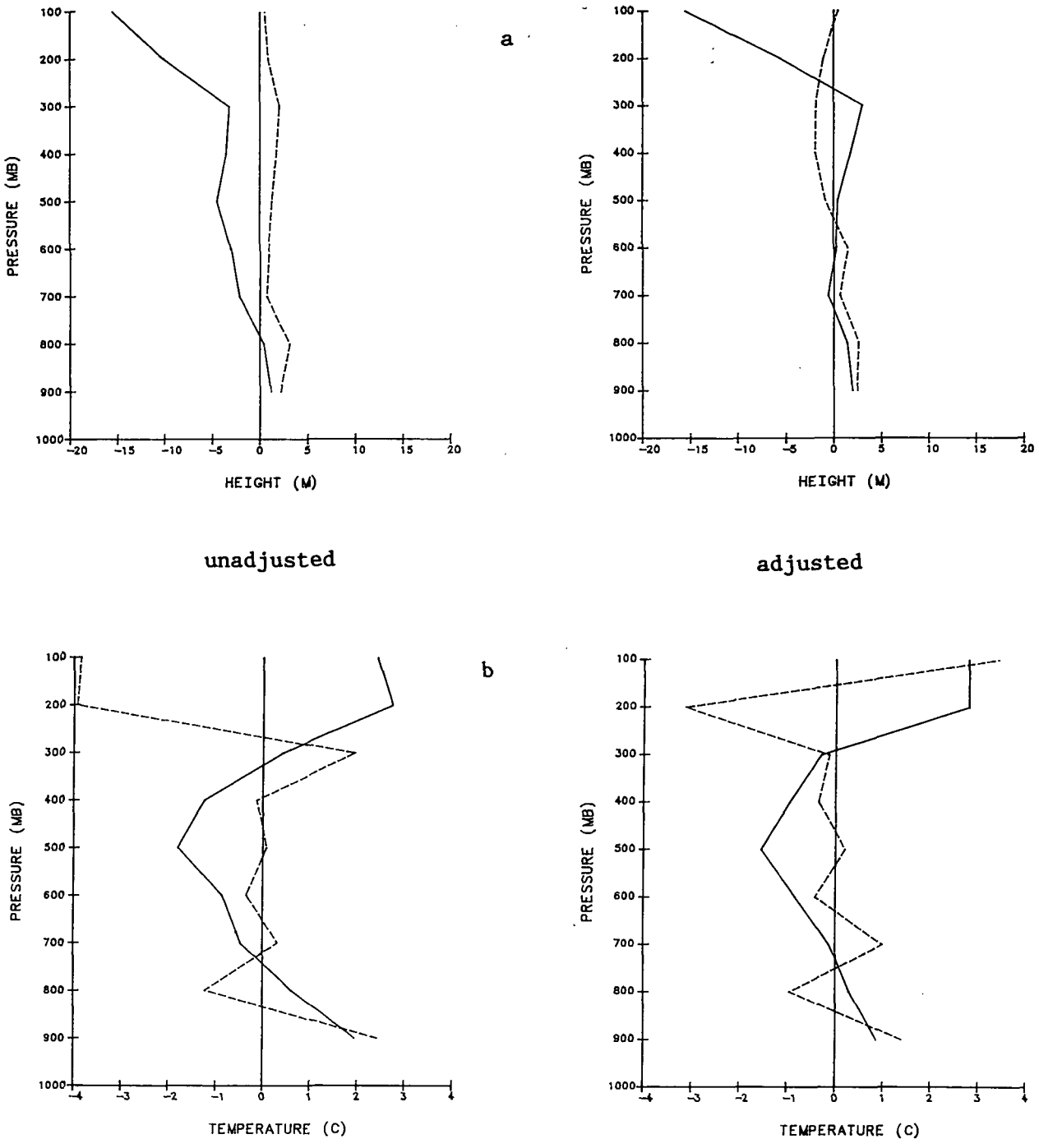

Fig. 4. RMS differences between unadjusted (adjusted) fields and observations after removal of standard observation error (solid lines) and means of differences between unadjusted (adjusted) fields and observations (dashed lines) for a) heights, b) temperatures, c) u-comp, and d) v-comp.

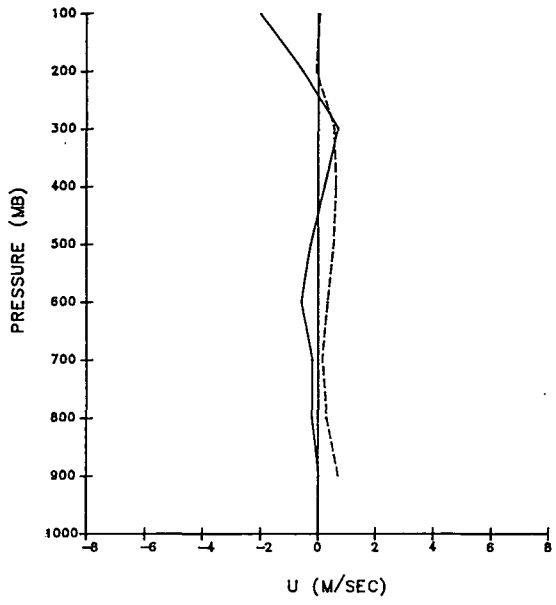

unadjusted

c

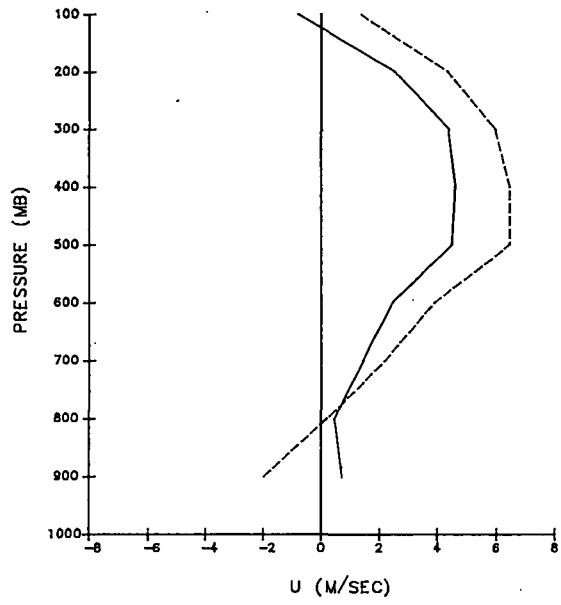

adjusted

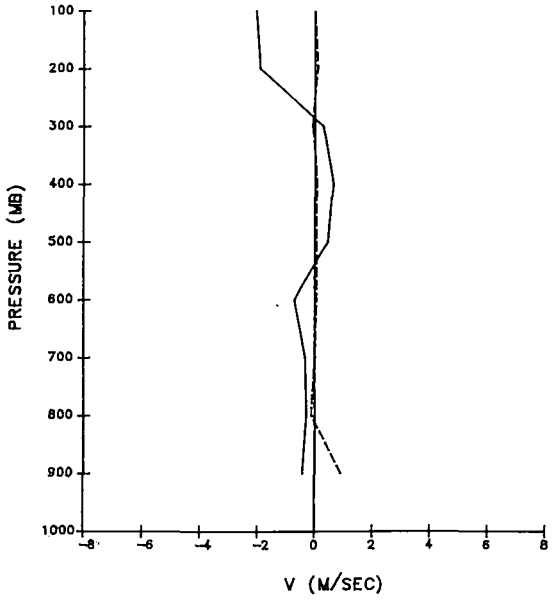

d

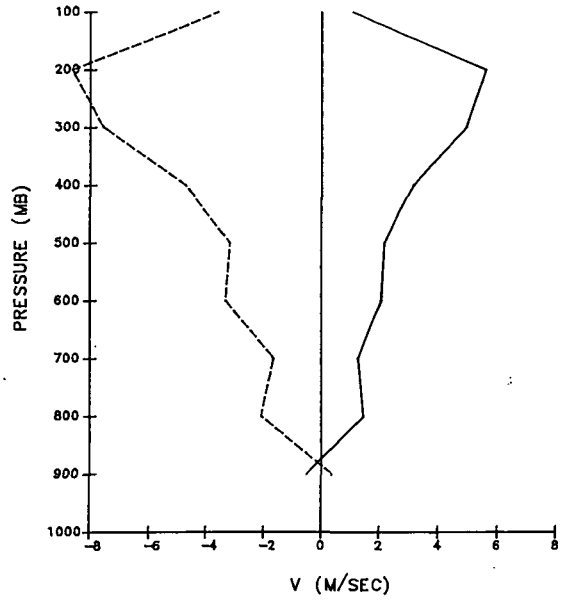

a b

300 mb

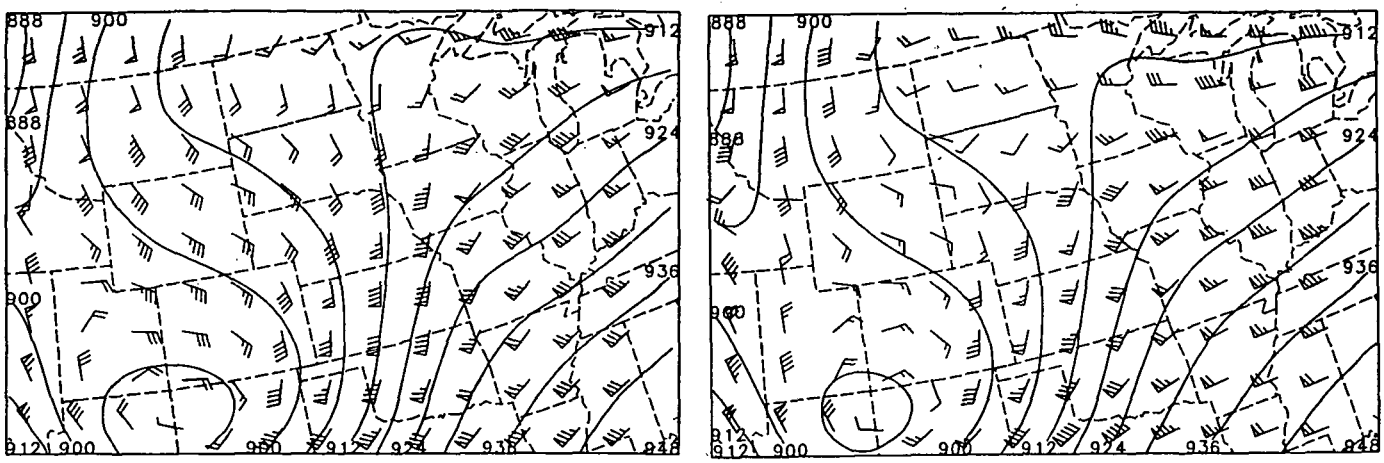

500 mb

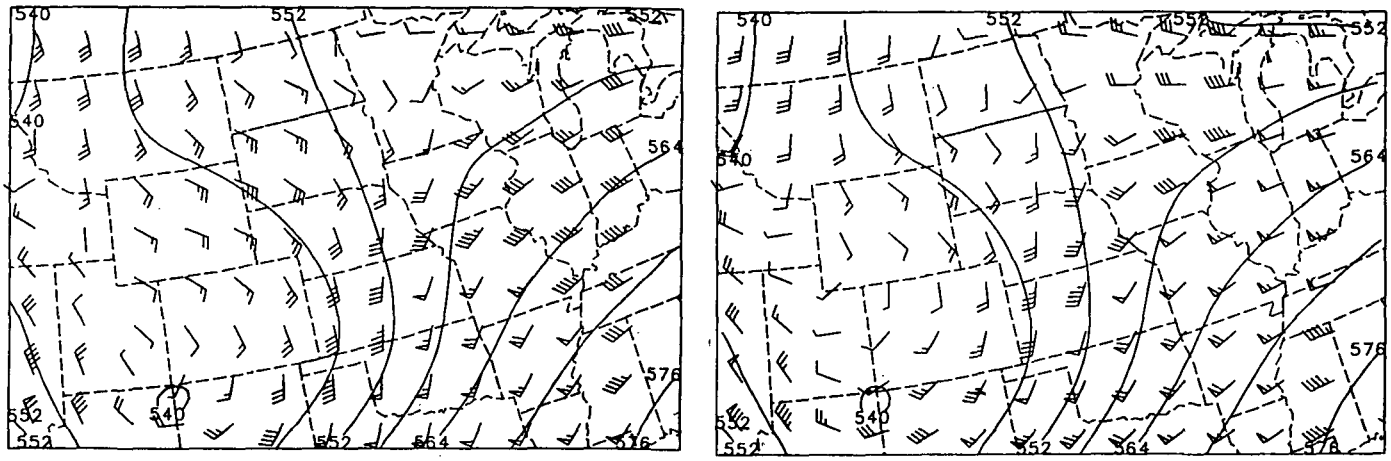

800 mb

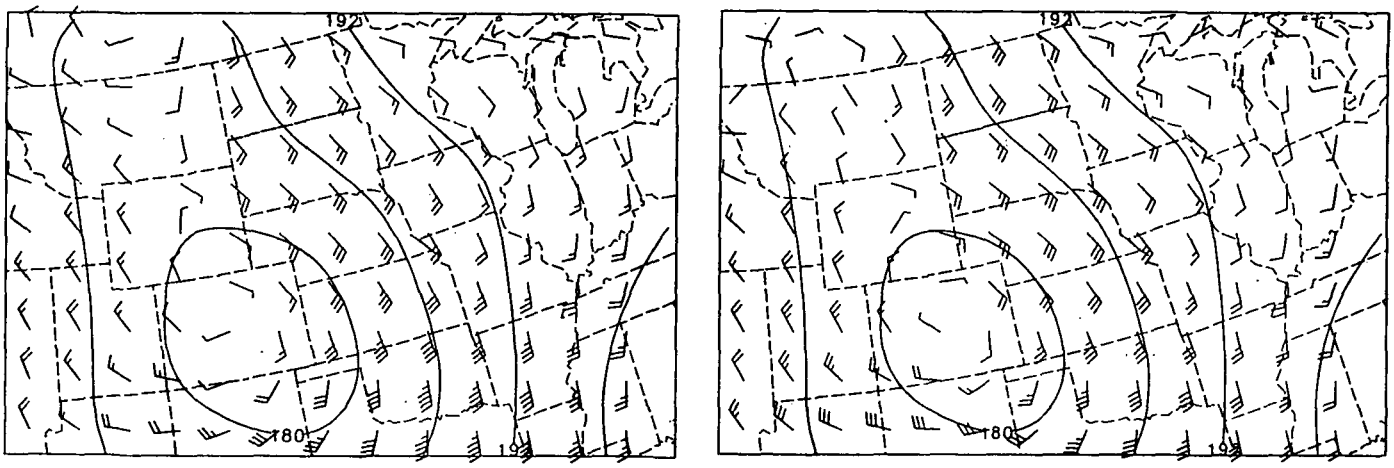

Fig. 5. Heights and wind vectors at 800 mb, 500 mb, and 300 mb for a) unadjusted and b) adjusted fields.

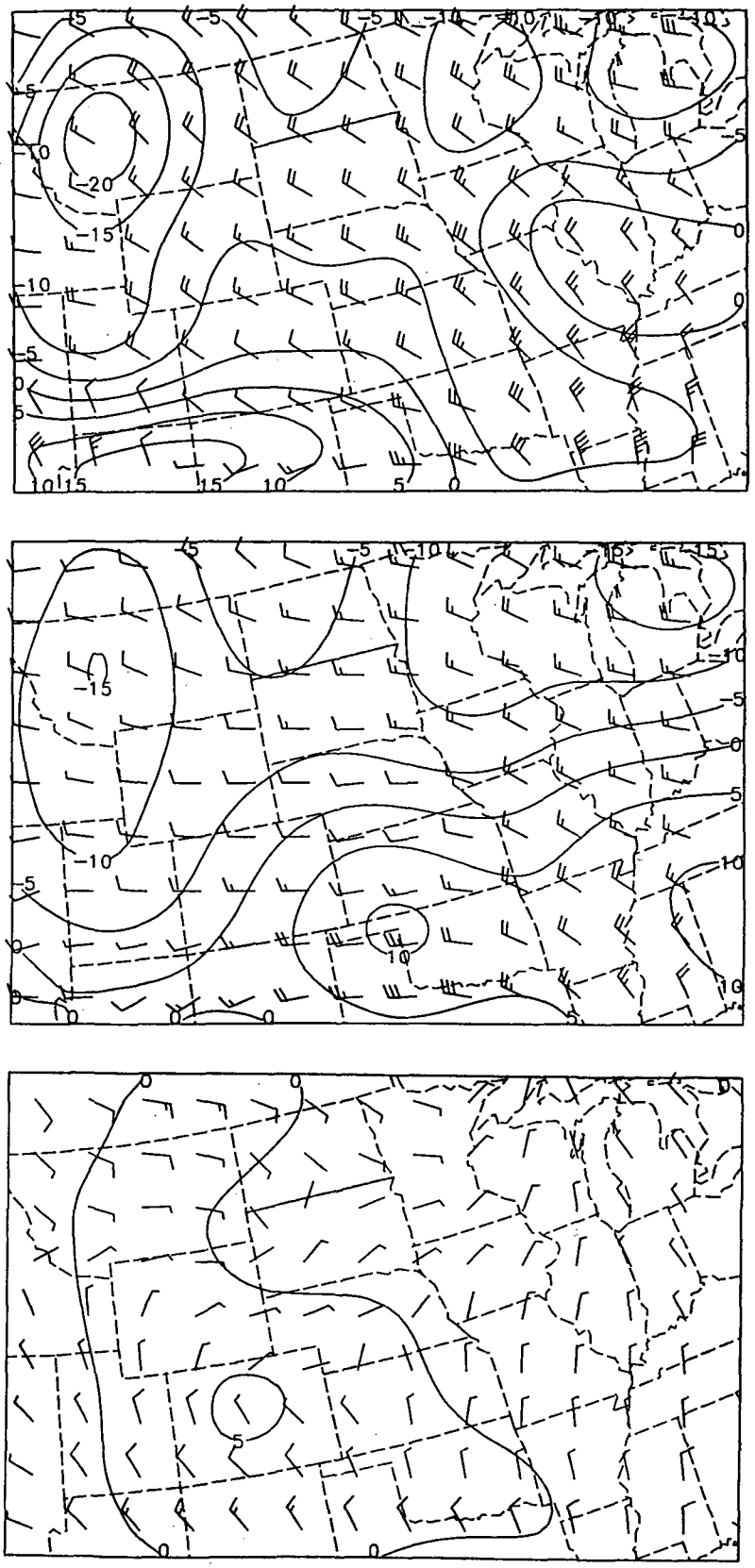

Fig. 6. Differences between adjusted and unadjusted heights and vector winds at 800 mb, 500 mb, and 300 mb.

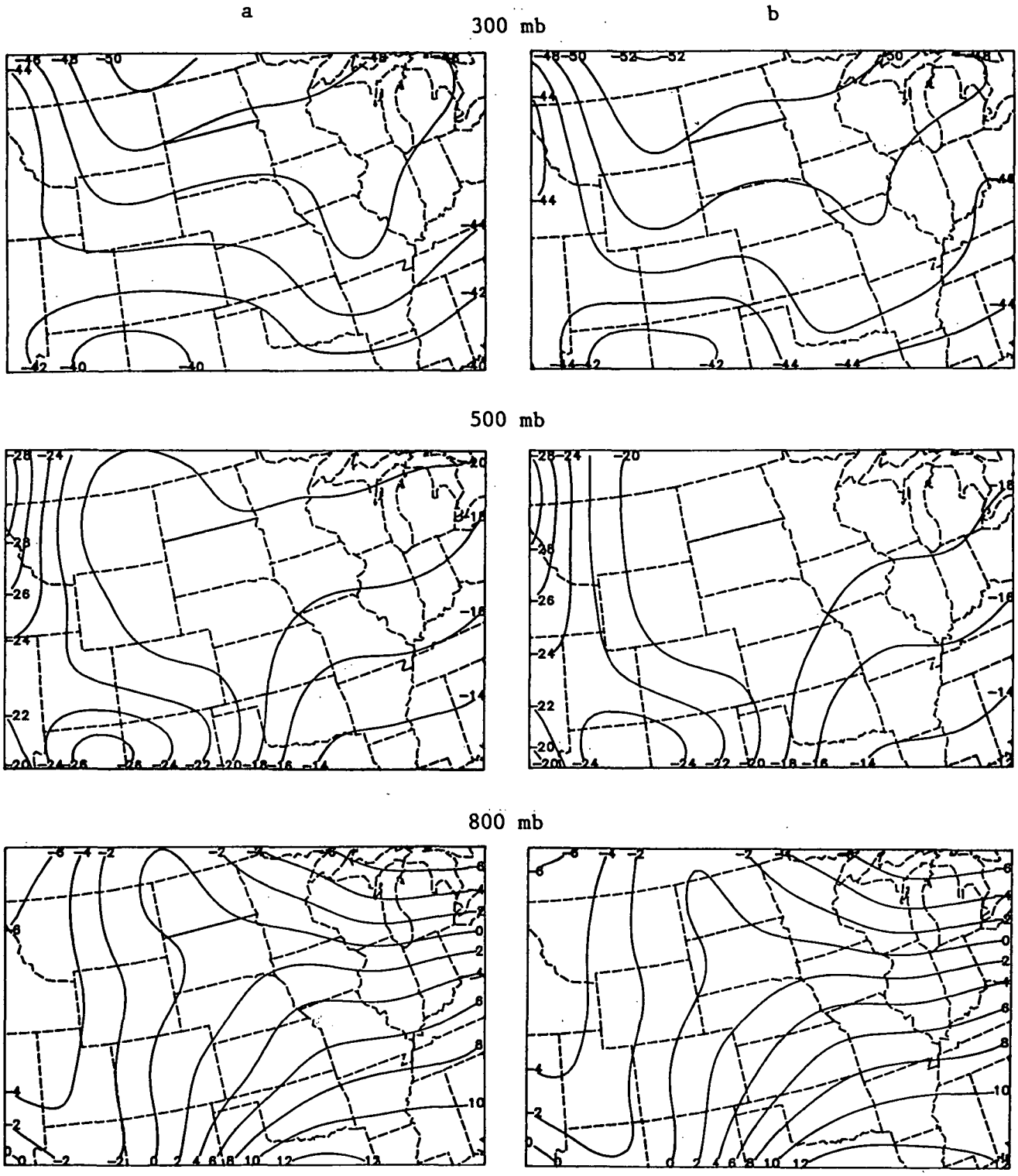

Fig. 7. Same as Fig. 5 but for temperature.

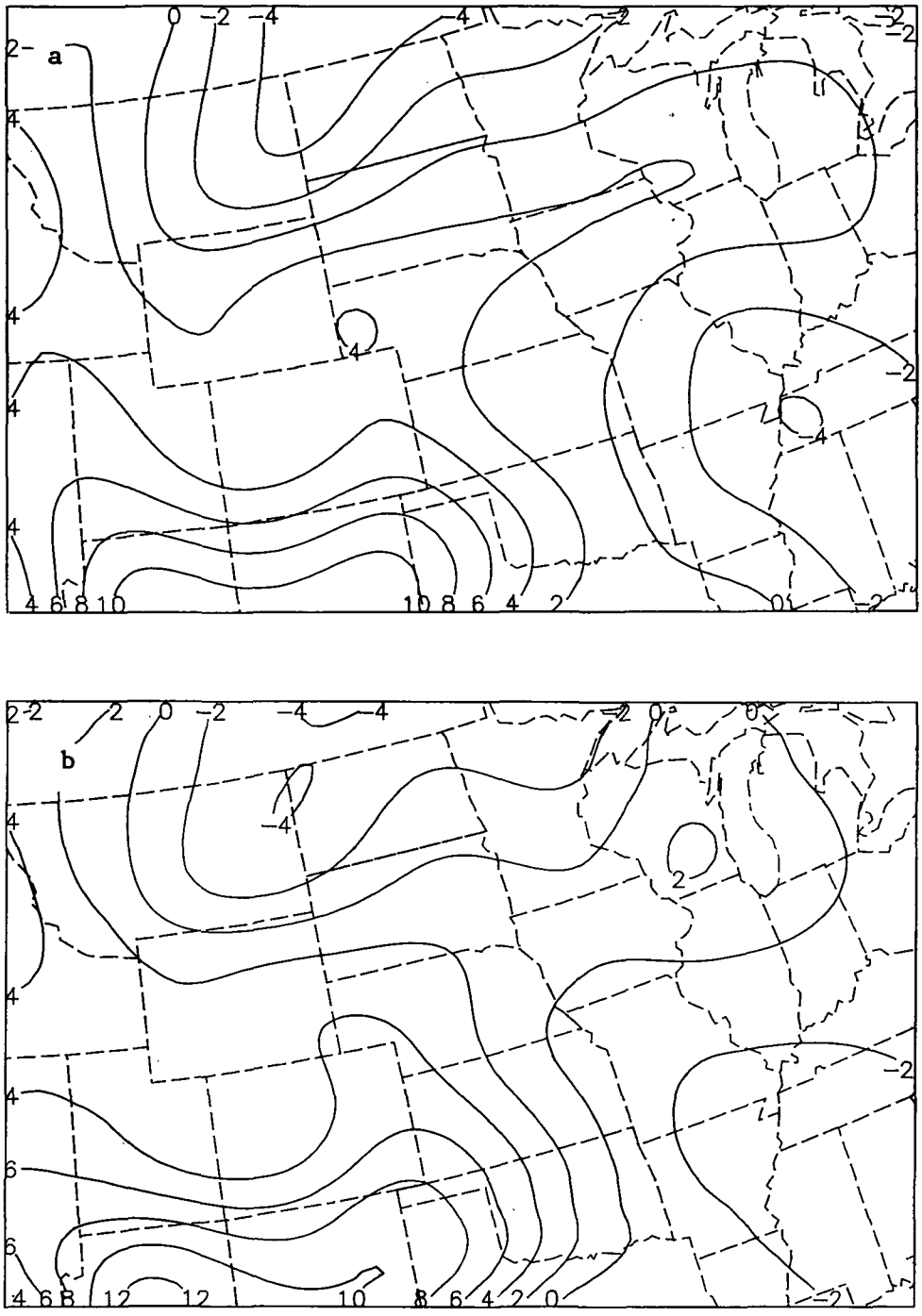

Fig. 8. Relative vorticities at 500 mb, a) unadjusted and b) adjusted.

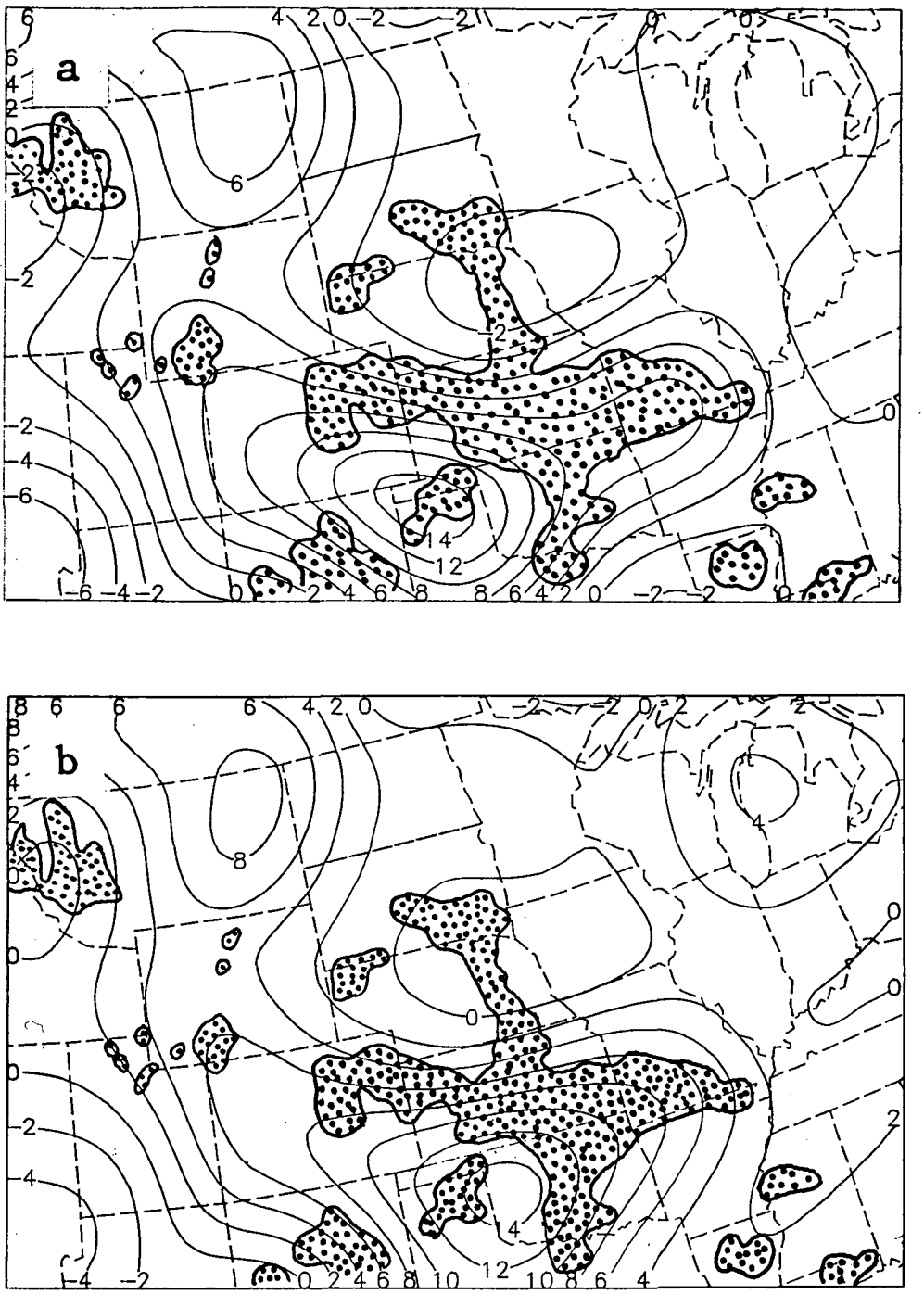

Fig. 9. a) unadjusted, b) adjusted vertical velocities (cm sec^{-1}) at 500 mb. Precipitation areas are stippled.

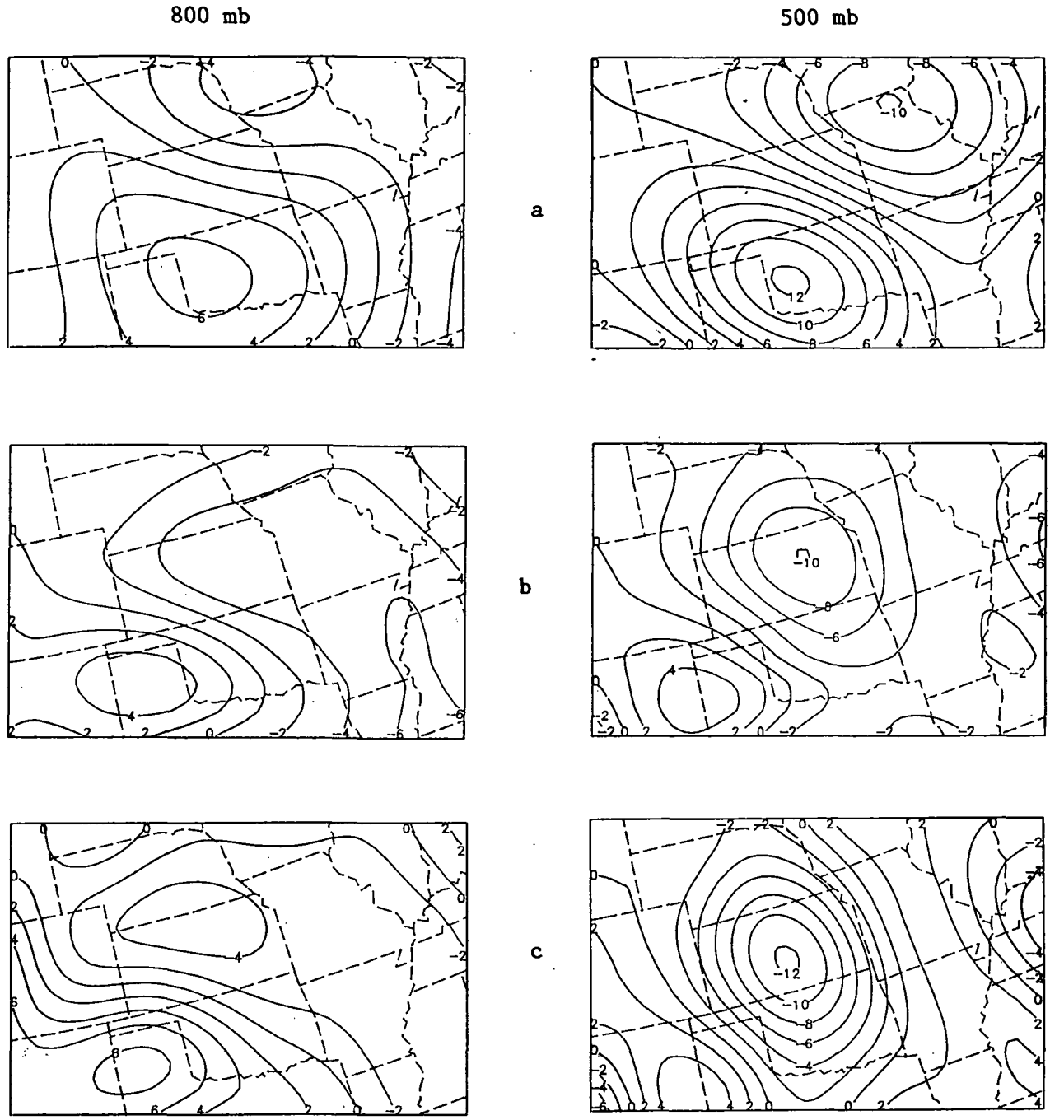

Fig. 10. u-component tendencies for 800 mb (left panels) and 500 mb (right panels) for a) observed, b) unadjusted, and c) adjusted fields in m sec^{-1} 3-hr^{-1}.

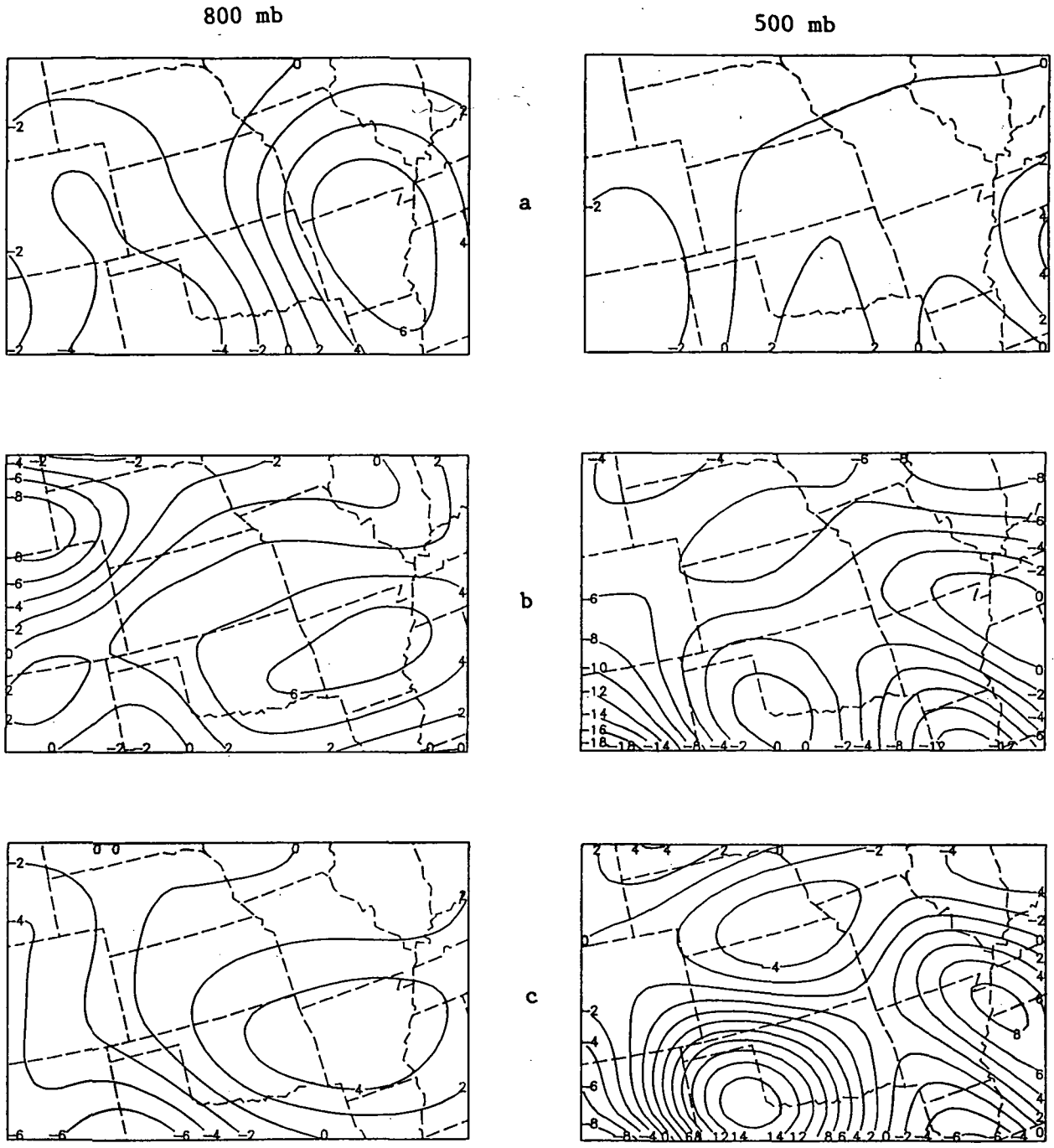

Fig. 11. Same as Fig. 10 but for the v-component.

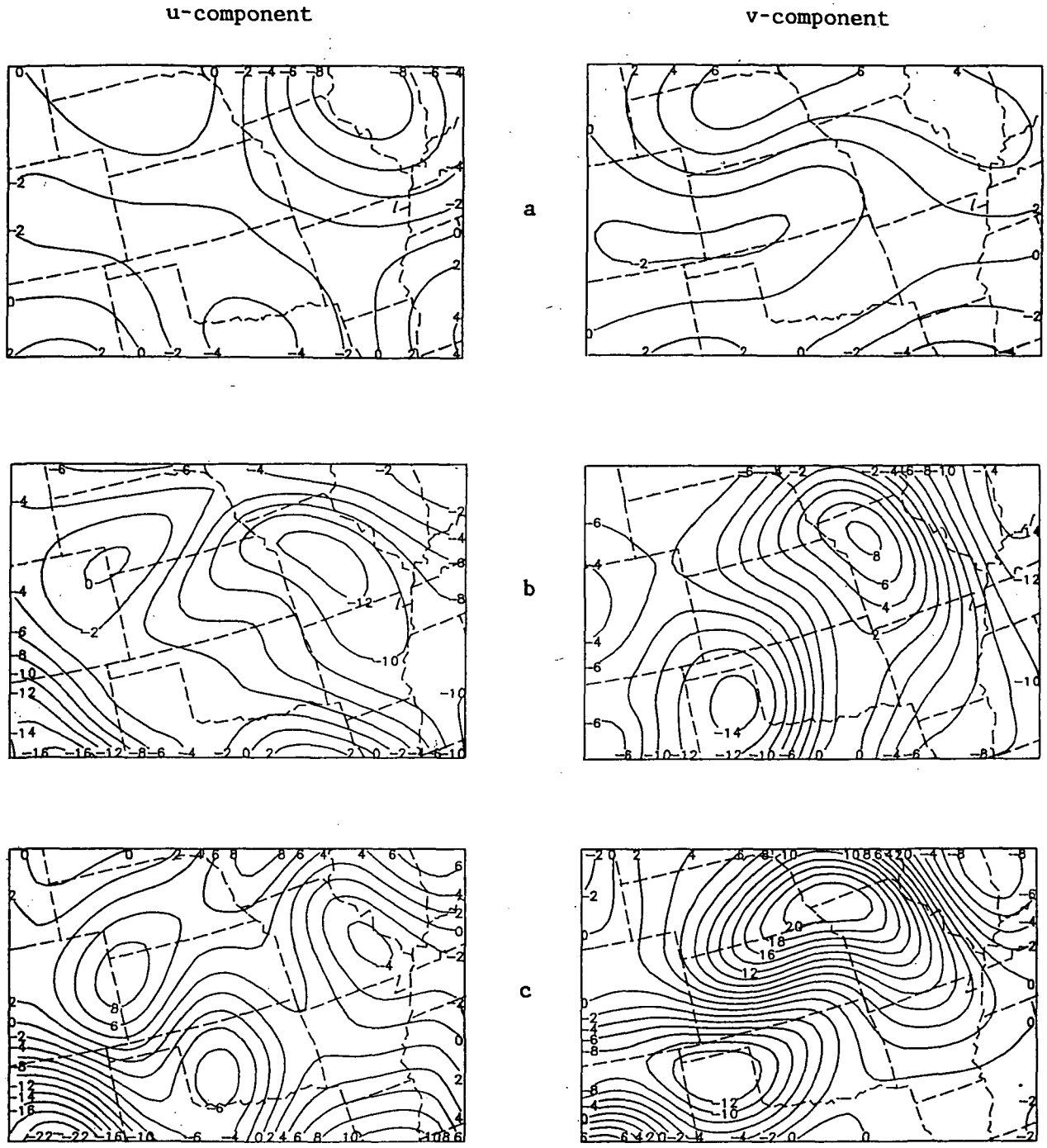

Fig. 12. u-component tendencies (left panels) and v-component tendencies (right panels) at 300 mb for a) observed, b) unadjusted, and c) adjusted fields in m sec^{-1} 3-hr^{-1}.

Chapter IV

A Variational Formalism for the Radiative Transfer Equation: Prelude to MODEL III

Gary L. Achtemeier
Office of Climate and Meteorology
Division of Atmospheric Sciences
Illinois State Water Survey
Champaign, IL 61820

1. Introduction

The MODEL III variational data assimilation model is the third of four general assimilation models designed to blend weather data measured from space-based platforms into the meteorological data mainstream in a way that maximizes the information content of the satellite data. Because there are many different observation locations and there are many instruments with different measurement error characteristics, it is also necessary to require that the blending be done to maximize the information content of the data and simultaneously to retain a dynamically consistent and reasonably accurate description of the state of the atmosphere. This is ideally a variational problem for which the data receive relative weights that are inversely proportional to measurement error and are adjusted to satisfy a set of dynamical equations that govern atmospheric processes. Because of the complexity of this type of variational problem, we have divided the problem into four variational models of increasing complexity. The first, MODEL I, includes as dynamical constraints the two horizontal momentum equations, the hydrostatic equation, and an integrated continuity equation. The second, MODEL II includes as dynamical constraints, the equations of MODEL I plus the thermodynamic equation for a dry atmosphere. MODEL III includes the equations of MODEL II plus the radiative transfer equation.

The advantage of MODEL III over the previous two models is that radiance, the atmospheric variable measured by satellite, becomes a dependent variable. In the previous versions, mean layer temperatures that had been retrieved from the radiances by some method, were included in the assimilation by substituting them in place of the rawinsonde temperatures. Now both rawinsonde temperatures and satellite radiances are included independently in the assimilation.

Our approach to the development of MODEL III has been to divide the problem into three steps of increasing complexity. Chapter IV deals with the first step, a variational version of the classical temperature retrieval problem that includes just the radiative transfer equation as a constraint. The radiances for each of the four TOVS MSU microwave channels are dependent variables. These plus temperature constitute a set a five adjustable variables. Each radiance is related to the temperature through its radiative transfer equation. There are therefore four dynamic constraints in this first variational problem.

Chapter V summarizes the second step which combines the four radiative transfer equations of the first step with the equations for a geostrophic and hydrostatic atmosphere. This step is intended to bring radiance into a three-dimensional balance with wind, height, and temperature. The use of the geostrophic approximation in place of the full set of primitive equations allows for an easier evaluation of how the inclusion of the radiative transfer equation increases the complexity of the variational equations.

The third and final step includes the four radiative transfer equations with the fully nonlinear set of primitive equations, ie., MODEL III.

2. A Variational Retrieval Algorithm

The radiative transfer equation is the only variational constraint. It takes the form

$$B - B_o w_o - \int_0^\infty w' T dz = 0 \qquad (1)$$

where B is the brightness temperature as computed from radiance measured at the satellite and T is the mean layer temperature of an incremental depth of the atmosphere, dz. The weight, w_0, is the transmittance of the total atmosphere from the surface (where the surface brightness temperature, B_0, is measured) to the space-based observation platform. The weights, w', are proportional to the transmittance from some level within the atmosphere to the satellite. In order to make the variational derivations from (1) compatible with the larger set of variational equations in MODEL I and MODEL II, we will make the following modifications in (1). First, the brightness temperature is replaced by the skin temperature, T_0, and the weight, w_0, will become a skin level surface weight. Second, (1) is converted from the z to the sigma vertical coordinate. In this conversion,

$$\int_0^\infty w'Tdz-\int_0^\infty w'T[f(T)]\,d\sigma-\int_0^\infty wTd\sigma \tag{2}$$

Now f(T), a small conversion term that results from the changeover to sigma coordinates, will be combined with the weights and not subjected to variation. This approach avoids complicated nonlinear equations that will otherwise arise through the variational formations. The f(T) and the weak temperature dependence in the weights will not be held constant however. At each step of a converging iterative process, the small temperature dependencies will be updated with adjusted temperatures. With these modifications, (1) becomes,

$$B-\int_0^\infty wTd\sigma=0 \tag{3}$$

The next step is to bring (3) into dimensional compatibility with the more general variational models. Let,

$$T=\theta T'=\frac{gH}{R}T' \tag{4}$$

and

$$T'=T_R+\frac{F}{R_o}T'' \tag{5}$$

so that,

$$T = \frac{gH}{R}\left(T_R + \frac{F}{R_o}T''\right) \tag{6}$$

Here g is gravity, H=10 km is a reference height, R is the universal gas constant, F is the Froude number, and R_o is the Rossby number. The subscript R refers to a reference atmosphere and the notation " refers to departures from the reference atmosphere. Substitution of (6) in place of T in (3) gives,

$$B - \frac{gH}{R}\left[\int_0^\infty wT_R\,d\sigma + \frac{F}{R_o}\int_0^\infty wT''\,d\sigma\right] = 0 \tag{7}$$

Further, we partition $B = B_R + B_m$ and define

$$B_R = \frac{gH}{R}\int_0^\infty T_R\,d\sigma \tag{8}$$

It follows then, that

$$B'' = \frac{gH}{R}\frac{F}{R_o}B_m \tag{9}$$

Finally, upon suppression of the double primes, the radiative transfer equation becomes,

$$B-\sum_{k-1}^{K} w_k T_k=0 \tag{10}$$

Now there are four TOVS microwave channels each with an independent measurement of the brightness temperature. Let B_j be the brightness temperature perturbation for the jth channel. The J constraining equations are,

$$m_j=B_j-\sum_{k-1}^{K} w_{kj} T_k=0 \tag{11}$$

The functional to be minimized is

$$F=\int I d\sigma \tag{12}$$

where

$$I=\sum_{k-1}^{K} \pi_k (T_k-T_k^o)^2+\sum_{j-1}^{J} \pi_j (B_j-B_j^o)^2+2\sum_{j-1}^{J} \lambda_j m_j \tag{13}$$

Performing the variations upon T and B as shown by Achtemeier, et al. (1986) yields the following Euler-Lagrange equations,

$$\delta T: \quad \pi_k (T_k-T_k^o) -\sum_{j-1}^{J} w_{kj} \lambda_j=0 \tag{14}$$

for each k and,

$$\delta B: \quad \pi_j (B_j - B_j^o) + \lambda_j = 0 \tag{15}$$

for each j. Variation upon the J Lagrange multipliers restore the original constraints (11). These equations are linear and may be easily reduced to one diagnostic equation in temperature. First, eliminate reference to the Lagrangian multipliers by substituting (15) into (14). Then substituting for B_j gives the adjusted temperature as a function of weight functions and observed variables,

$$\pi_k T_k + \sum_{i=1}^{K} \sum_{j=1}^{J} \pi_j w_{kj} w_{ij} T_i - F_k = 0 \tag{16}$$

for each k. Here

$$F_k = \pi_k T_k^o + \sum_{j=1}^{J} \pi_j B_j^o \tag{17}$$

Equation (16) can be easily solved with a standard matrix inversion package to retrieve the variationally adjusted temperature profile. At most two cycles with the weight functions updated with adjusted temperatures are required for convergence to a final adjusted temperature.

4. Results

In order to properly interpret the results of the example of variational adjustment with the radiative transfer equation, one must be aware that three sets of weights appear in (16). The weights, w_{ij}, are the transmittance weights for the ith level and the jth microwave channel. They are not subject to the variational adjustment and remain unchanged with the exception of minor adjustments for temperature sensitivity. The variational weights, π_j and π_k, carry the relative importance of the jth microwave channel and the temperature at the kth level. It is the choice of the variational weights that are important in interpreting the results.

Consider a temperature profile that is to be retrieved from MSU brightness temperatures. It is to be made halfway between two rawinsonde sites. The rawinsonde soundings are given by A and B in Fig. 1. Sounding A is cold up to the tropopause (about 220 mb) and then it becomes isothermal up to 60 mb. Sounding B is warm from the surface to 170 mb and then becomes colder than A in the layer from 170 mb to 60 mb. Its tropopause is located at 100 mb.

The first guess or "observed" sounding that will enter into the temperature part of the variational analysis is the mean of A and B. It is given by M in Fig. 1. Now suppose that the true sounding is given by T. Note that M=T from the surface to 230 mb and from 50 mb to the top.

Next, the brightness temperatures, B_j, were calculated from (10) using the true temperature sounding. Thus the B_j° that enter (17) are true and the T_k° are approximate. However, only the temperatures between 100-230 mb need adjustment. The observational error for the temperature was 0.7 K and the weight accorded to the temperature was,

$$\pi_k = \frac{1}{2\sigma_T^2} = 1.0 \qquad (18)$$

Fig. 2 shows the results of three retrievals between 500 mb and the top. The dashed line is the difference M-T between the true and first guess temperature soundings. The other curves are the differences between the adjusted and the true temperatures for π_j that ranged in values from 10 to 100 to 1000. Note that the weights for the four MSU channels and hence the brightness temperatures were always equal.

Fig. 2 shows that increasing the brightness temperature weights progressively reduced the differences between the adjusted and true temperature soundings but by only 2.5 K. However, the retrievals also spread the adjustments throughout the depth of the sounding. Therefore, improvements where the M-T residuals were nonzero were offset by degraded temperatures throughout the reminder of the sounding - the errors being almost 2 K at 250 mb with lesser error elsewhere.

A more extensive analysis of the behavior of (16) found that the retrievals were sensitive to the vertical distribution of the

weights for the temperature hence the errors of observation for the temperature. If there existed some independent observations that could be used to estimate the accuracy of the first guess temperature as a function of height, then the retrievals could be focused into those locations where the M-T residuals were greatest. Consider possible accuracy functions given in Fig. 3. The effective temperature error at 150 mb is doubled by f(1) and is tripled by f(2). Therefore, the weights accorded to the temperature there are decreased by a factor of four for f(1) and a factor of nine for f(2).

Fig. 4 shows the residuals between the adjusted and true temperature profiles for the three retrievals when the accuracy function f(1) was applied to the temperature weights. The initial residual has been reduced by approximately 6 K. Fig. 5 shows the results for f(2). Additional reductions in the residuals over f(1) results were found between 150 and 100 mb. Fig. 6 summarizes the resulting temperature soundings for f(0), f(1), and f(2) if the weights for the brightness temperatures were π_j = 1000. The improvement of f(2) over f(1) is apparent between 150 and 100 mb but elsewhere the differences between the two retrievals are only a few tenths of a degree. This suggests that it is the shape of the accuracy function, not the magnitude, that determines where the variational adjustment will be focused.

Fig. 7 shows part of the temperature soundings T and M between 250 mb and 50 mb. The curve identified by V1 is the sounding that was obtained with the conditions that the weights for the first

guess temperature were constant with height. The sounding V2 results from the application of f(2) to the temperature weights.

The first step in the variational analysis of the radiative transfer equation succeeded in producing a variational algorithm that could be used to retrieve temperature from the four MSU channel brightness temperatures given a first guess temperature sounding. The results showed that the variational retrievals were subject to the same limitations as are retrievals by other methods, inability to accurately resolve temperatures near the tropopause spreads error though the whole retrieved sounding, unless some temperature accuracy function is employed to focus the retrieval. The identification of a data set that could be used for a temperature accuracy function and the derivation of the same is beyond the scope of this study.

REFERENCE

Achtemeier, G. L., H. T. Ochs, III, S. Q. Kidder, R. W. Scott, J. Chen, D. Isard, and B. Chance, 1986: A variational assimilation method for satellite and conventional data: Development of basic model for diagnosis of cyclone systems. NASA Con. Rept. 3981, 223 pp.

FIGURE CAPTIONS

Figure 1. Two typical temperature soundings A and B; the mean of A and B, sounding M; and true temperature sounding T used for sensitivity studies of variational temperature retrievals.

Figure 2. Dashed line: differences between the mean or first guess temperature sounding and true sounding. Solid lines: differences between variational temperature retrievals and true temperature sounding for the following choices of brightness temperature weights; sounding 1 (10), sounding 2 (100), sounding 3 (1000).

Figure 3. Curves for hypothesized temperature accuracy functions.

Figure 4. Same as Fig. 2 but for f(1).

Figure 5. Same as Fig. 4 but for f(2).

Figure 6. Differences between first guess and true temperature (dashed line) and variational temperature retrievals and true temperature for brightness temperature weights equal to 1000 for f(0), f(1), and f(2).

Figure 7. Parts of temperature soundings T and M between 250 mb and 50 mb. Sounding V1 is temperature retrieval with f(0) and sounding V2 is temperature retrieval with f(2).

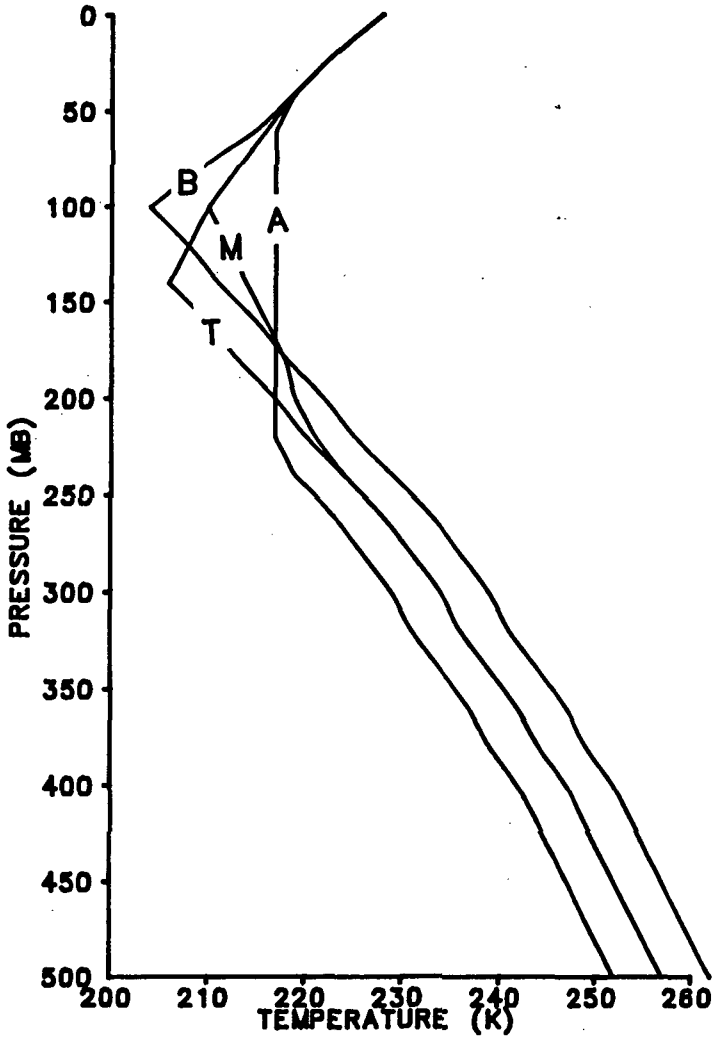

Figure 1. Two typical temperature soundings A and B; the mean of A and B, sounding M; and true temperature sounding T used for sensitivity studies of variational temperature retrievals.

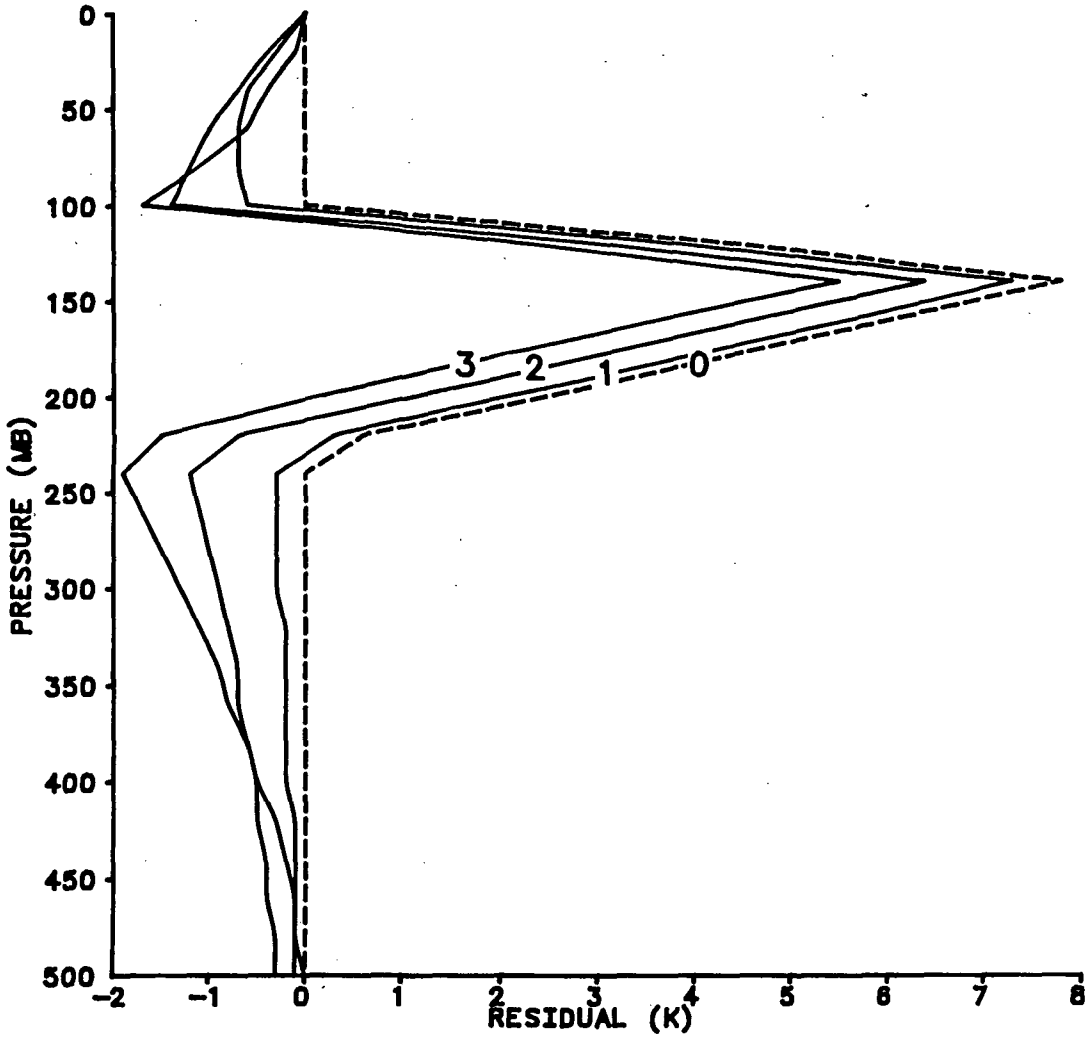

Figure 2. Dashed line: differences between the mean or first guess temperature sounding and true sounding. Solid lines: differences between variational temperature retrievals and true temperature sounding for the following choices of brightness temperature weights; sounding 1 (10), sounding 2 (100), sounding 3 (1000).

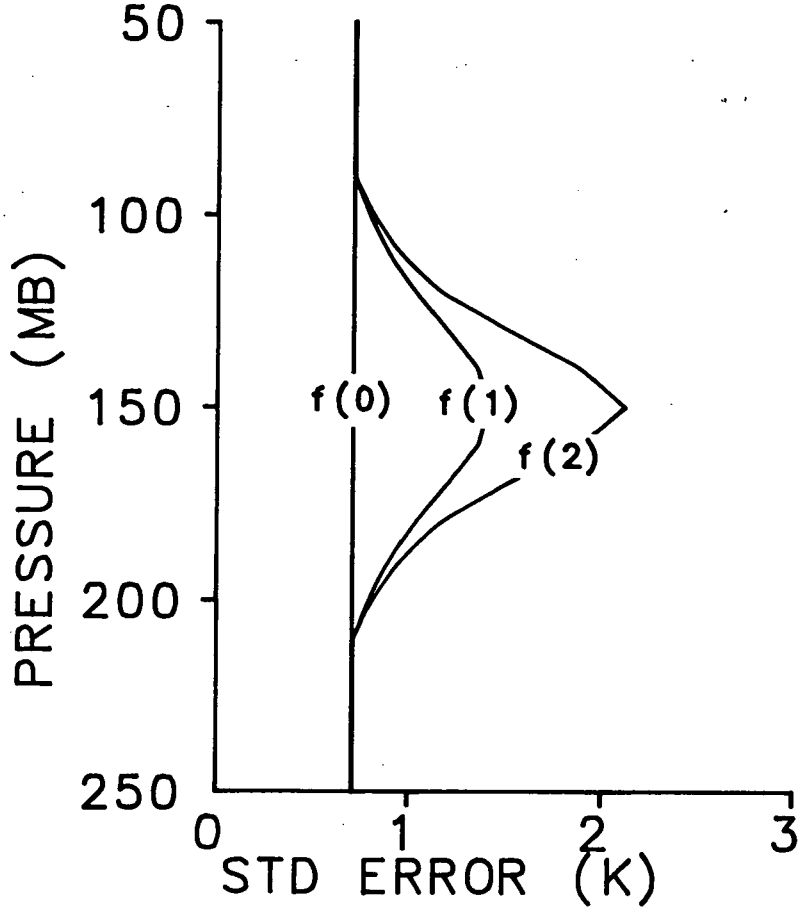

Figure 3. Curves for hypothesized temperature accuracy functions.

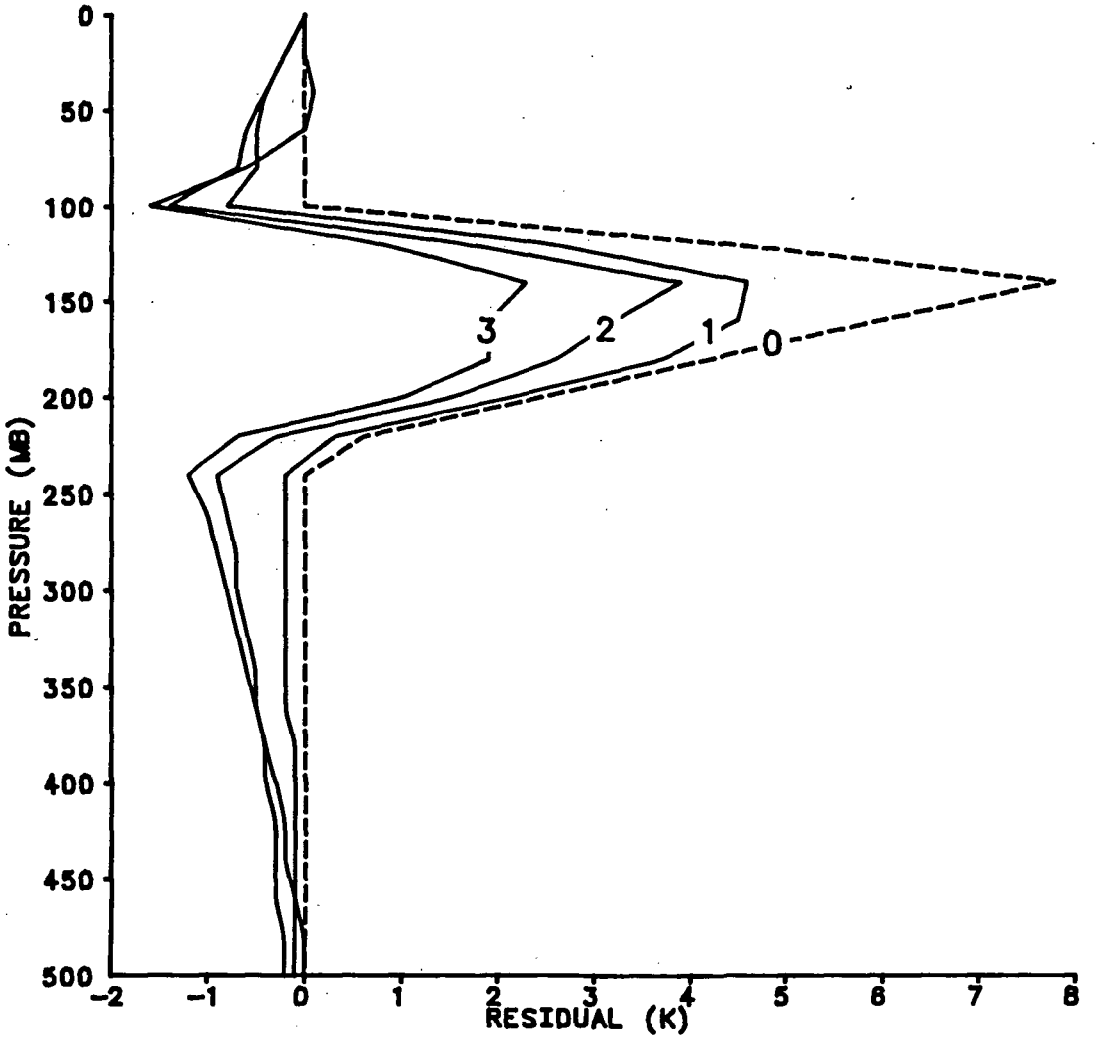

Figure 4. Same as Fig. 2 but for f(1).

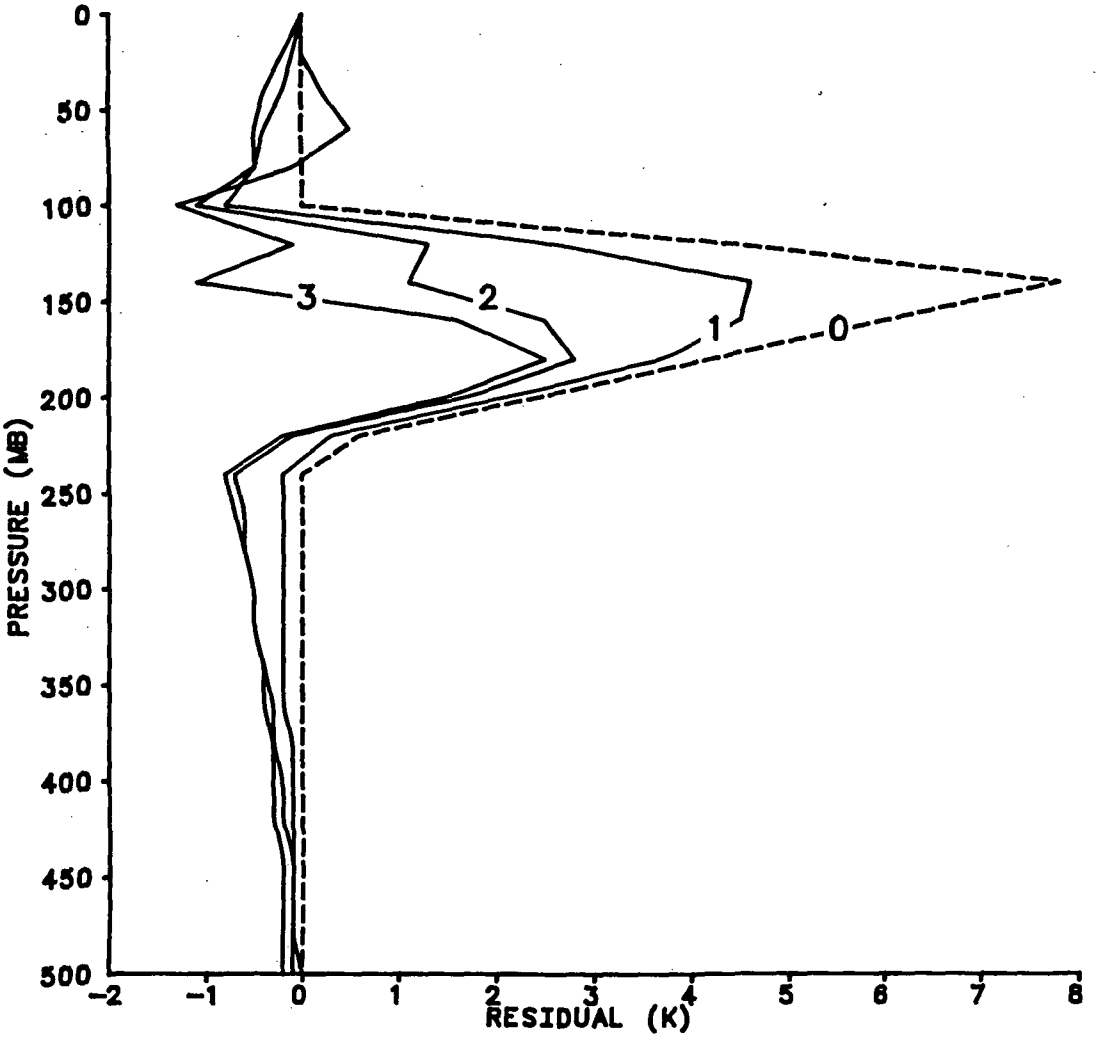

Figure 5. Same as Fig. 4 but for f(2).

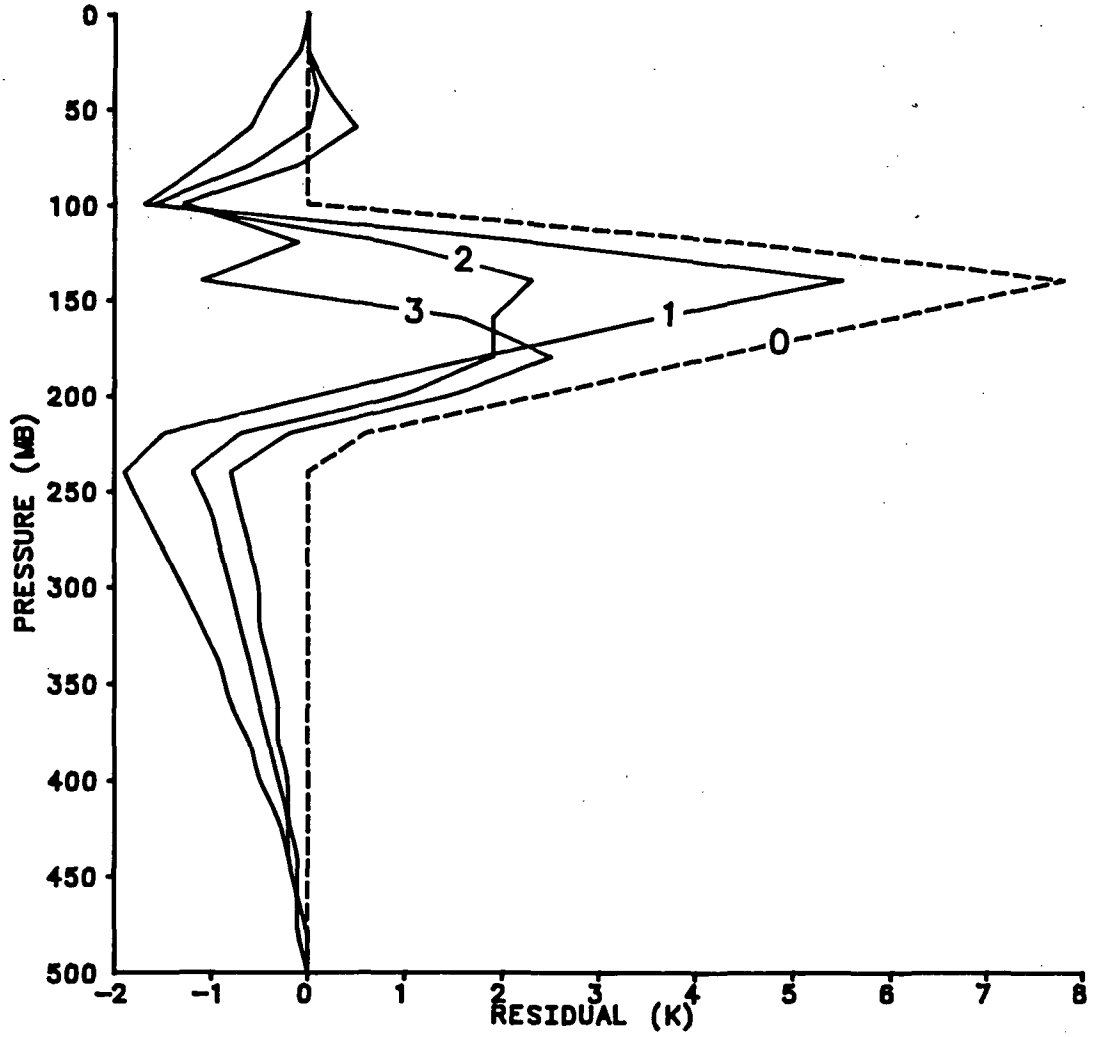

Figure 6. Differences between first guess and true temperature (dashed line) and variational temperature retrievals and true temperature for brightness temperature weights equal to 1000 for f(0), f(1), and f(2).

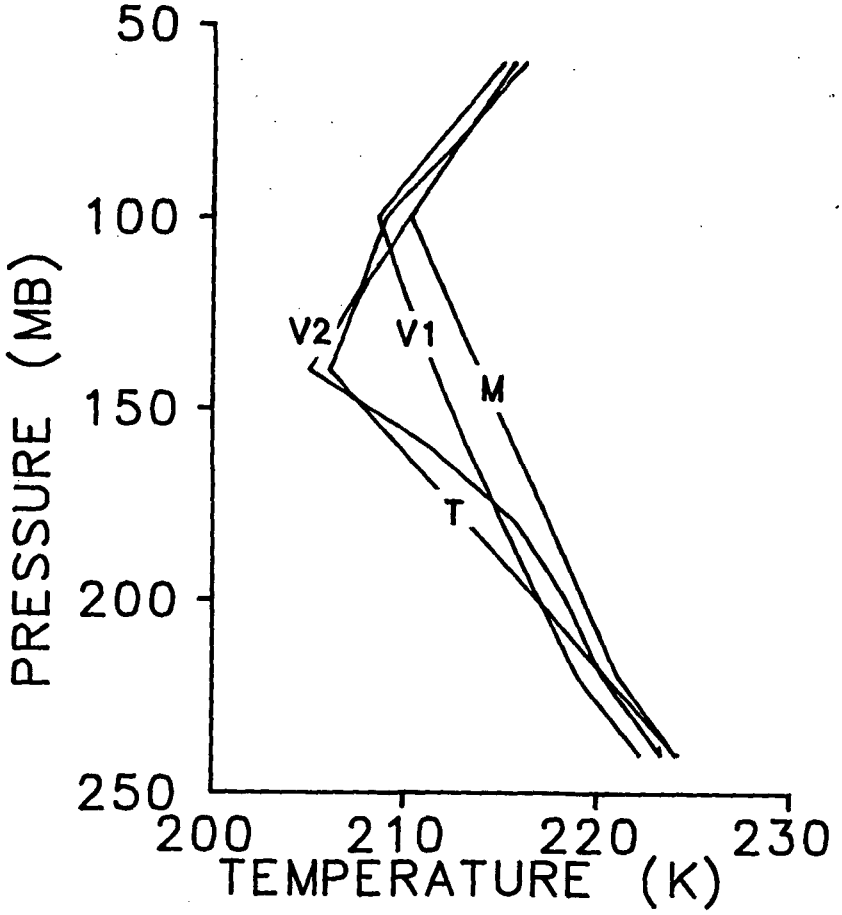

Figure 7. Parts of temperature soundings T and M between 250 mb and 50 mb. Sounding V1 is temperature retrieval with f(0) and sounding V2 is temperature retrieval with f(2).

Chapter V

A Variational Formalism for the Radiative Transfer Equation and a Geostrophic, Hydrostatic Atmosphere: Prelude to MODEL III

Gary L. Achtemeier
Office of Climate and Meteorology
Division of Atmospheric Sciences
Illinois State Water Survey
Champaign, IL 61820

1. Introduction

The approach to the development of MODEL III has been to divide the problem into three steps of increasing complexity. In Chapter IV we successfully developed a variational algorithm for the classical temperature retrieval problem that includes just the radiative transfer equation as a constraint. The radiances for each of the four TOVS MSU microwave channels were dependent variables.

Chapter V summarizes the second step which combines the four radiative transfer equations of the first step with the equations for a geostrophic and hydrostatic atmosphere. This step is intended to bring radiance into a three-dimensional balance with wind, height, and temperature. The use of the geostrophic approximation in place of the full set of primitive equations allows for an easier evaluation of how the inclusion of the radiative transfer equation increases the complexity of the variational equations.

It should be noted that the variational method is a powerful mathematical tool and a powerful method for diagnosing the physical role of the observations in the adjustment. We developed seven different variational formulations for the geostrophic, hydrostatic and radiative transfer equations. The first derivation was too complex to yield solutions that were physically meaningful. For the remaining six derivations, the variational method gave the same physical interpretation - the observed brightness temperatures could provide no meaningful input into a geostrophic, hydrostatic balance - at least through the problem-solving methodology employed

in these studies. It would be axiomatic therefore, that the brightness temperatures could provide no meaningful input into a variational assimilation with the primitive equations.

During the writing of this chapter, the equations were reviewed and a conceptual error regarding one of the Lagrange multipliers was discovered.

In the following section, the variational methodology is presented and the Euler-Lagrange equations rederived for the geostrophic, hydrostatic and radiative transfer equations. Then the equations are reduced in number through elimination of variables to produce a single equation for the geopotential height. It is shown that the single equation is too difficult to solve but that a three equation set can be solved iteratively. It is also shown that space-based thermodynamic data can be assimilated into the meteorological data mainstream and that none of the difficulties associated with traditional temperature retrievals will be encountered.

2. A Variational Assimilation Theory for the Geostrophic, Hydrostatic and Radiative Transfer Equations

The variational formalism will be derived for the four radiative transfer equations in integral form. Let the dynamical constraints be,

$$m_2 - \phi_\sigma + \gamma T + \beta = 0 \qquad (2)$$

$$\sum_{j-1}^{J} m_{1j} - \sum_{j-1}^{J} \left(B_j - \int_0^{\infty} w_j T d\sigma - 0\right) \tag{1}$$

$$m_3 = v - \phi_x - F_5 = 0 \tag{3}$$

$$m_4 = u + \phi_y + F_6 = 0 \tag{4}$$

For additional simplification, set the terrain correction term ß=0. The forcing functions F_5 and F_6 (see Chapter II) are simplified through setting $R_o = 0$.

The integrand of the functional to be minimized is,

$$\begin{aligned} I = {} & \pi_1 (u-u^o)^2 + \pi_1 (v-v^o)^2 + \pi_2 (T-T^o)^2 + \pi_3 (\phi-\phi^o)^2 \\ & + \sum_{j-1}^{J} \pi_{4j} (B_j - B_j^o)^2 + 2\sum_{j-1}^{J} \lambda_{1j} m_{1j} + 2\lambda_2 m_2 + 2\lambda_3 m_3 + 2\lambda_4 m_4 \end{aligned} \tag{5}$$

where the π_i are the relative weights accorded to the observations.

Performing the variations for the eight dependent variables, u, v, Φ, T, and B_j (j=1,4), yields the following Euler-Lagrange equations,

$$\delta u: \quad \pi_1 (u-u^o) + \lambda_4 = 0 \tag{6}$$

$$\delta v: \quad \pi_1 (v-v^o)+\lambda_3=0 \tag{7}$$

$$\delta \phi: \quad \pi_3 (\phi-\phi^o)-\lambda_{2\sigma}+\lambda_{3x}-\lambda_{4y}=0 \tag{8}$$

$$\delta T: \quad \pi_2 (T-T^o)+\gamma\lambda_2-\sum_{j-1}^{J}\lambda_{1j}\int_0^{\infty} w_j d\sigma=0 \tag{9}$$

$$\delta B: \quad \sum_{j-1}^{J}[\pi_{4j}(B_j-B_j^o)+\lambda_{1j}=0] \tag{10}$$

These eight equations plus the seven original constraints constitute a set of 15 algebraic and linear partial differential equations to be solved. The number of equations may be reduced through the elimination of variables. There results a single diagnostic equation with geopotential height as the dependent variable. We develop a diagnostic equation for the geostrophic, hydrostatic adjustment first and then include the contribution from the radiative transfer equations. Two Lagrange multipliers are eliminated by combining (6), (7), and (8). Then, forming the vorticity from (3) and (4) and combining with (8) gives,

$$\pi_1\nabla^2\phi-\pi_3\phi+\lambda_{2\sigma}-\pi_1(v_x^o-u_y^o)+\pi_3\phi^o+\pi_1(F_{5x}+F_{6y})=0 \tag{11}$$

Reducing the thermodynamic variables is done as follows. Divide (9) by γ and operate by σ. Eliminate brightness temperature between (1) and (10). There results two equations,

$$\frac{\partial}{\partial\sigma}\left[\frac{\pi_2}{\gamma}(T-T^o)\right]+\lambda_{2\sigma}-\sum_{j-1}^{J}\lambda_{1j}\epsilon_j=0 \tag{12}$$

where,

$$\epsilon_j=\frac{\partial}{\partial\sigma}\left[\frac{1}{\gamma}\int_0^\infty w_j d\sigma\right] \tag{13}$$

and,

$$\sum_{j-1}^{J}\left[\pi_{4j}\left(\int_0^\infty w_j T d\sigma - B_j^o\right)+\lambda_{1j}=0\right] \tag{14}$$

Combining (12) with (14) and substituting (2) gives,

$$\begin{aligned}\lambda_{2\sigma}=&-\frac{\pi_2}{\gamma^2}\phi_{\sigma\sigma}+\left(\frac{\pi_2\phi_\sigma}{\gamma^2}\right)_\sigma+\sum_{j-1}^{J}\epsilon_j\pi_{4j}\int_0^\infty\frac{w_j\phi_\sigma}{\gamma}d\sigma\\&+\left(\frac{\pi_2}{\gamma}T^o\right)_\sigma+\sum_{j-1}^{J}\epsilon_j\pi_{4j}B_j^o\end{aligned} \tag{15}$$

Eliminating the Lagrangian multiplier between (11) and (15) yields a diagnostic equation in the geopotential height,

$$\pi_1\nabla^2\phi+\frac{\pi_2}{\gamma^2}\phi_{\sigma\sigma}+\left(\frac{\pi_2\phi_\sigma}{\gamma^2}\right)_\sigma-\pi_3\phi+\sum_{j=1}^{J}\epsilon_j\pi_{4j}\int_0^\infty\frac{w_j\phi_\sigma}{\gamma}d\sigma+F=0 \qquad (16)$$

where,

$$F=\pi_1(v_x^o-u_y^o)+\pi_3\phi^o+\left(\frac{\pi_2}{\gamma}T^o\right)_\sigma+\sum_{j=1}^{J}\epsilon_j\pi_{4j}B_j^o+\pi_1(F_{5x}+F_{6y}) \qquad (17)$$

Much effort was spent programming for (16). The resulting solution was not considered satisfactory. Given the complex coefficient structures and the delicate convergence criteria, much additional effort was expended through six subsequent derivations to express the variational formalism in forms easier to understand and easier to solve. These efforts eventually led away from a direct inclusion of the radiative transfer equation in a geostrophic, hydrostatic atmosphere.

In retrospect, it seems that the solution could have been more easily obtained if the 15 equation set was reduced to the following 3 equation set:

$$\pi_1\nabla^2\phi-\pi_3\phi=-\lambda_{2\sigma}+\pi_1(v_x^o-u_y^o)-\pi_3\phi^o-\pi_1(F_{5x}+F_{6y}) \qquad (18)$$

$$T=-\frac{1}{\gamma}(\phi_\sigma+\beta) \qquad (19)$$

$$\lambda_2 = -\frac{\pi_2}{\gamma}(T-T^o) - \sum_{j-1}^{J}\left[\frac{\pi_{4j}}{\gamma}\int_0^\infty w_j d\sigma \left(\int_0^\infty w_j T d\sigma - B_j^o\right)\right] \qquad (20)$$

These equations can be solved iteratively by first setting $\lambda_2 = 0$ and solving (18) for Φ. Then (19) is solved for T and the temperature substituted into (20) to derive an updated λ_2. Then the updated values are entered into (18) and the cycle repeated until a satisfactory level of convergence is attained.

3. Results

There are three important points to consider regarding (18) - (20).

a) NO RETRIEVAL OF TEMPERATURE IS REQUIRED TO BLEND SATELLITE OBSERVED BRIGHTNESS TEMPERATURES INTO THE METEOROLOGICAL DATA MAINSTREAM. This means that none of the problems associated with temperature retrievals will be encountered. The integral term appears on the right hand side of (20) not as a term to be solved. This is analogous to solving the radiative transfer equation for the brightness temperature - a very easy exercise. This single finding may make it worth while to pursue the formal variational approach to assimilation of microwave channel data especially if higher resolution radiance data becomes available in the future.

b) There must be observations of geopotential height or winds or both of equivalent accuracy with the satellite measurements in order for the (18) - (20) to work. Accurate observations of temperature apart from space-based measurements are not necessary. The caveat is that geopotential height must be known at the boundaries of the domain in order to obtain a solution for (18). Lateral boundaries would vanish for the equations written on the sphere and the top boundary conditions can be removed to the top of the atmosphere or to some level where model predictions or climatology give satisfactory estimates.

c) It is highly probable that (18) - (20) converge to a solution. The same equation set with the absence of the second term of (20) (the radiative transfer equation contribution) is known to converge. The second term of (20) is an integral term which should further stabilize the solution.

The main goal of the variational assimilation project was to blend satellite-derived thermodynamic data into the meteorological data mainstream in a dynamically consistent way. The classical variational calculus method used to achieve that goal typically yields sets of complicated equations that require innovative methods for solution and also involve immense programming efforts. Therefore the effort was broken down into several simpler models that could be solved.

The attempt to reduce the equation set from 15 equations to one diagnostic equation in geopotential height resulted in equation (16). After an extensive programming effort, a satisfactory solution was not obtained. I was unable to devise a scheme that could determine whether the problems were mathematical or programmatical. During the six other efforts to derive a more tractable diagnostic equation a conceptual error was made, namely, λ_{1j} was treated as a variable that could be differentiated with respect to σ. The observed brightness temperature dropped out of the equations. This led to the conclusion that the satellite data could not be successfully included in a classical variational assimilation.

With the discovery of this error during the writing of Chapter 5 of this final report, that conclusion is no longer valid. It appears, instead, that the satellite data can be successfully incorporated into a variational assimilation and that the blending can be done without any of the problems typically encountered with temperature retrievals.

Chapter VI

On the Concept of Varying Influence Radii for a Successive Corrections Objective Analysis

Gary L. Achtemeier
Office of Climate and Meteorology
Division of Atmospheric Sciences
Illinois State Water Survey
Champaign, Illinois 61820

ABSTRACT

There has been a long-standing concept by those who use successive corrections objective analysis that the way to obtain the most accurate objective analysis is first, to analyze for the long wavelengths and then to build in the details of the shorter wavelengths by successively decreasing the influence of the more distant observations upon the interpolated values. Using the Barnes method, we compared the filter characteristics for families of response curves that pass through a common point at a reference wavelength. It was found that the filter cutoff is a maximum if the filter parameters that determine the influence of observations are unchanged for both the initial and corrections passes. This

information was used to define and test the following hypothesis. If accuracy is defined by how well the method retains desired wavelengths and removes undesired wavelengths, then the Barnes method gives the most accurate analyses if the filter parameters on the initial and corrections passes are the same. This hypothesis does not follow the usual conceptual approach to successive corrections analysis.

Theoretical filter response characteristics of the Barnes method were compared for filter parameters set to retrieve the long wavelengths and then build in the short wavelengths with the method for filter parameters set to retrieve the short wavelengths and then build in the long wavelengths. The theoretical results and results from analyses of regularly spaced data show that the customary method of first analyzing for the long wavelengths and building in short wavelengths is not necessary for the single correction pass version of the Barnes method. Use of the same filter parameters for initial and corrections passes improved the analyses from a fraction of a percent for long wavelengths to about ten percent for short but resolvable wavelengths.

However, the more sparsely and irregularly distributed the data, the less the results are in accord with the predictions of theory. Use of the same filter parameters gave better overall fit to the wavelengths shorter than eight times the minimum resolvable wave and slightly degraded fit to the longer wavelengths. Therefore, in the application of the Barnes method to irregularly spaced data, successively decreasing the influence of the more

distant observations is still advisable if longer wavelengths are present in the field of data.

It also was found that no single selection of filter parameters for the two-pass Barnes method gives the best analysis for all wavelengths. A three-pass hybrid method is shown to reduce this problem.

REFERENCE

Achtemeier, G. L., 1987: On the Concept of Varying Influence Radii for a Successive Corrections Objective Analysis. Mon. Wea. Rev., 115, 1760-1771.

Chapter VII

Modification of a Successive Corrections Objective Analysis for Improved Derivative Calculations

by

Gary L. Achtemeier
Climate and Meteorology Section
Illinois State Water Survey
Champaign, IL 61820

Abstract

The use of objectively analyzed fields of meteorological data for complex diagnostic studies and for the initialization of numerical prediction models places the requirements upon the objective method that derivatives of the gridded fields be accurate and free from interpolation error. A modification of an objective analysis developed by Barnes provides improvements in analyses of both the field and its derivatives. Theoretical comparisons, comparisons between analyses of analytical monochromatic waves, and

comparisons between analyses of actual weather data are used to show the potential of the new method. The new method restores more of the amplitudes of desired wavelengths while simultaneously filtering more of the amplitudes of undesired wavelengths. These results also hold for the first and second derivatives calculated from the gridded fields. Greatest improvements were for the Laplacians of the height field; the new method reduced the variance of undesirable very short wavelengths by 72 percent. Other improvements were found in the divergence of the gridded wind field and near the boundaries of the field of data.

REFERENCE

Achtemeier, G. L., 1989: Modification of a Successive Corrections Objective Analysis for Improved Higher Order Calculations. Mon. Wea. Rev., 117, 78-86.

OMIT TO END

Chapter VIII

PROJECT PUBLICATIONS

The following is a list of publications produced as part of the variational assimilation project.

REFERRED PUBLICATIONS

Achtemeier, G. L., 1986: On the impact of data boundaries upon the objective analysis of limited-area data sets. Mon. Wea. Rev., 114, 40-49.

Kidder, S.Q., and G. L. Achtemeier, 1986: Day-night variation in operationally-retrieved TOVS temperature biases. Mon. Wea. Rev., 114, 1175-1178.

Achtemeier, G. L., H. T. Ochs III, S. Q. Kidder, and R. W. Scott, 1986: Evaluation of a multivariate variational assimilation of conventional and satellite data for the diagnosis of cyclone systems. 49-54. Variational Methods in Geosciences. Developments in Geomathematics 5, Y. Sasaki, ed. Elsevier, Amsterdam, 309 pp.

Achtemeier, G. L., 1987: On the Concept of Varying Influence Radii for a Successive Corrections Objective Analysis. Mon. Wea. Rev., 115, 1760-1771.

Achtemeier, G. L., 1989: Modification of a Successive Corrections Objective Analysis for Improved Higher Order Calculations. Mon. Wea. Rev., 117, 78-86.

CONFERENCE PROCEEDINGS

Achtemeier, G. L., 1985: On the impact of data boundaries upon the objective analysis of limited-area data sets. Preprints, 7th Conf. on Num. Wea. Pred., Montreal, Que., Canada, 17-20 June 1985, Amer. Meteor. Soc.

Achtemeier, G. L., S.Q. Kidder, H. T. Ochs III, 1985: Variational Objective Analyses for Cyclone Studies. NASA/MSFC FY-85 Atmospheric Processes Research Review, NASA Conf. Pub. 2402, Columbia MD, 8-12 July 1985, pp. 26-28.

Achtemeier, G. L., H. T. Ochs III, S. Q. Kidder, and R. W. Scott, 1986: Evaluation of a multivariate variational assimilation of conventional and satellite data for the diagnosis of cyclone systems. PREPRINTS, 2nd Conf. on Sat. Meteor./Rem. Sensing and Appl. Williamsburg, VA, 13-16 May 1986, Amer. Meteor. Soc.

Kidder, S. Q., and G. L. Achtemeier, 1986: Preparation of satellite soundings for insertion in a variational objective analysis model. PREPRINTS, 2nd Conf. on Sat. Meteor./Rem. Sensing and Appl. Williamsburg, VA, 13-16 May 1986, Amer. Meteor. Soc.

Chance, B. A., and G. L. Achtemeier, 1986: Application of satellite data to the variational analysis of the three dimensional wind field. PREPRINTS, 2nd Conf. on Sat. Meteor./Rem. Sensing and Appl. Williamsburg, VA, 13-16 May 1986, Amer. Meteor. Soc.

Achtemeier, G. L., 1987: A 3-pass near optimum Barnes method for the univariate objective analysis of mesoscale phenomena. 3rd Conf. Mesoscale Proc., Vancouver, B.C., Canada, 21-26 Aug. 1987, 126-127. (Poster paper)

Achtemeier, G. L., 1990: Coupling divergence in direct variational analysis of the five "primitive" model equations. International Symposium on Assimilation of Observations in Meteorology and Oceanography, Clermont-Ferrand, France 9-13 July 1990, pp. 371-376.

TECHNICAL AND CONTRACT REPORTS

Achtemeier, G.L., S.Q. Kidder, and H.T. Ochs, 1985: Variational Objective Analysis for Cyclone Studies. Abstract Digest for the Panel Review of Data Analysis, Modeling, and Theoretical Research in the NASA Global Scale Atmospheric Processes Research Program. Columbia, MD, 8-12 July, pp. 39-42.

Achtemeier, G. L., H. T. Ochs III, S. Q. Kidder, R. W. Scott, J. Chen, D. Isard, and B. Chance, 1986: A Variational Assimilation Method for Satellite and Conventional Data: Development of Basic Model for Diagnosis of Cyclone Systems. Nasa Contractor Report 3981, 223 pp.

Achtemeier, G.L., 1986: Modification of a Variational Objective Analysis Model for New Equations for Pressure Gradient and Vertical Velocity in the Lower Troposphere and for Spatial Resolution and Accuracy of Satellite Data. Final Report to USRA, Contract NAS 8-36474, 28 pp.

Achtemeier, G. L., 1988: Application of Satellite Data in Variational Analysis for Global Cyclonic Systems. Status Report, Grant NAG8-059, 27 pp.

Achtemeier, G.L., 1989: Smoke Management Numerical Wind Prediction Model. Final Report, Con. AG Forest 29-412, 23 pp.

ABSTRACTS AND SHORT ARTICLES

Achtemeier, G. L., 1987: A 3-Pass Near Optimum Barnes Method for the Univariate Objective Analysis of Mesoscale Phenomena. Third Conference on Mesoscale Processes, August 21-26, 1987, Vancouver, B.C., Canada, 126-127.

Achtemeier, G. L., 1988: Variational Blending of Space Observed Radiance with Conventional Weather Data Through Coupling Radiative Transfer with the Truncated Navier-Stokes Equations. European Geophysical Society XIII General Assembly, Bologna, Italy, 21-25 March 1988, Annales Geophysicae, 6, 97.

UNPUBLISHED MANUSCRIPTS

Achtemeier, G. L., and H. T. Ochs, III, 1986: Hybrid Vertical Coordinate and Pressure Gradient Formulations for a Numerical Variational Analysis Model for the Diagnosis of Cyclone Systems. (Submitted to Monthly Weather Review)

Achtemeier, G. L., and H. T. Ochs III, 1988: A Variational Objective Analysis - Assimilation Method, Part I: Development of the Basic Model. (Submitted to Tellus 20 April 1988)

Achtemeier, G. L., S. Q. Kidder, and R. W. Scott, 1988: A Multivariate Variational Objective Analysis - Assimilation Method, Part II: Case Study Results with and without Satellite Data. (Submitted to Tellus 20 April 1988)